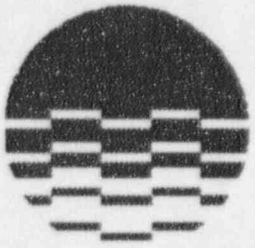

ENTERGY

ARKANSAS NUCLEAR ONE

UNIT TWO

STEAM GENERATOR

CIRCUMFERENTIAL CRACKING EVALUATION

February 1995

Table of Contents

1.0 INTRODUCTION

Arkansas Nuclear One, Unit Two (ANO-2), first experienced circumferential cracking in March 1992. Cracking was discovered as a result of primary-to-secondary leakage from a crack in the "A" steam generator (SG). The first inspection for circumferential cracking was performed during this forced outage. Since that time, four additional comprehensive examinations for circumferential cracking (during two refueling and two planned inspection outages) have been conducted. In order to assess the safety implications of continued operation of the unit, a comprehensive evaluation was performed to assess the impact of the circumferential cracks on the structural integrity of the SG tubing. This evaluation, which is a compilation of several related engineering calculations, follows.

2.0 SUMMARY

The ANO-2 steam generators have experienced several forms of tubing degradation, most notably stress corrosion cracking (SCC) at the tube support plates (axially oriented) and at the expansion transition region (ETR) at the top of the hot leg (HL) tubesheet in the sludge pile region. The indications at the tubesheet have primarily been circumferentially oriented, but have also included axially oriented, as well as volumetric indications. This evaluation is limited to the circumferential cracks at the ETR, since these have been the only flaw detected in the SGs which could potentially challenge structural margin requirements.

As a result of comprehensive inspections, application of NRC Regulatory Guide (RG) 1.121 safety factors, use of statistically valid (95/95) material properties, statistically based degradation projections, and tube burst test data, it is concluded that the ANO-2 steam generators can safely operate for the remainder of the current cycle with an acceptable level of risk of compromising the structural integrity requirements for the tubing. From a risk perspective, full cycle operation is also assured at an acceptable level. The next cycle's operation will be evaluated again following data collection from the September 1995 refueling outage (2R11). Details of the evaluations performed are described in the remaining sections of this report.

3.0 ANO-2 STEAM GENERATOR DESCRIPTION

The ANO-2 steam generators are of the U-tube design manufactured by Combustion Engineering (model 2815). Each steam generator contains 8411 tubes constructed of high temperature mill annealed (HTMA) Inconel alloy 600 material with an outside diameter of 3/4 inches and a wall thickness of 0.048 inches. The tubes are explosively expanded to the full depth of the tube sheet. There are seven full eggcrate tube support plates (TSP), two partial eggcrate TSPs, and two partial drilled TSPs. The SG layout is shown in Figure 3.0-1. The reactor went into commercial operation in March 1980, and utilizes all volatile treatment (AVT) chemistry. Secondary side boric acid addition was initiated in 1983 to arrest denting at the partial drilled TSPs. The hot leg operating temperature was initially 607° F, but was reduced to ~600° F following the ninth refueling outage in the fall of 1992.

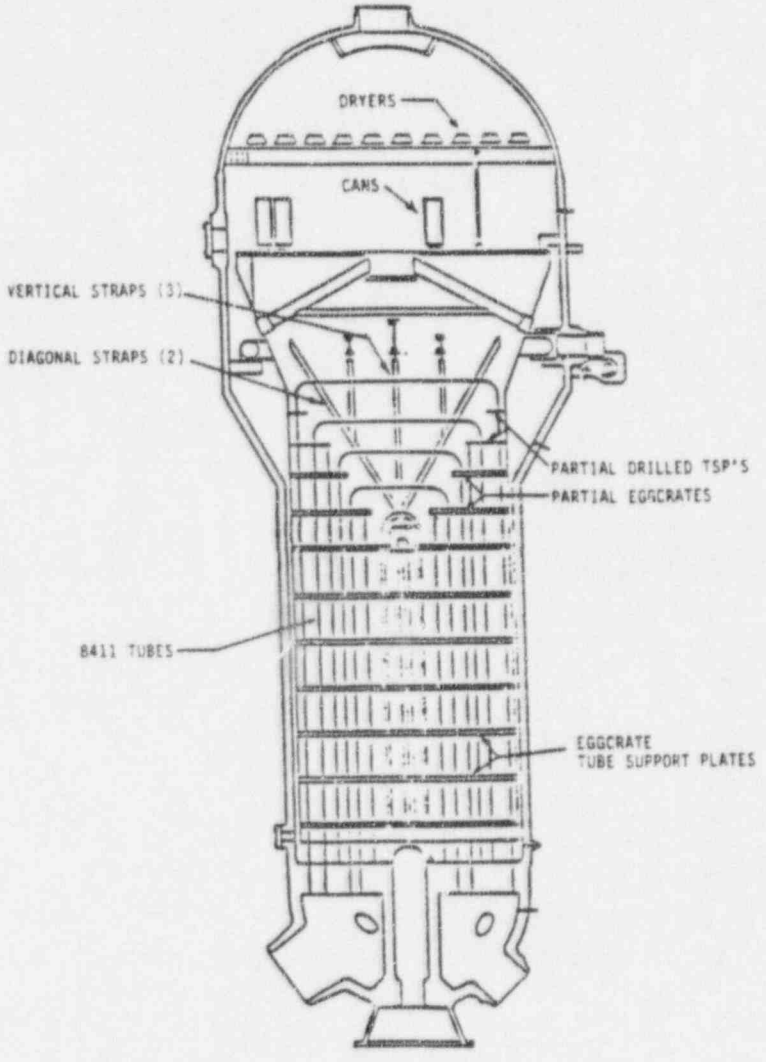

Figure 3.0-1
ANO-2 Steam Generator

4.0 STEAM GENERATOR INSPECTION/REPAIR HISTORY

4.1 Operational History

The ANO-2 SGs began commercial operation with 44 tubes plugged (15 in "A" and 29 in "B"). These preservice repairs were done primarily as a result of a "post rim cut" of the drilled TSPs around the periphery to prevent cracking of the solid ligaments between the drilled holes of the TSPs due to denting. An inspection of the periphery was performed to ensure that any tubes damaged during the modification were repaired.

ANO-2 historically performed the technical specification minimum inspection sample size of 3% per SG through the eighth refueling outage. Early on, denting of the tubes at the partial drilled TSPs (TSPs 10 and 11) was of concern. Changes to the secondary plant, including removal of the CuNi tubing in the feedwater heaters, oxygen control modifications to the condensate storage tanks, boric acid treatment, and adoption of the Electric Power research Institute (EPRI) Secondary Water Chemistry Guidelines, arrested the denting rate and all but eliminated that concern. These changes/enhancements were completed by the end of the third refueling outage (1983).

The next area of interest that developed was flow induced vibration in the form of wear at the upper bundle vertical and diagonal support straps (commonly referred to as "batwings"). In the sixth refueling outage (1988), expanded testing was performed in the "B" SG due to wear induced damage. The initial sample plan was 8% in "A" and 5% in "B." In accordance with the technical specifications, a second inspection sample (6%) for a total of 11% was performed in the "B" SG. Six tubes were plugged as a result. The "A" SG had no repairable indications in the first sample, and thus no expansion was required.

In August 1990, the first indication of primary-secondary leakage occurred. Evidence of leakage was detected following a full power reactor trip and decreased upon return to full power to a low level (<0.01 GPM).

In 1991, during the eighth refueling outage, the initial inspection of the "B" SG (3%) was categorized as C-3 (>1% of the sample defective per the technical specifications) due to TSP indications, and thus a 100% inspection was required. Additionally, a second sample inspection was required in the "A" SG as a result of the C-3 categorization in the "B" SG. The 9% total sample of "A" did not yield defective tubes and no further inspections were performed. An attempt was made in 2R8 to locate the leaker with a pressure/helium test, but no indication of leakage was found.

In October 1991, following a full power reactor trip, indications of primary-secondary leakage again occurred. Following a return to full power, the leakage gradually decreased to a very small level (<0.01 GPM).

On March 9, 1992, primary-secondary leakage took a step increase and the plant was subsequently shut down. The calculated maximum leak rate was 0.25 GPM. During

the outage, the leak was determined to be from a circumferential crack at the top of tubesheet (TTS) ETR on the hot leg of the "A" steam generator. Rotating pancake coil (RPC) inspections were performed on 100% of the hot leg ETR of both SGs, and 20% of the sludge pile region in the cold leg (CL). In addition, all tubes with potential indications were tested full length with a bobbin coil probe. In total, 421 tubes were repaired in "A" and 67 in "B". Of those numbers, 392 tubes in "A" and 56 in "B" were repaired via sleeving. The remainder of the tubes were removed from service with plugs and stabilizers. Subsequent detailed evaluations indicated that only 208 tubes in "A" and 11 in "B" had circumferential cracks, with the remainder being volumetric or axial indications. The results of the outage were presented to the NRC staff in a meeting on April 16, 1992[1].

Five tubes were removed during this outage. Three contained circumferential cracks and two contained axial indications at three support elevations. The results of the tube pull and additional analysis were presented to the NRC staff in a meeting on August 26, 1992[2].

The unit operated following the forced outage for approximately four months until the ninth refueling outage in September 1992 (2R9). During that outage, 25 circumferential cracks (17 in "A" and 8 in "B") were detected as a result of an inspection of 100% of the hot leg ETR and 20% of the cold leg sludge pile region in each SG. The largest flaw was pressure tested prior to removal. The test demonstrated the flaw was able to withstand three times the normal operating differential pressure (3ΔP). Two tubes with circumferential cracks were removed during the outage. The inspection and pulled tube results were presented to the NRC staff in a meeting on December 3, 1992[3].

As a result of concern for possible high growth rate and potential for leakage, a mid-cycle outage (2P93-1) was planned. The outage was conducted after approximately six months of operation from the refueling outage. During that outage, inspections of both SGs were performed concentrated in the sludge pile region (100% of sludge pile area, ~70% of the total bundle). Forty-five circumferential cracks were found in the "A" SG and three in the "B" SG. In addition, two volumetric indications were discovered in the "A" SG. All indications were plugged and stabilized. The results of the outage were presented to the NRC staff in a meeting on August 30, 1993[4].

ANO-2 operated until the next refueling outage (2R10, beginning in March 1994) with no detectable leakage. During this outage, 170 circumferential cracks were discovered (147 in "A" and 23 in "B") as a result of an inspection of 100% of the hot leg ETR and 20% of the cold leg sludge pile region in each SG. In-situ pressure testing was performed on three tubes. A detailed discussion of the pressure testing is provided in Section 5.3.3. Subsequent evaluations indicated that all tubes met RG 1.121 structural margin requirements, and probabilistic analysis showed that full cycle operation was acceptable (see Section 6). However, in order to provide additional data, a subsequent mid-cycle outage was scheduled. The results of the 2R10 outage were presented to the NRC staff in a meeting on July 14, 1994[5].

ANO-2 operated from 2R10 until the mid-cycle outage in January 1995 (2P95-1), with no detectable leakage. The mid-cycle outage was performed with a planned scope of RPC testing at the ETR of the entire hot leg sludge pile region of both steam generators. The results were 283 circumferential cracks (203 in "A" and 80 in "B"). In addition, 17 other flaws (12 in "A" and 5 in "B") were detected. These flaws were generally axially oriented or volumetric in nature. All tubes containing detected flaws were plugged and those tubes containing circumferential cracks were also stabilized. A summary listing of the 2P95-1 results is included in Appendix A. The listing contains all tubes plugged during the outage and satisfies the ANO-2 technical specification reporting requirement.

The largest flaw detected was sized at 304° arc length, 81% maximum depth, and calculated average depth of 69%. In-situ pressure testing was performed on this tube and two additional tubes. A detailed discussion of the pressure testing is provided in Section 5.3.3. Based on the RPC data and the in-situ pressure testing, all flaws met the RG 1.121 structural requirements. Additional probabilistic and statistical analysis show that operation for the remainder of the cycle is acceptable (see Sections 5.2 and 6).

4.2 Eddy Current/Repair Summary

The following tables summarizes the ANO-2 inspection history since 1991 (Table 4.2-1) and the repair summary since pre-operation (Table 4.2-2) for all defects.

Table 4.2-1

ANO-2 Inspection History

"A" Steam Generator % Tubes Inspected

Type of Inspection	2R8	2F92	2R9	2P93-1	2R10	2P95-1
HL TTS RPC (ETR)	0	100	100	71*	100	66*
CL TTS RPC (ETR)	0	20**	20**	0	20**	0
Bobbin Full Length	9	5	100	0	100	0
Dent Inspection (RPC)	0	0	0	0	8	0
Sleeve Inspection	N/A	100	0	0	100	0

"B" Steam Generator % Tubes Inspected

Type of Inspection	2R8	2F92	2R9	2P93-1	2R10	2P95-1
HL TTS RPC (ETR)	0	100	100	72*	100	71*
CL TTS RPC (ETR)	0	0	20**	0	20**	0
Bobbin Full Length	100	1	100	0	100	0
Dent Inspection (RPC)	0	0	0	0	33	0
Sleeve Inspection	N/A	100	0	0	100	0

* Percentage of non-plugged and non-sleeved tubes in the entire bundle. 100% of the sludge pile region was inspected.

** Percentage of the sludge pile region.

Table 4.2-2

Repair Summary

			SG "A"		SG "B"	
YEAR	EFPY	OUTAGE	PLUGS	SLEEVES	PLUGS	SLEEVES
1978	0.00	MFG	15	0	29	0
1981	0.89	2R1	0	0	0	0
1982	1.69	2R2	0	0	1	0
1983	2.33	2R3	0	0	0	0
1985	3.31	2R4	0	0	0	0
1986	4.16	2R5	0	0	0	0
1988	5.38	2R6	0	0	6	0
1989	6.52	2R7	0	0	0	0
1991	7.67	2R8	0	0	73	0
1992	8.51	2F92	29	392	11	56
1992	8.85	2R9	67*	0*	132	0
1993	9.36	2P93-1	47	0	3	0
1994	10.16	2R10	170	0	77	0
1995	10.86	2P95-1	215	0	85	0
Total # Repaired:			543	388*	417	56
Total % Equivalent Plugged:			6.71		4.99	

* Four tubes previously sleeved at the tubesheet were plugged due to flaws at tube support plates. The total number of inservice sleeves in the "A" SG is 388.

Note: Eighteen sleeves are equivalent to one plug in reduction of reactor coolant system (RCS) flow.

5.0 TECHNICAL EVALUATION

5.1 Inspection Techniques/Improvements

Nondestructive Examination (NDE) is a critical element in assessing the structural significance of SG tubing flaws, and the inspection method must provide a reliable measurement of crack dimensions. Additionally, the inspection process can provide crack growth data which is required to establish allowable crack sizes and operating intervals for various conditions.

Conventional bobbin coil technology, used for routine steam generator examinations, has limitations in inspecting expansion transitions, and circumferentially oriented flaws are essentially undetectable with the bobbin coil. The use of RPC eddy current technology provides an important field diagnostic tool for detecting and measuring circumferential cracks.

RPC tube inspection is accomplished using a surface-riding coil which is rotated around the tube axis. The coil is spring loaded to maintain contact with the tube inner surface as it moves through the expansion transition region. Lift-off variations between the coil and the tube surface, caused by a change in tube diameter due to the expansion, are significantly reduced when compared with the bobbin coil. As the probe is translated and rotated through the tube it describes a helical path. A linear discontinuity is scanned once during each rotation of the probe. The coil output voltage from a given rotation is used to generate a line scan which represents signal amplitude as a function of coil position around the tube circumference[6]. Multiple line scans are typically displayed in a three dimensional format (known as C-Scan) to provide a tool for evaluating potential flaws.

Entergy Operations has previously utilized an approach to predict the average circumferential crack depth as the product of the maximum depth from the RPC phase angle analysis and the circumferential crack length divided by 360°:

$$\bar{d} = \frac{d_{max} l}{360}$$

where: d_{max} = crack maximum depth (based on phase analysis), % throughwall (TW)
l = crack arc length (largest of clip plot or crack map), degrees

The intent of the average depth approach is to define the flawed area in order to assess structural integrity. Information related to this issue was presented to the NRC staff in a meeting on July 15, 1993[7].

In Belgium, a similar approach is used where the "crack area" is calculated by using the percent depth times the length in degrees as determined by ultrasonic testing[8]. Average depth or crack area is the desirable product of the NDE because of its correlation to the structural adequacy of a circumferentially cracked tube. In the

absence of significant bending effects, the burst pressure of tubes with large circumferential cracks can be calculated by equating the axial load due to pressure (lb_f) to the net section remaining tube area (in^2) times a suitable flow strength (psi).

Figures 5.1-1 and 5.1-2 illustrate that the observed top of tubesheet circumferential cracking at ANO-2 is often comprised of a band of circumferential cracks. Small axial cracks are sometimes observed, with a resulting crack network morphology that has been termed cellular corrosion. The sound material which resists axial pressure forces is composed of uncracked material from the leading edge of partial throughwall circumferential cracks at different axial locations (see Figure 5.1-3). Machined circumferential flaws only simulate this first type of ligament. The ligaments of material between circumferential cracks at different axial locations in a band of circumferential cracks are not present in machined flaw geometries which have been tested to date[9].

Both average depth and crack area methods have shown reasonable agreement with the observations on pulled tubes; however, they appear to provide conservative assessments of burst strength of circumferential cracks as demonstrated by the use of in-situ pressure tests at ANO-2 and other sites. Assessments of the structural significance of circumferential cracks can be performed using arc length alone, as long as the length is short enough to support the necessary assumptions. When the crack lengths are longer, some other parameter must be factored in, and thus the average depth concept was created. However, the success of the average RPC depth hinges on the balance of overestimates and underestimates. The RPC maximum depth is typically an overestimate of the actual crack depth and the detected length is typically an underestimate of the actual crack length. It is expected that this procedure would be increasingly overconservative for very long cracks, since a detected length of about 360° cannot be an underestimate. However, the data available to date for crack lengths near 360° show that the RPC calculated average depth and the measured average depth are about equal. The present agreement between average crack depth and estimates from RPC may be fortuitous at very long crack lengths. For cracks of 360°, the cracked area estimate, and thus the burst strength estimate, is critically dependent on estimated maximum depth from RPC data. Sizing of nearly throughwall cracks must be considered a region of considerable uncertainty. While the RPC average depth approach is expected to be reasonably successful when cracking is not detected over the full tube circumference, this technique is subject to being overly conservative for very long and deep cracks, mostly due to the planar flaw presentation versus the flaw geometry containing ligaments described above. The RPC average depth concept is but one technique utilized at ANO to evaluate the structural significance of a given flaw. It is used to identify those flaws needing further evaluation via other means such as in-situ pressure testing, ultrasonic testing (UT), or RPC deconvolution analysis to evaluate the flaw[9].

Because of previous problems with data quality, three major hardware changes were incorporated for the 2R10 inspection to improve the data and enhance the detection and sizing of flaws. The first change was the use of a 0.115" diameter pancake coil, and an axial and circumferential coil. Previously, the pancake coil was 0.080". The 3-coil

RPC 0.080" shielded coil, which was developed for the detection and sizing of inside diameter (ID) initiated cracking, provides limited detection of low level outside diameter (OD) initiated cracking. This is, in part, due to the relatively high optimum frequency which results in the reduced density of eddy currents at the OD of the tube wall and because shallow OD flaws, coupled with the decreased current flow at the OD, cause minor perturbations of the eddy current field; these consequently limit detection of shallow OD flaws. The use of the 0.115" coil, coupled with overall system optimization has allowed for better detection capabilities[10]. The second change was the use of a low loss cable from the probe pusher to the MIZ-18 tester to provide a better signal to noise ratio. The third change involved the use of dedicated power supplies for each SG. None of these changes can be directly attributed to definitive improvements, although subjective evaluations have been performed indicating that the 1994 data quality appeared to be significantly better than that acquired in 1993[11].

One area related to analysis that was changed during the 2R10 outage involved the use of C-scan terrain plots to assess the data. The Eddy Current Testing (ECT) Guidelines did not previously require analysts to utilize the C-scan plots, even though it was common practice. A concern is that C-scan plots can produce flaw-like signals in good tubes (i.e., similar signals exist in steam generators never placed in service). Therefore, both C-scan and strip chart (lisajous) analysis must be performed in order to provide the best evaluation of the data. Analysts had previously relied on lisajous phase correlation between the base frequencies to evaluate signals. However, in many cases, the phase rotates completely out of a flaw plane. One would normally expect the phase spread between the base frequencies to be relatively narrow. For Tube 48-50 in 2R10, the spread was significant (from 62 degrees at 400 kHz to 353 degrees at 100 kHz). In addition, for that particular tube, a multi-frequency mix removes most of the signal response such that there is little to no evidence of a flaw being present. This is shown in Figure 5.1-4. Because of the above concerns with individual analysis tools, multiple analysis tools must be used to ensure that a thorough analysis of the data is performed.

For 2P95-1, the following changes were made:

- Data was acquired while pushing vs. pulling the probe to eliminate probe snap through the transition
- Rotational speed was increased from 300 RPM to 900 RPM
- Push speed was increased from 0.2 inches per second to 0.5 inches per second
- Terrain maps were required to be plotted for every tube.

These changes were made based on previous ANO and industry experience and yielded the best quality data to date (qualitative assessment). All of the above changes are enhancements Entergy Operations believes results in a comprehensive and conservative inspection.

For Tube 32-126, which was the largest flaw at 360° in 2R10, the previous outage results were classified as no detectable defect (NDD). The data does, however, provide some insight as to the formation of a flaw. The lisajous data for 2F92 and 2R9 (shown in Figure 5.1-5) at the base frequency with the pancake coil shows a flat response. The C-scan data does indicate a "ridge-like" response, but this is potentially a result of the effects of the expansion transition, conductive deposits, and the top of tubesheet (see Figure 5.1-6). In 2P93-1, while the lisajous by itself does not provide any indication of a flaw, it does show a change from the previous outage (see Figure 5.1-5). While this type of response could still be due to conductive deposits, it would be a cause for further evaluation. When conductive deposits exist in conjunction with the explosive expansion and top of tubesheet geometric distortions, comparison to previous data, even if the ECT response is not clearly indicative of a flaw, may be the best way to evaluate the data. Entergy Operations currently compares all tubes flagged with potential indications with the previous outage results.

A signal processing operation referred to as "deconvolution" has been used to obtain improved angular resolution of ANO-2 RPC data obtained from circumferential cracks at the top of the tubesheet. While deconvolution is not a new concept, its application to rotating probe eddy current data represents a first time application. Deconvolution provides a more detailed and accurate assessment of multiple closely spaced eddy current indications which, when coupled with leak rate data, can be used to provide a better estimate of tube integrity in the context of leakage and burst susceptibility. The deconvoluted eddy current data has also been compared with in-situ UT data with excellent agreement[9]. Figures 5.1-7 through 5.1-9 show the deconvoluted ECT data as compared to the UT.

ANO-2 has tested a total of 151 tubes with ultrasonic techniques and has received mixed results. The exams were performed in the 2F92, 2R10, and 2P95-1 outages.

During 2F92, 85 tubes were tested. The largest flaw was 360°, 100%TW maximum depth, and had an average depth of 67%, which is less than the RG 1.121 maximum of 79%.

UT was performed on 52 tubes with potential indications during 2R10. Of those, 13 of the 52 had no indication present. The largest flaw by UT was 360°, 100%TW maximum depth, and had an average depth of 76%, which is less than the RG 1.121 maximum of 79%, thus indicating the flaw would have sustained the required pressures with the margin included. A UT plot of the largest flaw in 2R10 is shown in Figure 5.1-10.

During 2P95-1, 14 tubes with indications as called by RPC were examined with UT. The results of the UT provided consistently poor correlation with the RPC results. The largest flaw by UT was 45°, 46%TW maximum depth, and an average depth of 3%. The same flaw by RPC was sized at 304°, 81%TW maximum depth and an average depth of 69%.

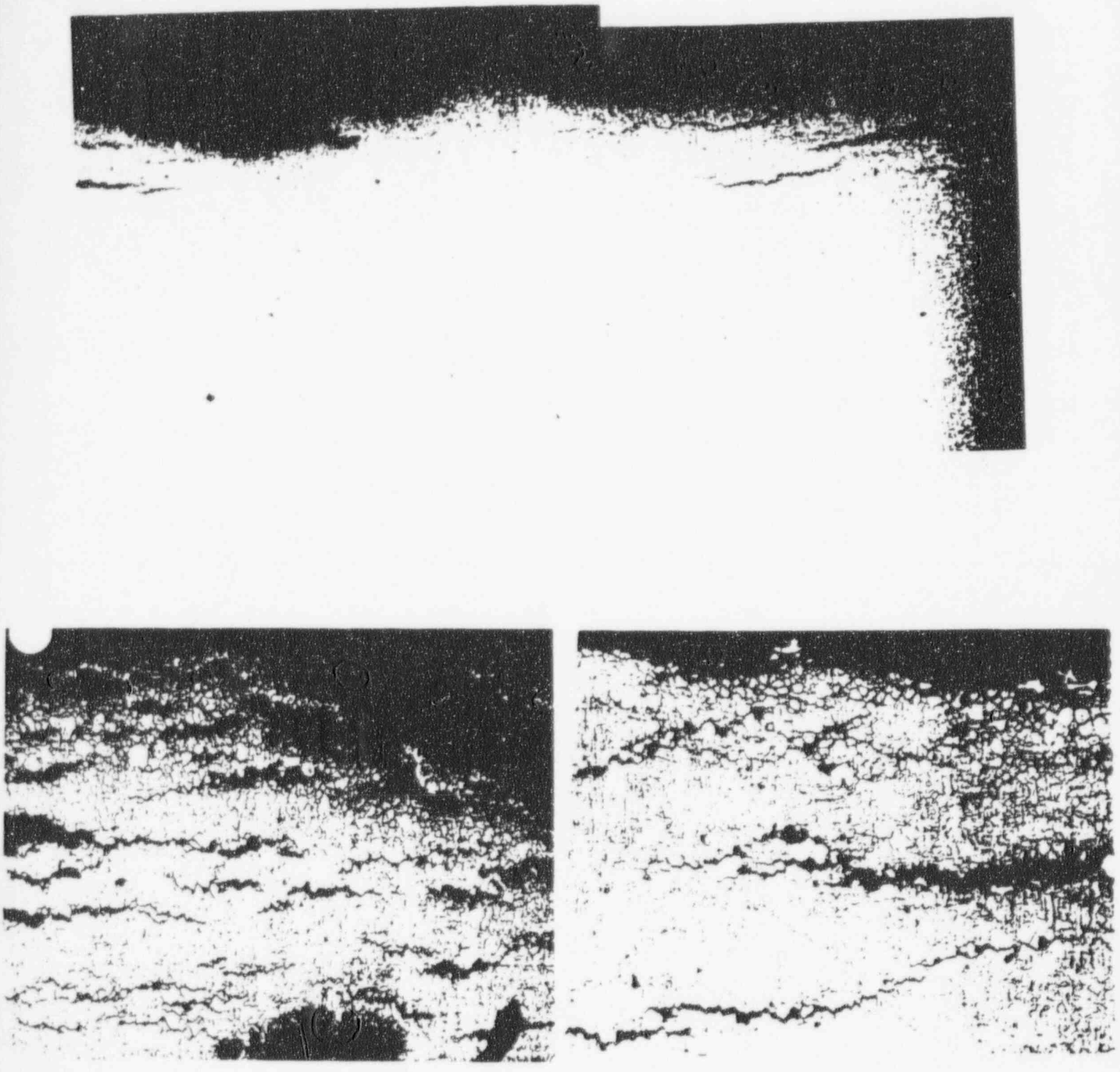

Figure 5.1-1
Tube A79-83

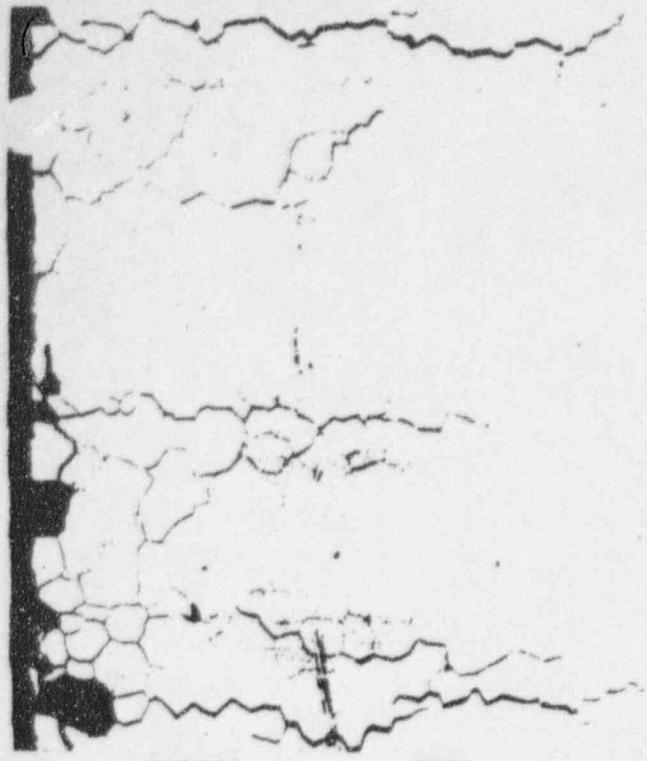

102080 200X
As Polished

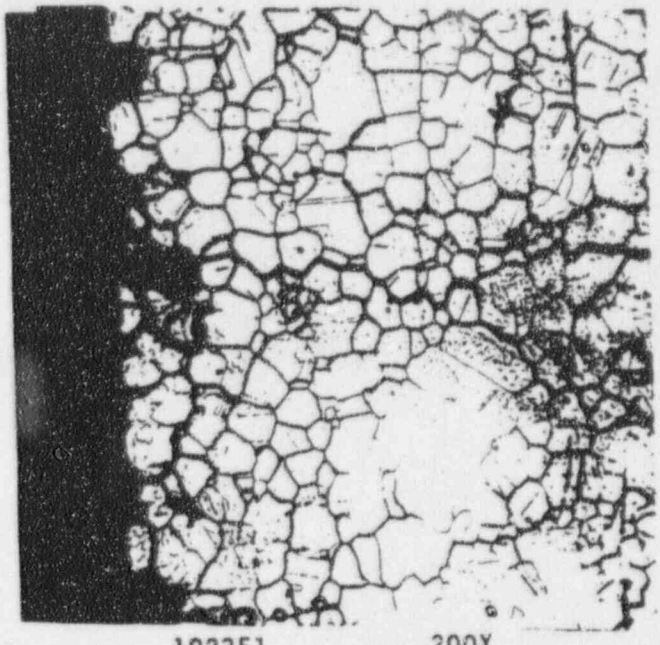

102351 200X
Glyceregia Etch

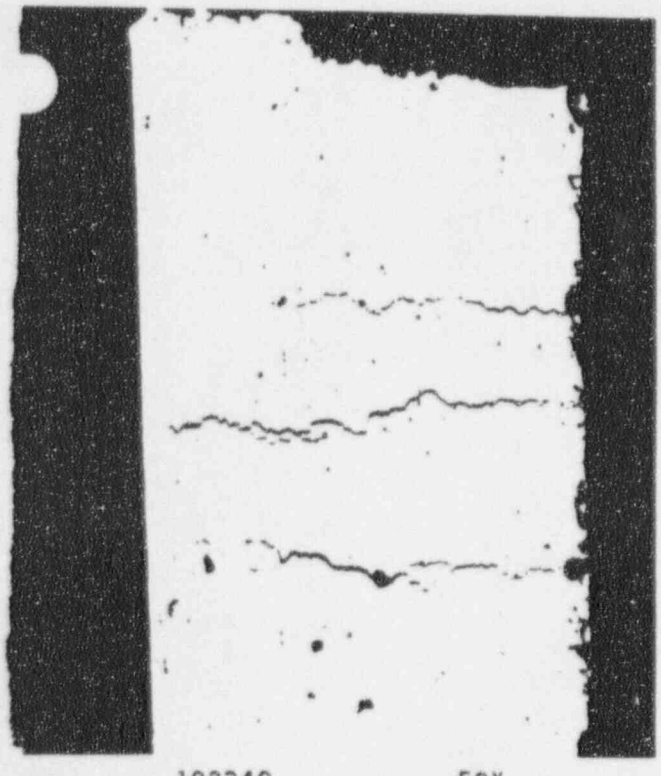

102349 50X
As Polished

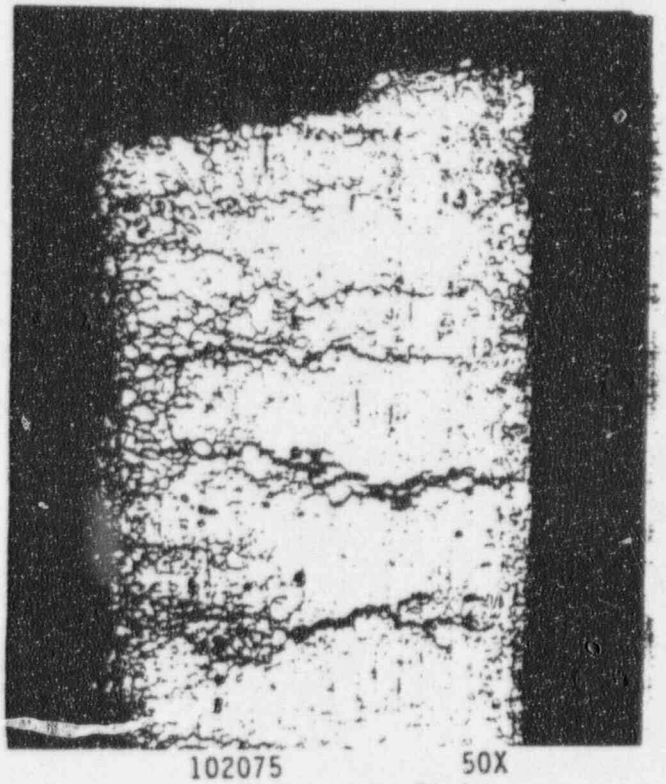

102075 50X
Glyceregia Etch

Figure 5.1-2
Tube A55-63

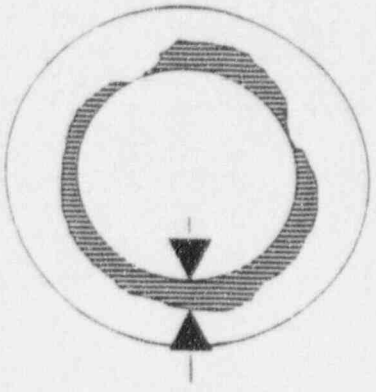

Depth Direction In-Plane Ligament

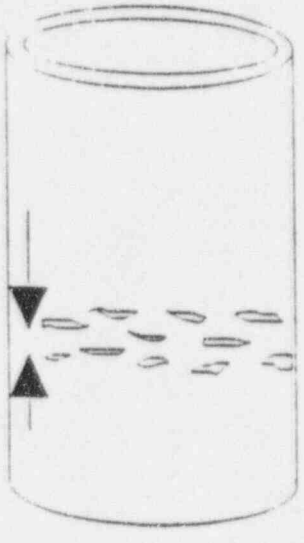

Non Co-Planar Ligaments

Figure 5.1-3
Schematic Illustration of a Band of Circumferential Cracking

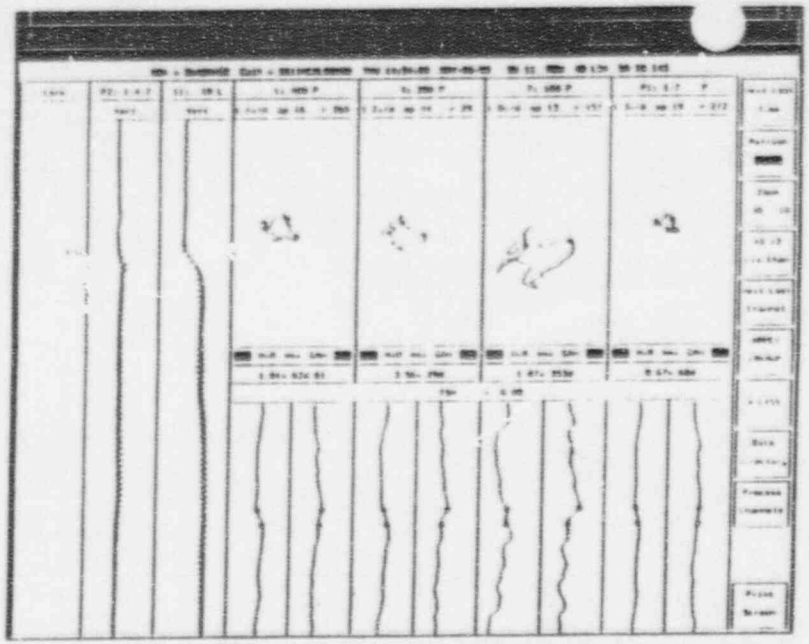

1994 LISAJOUS SHOWING PHASE SPREAD

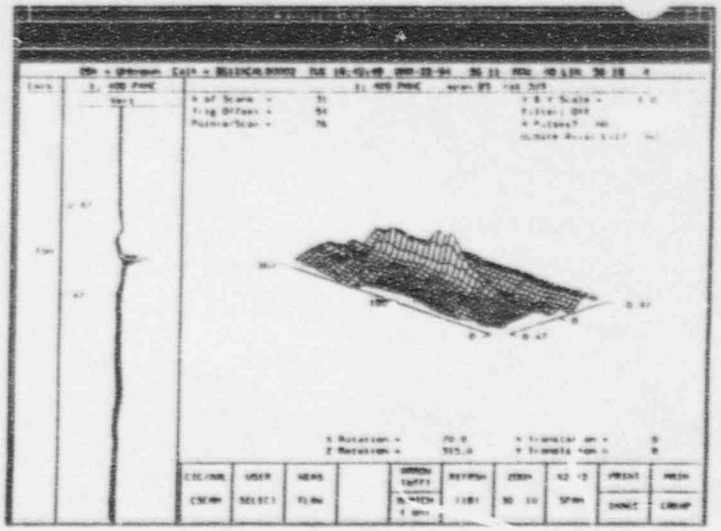

1994 C-SCAN PANCAKE COIL

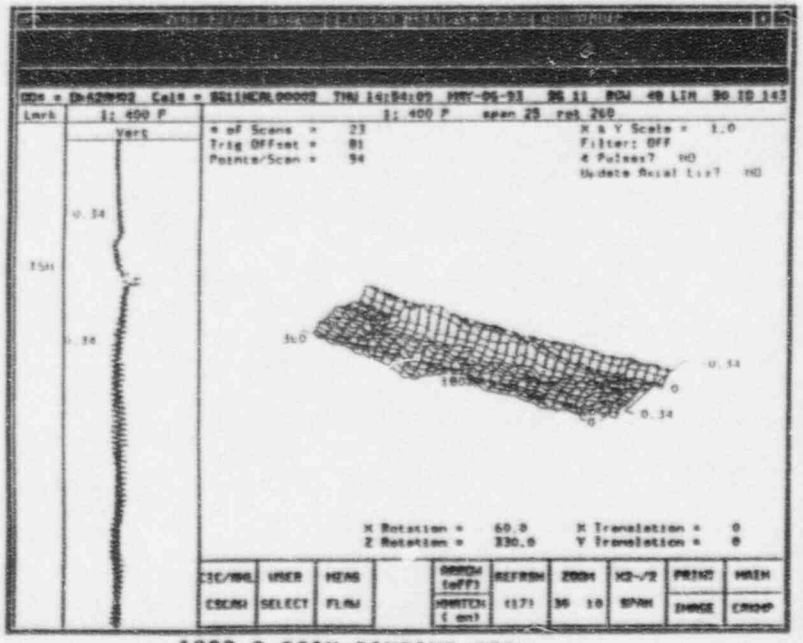

1993 C-SCAN PANCAKE COIL

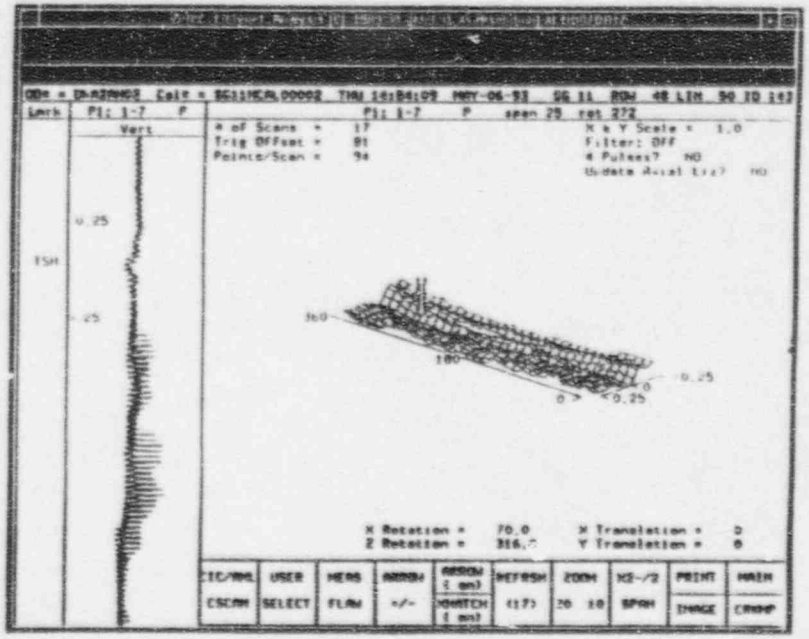

1993 C-SCAN MULTIFREQUENCY MIX

Figure 5.1-4
Tube 48-50

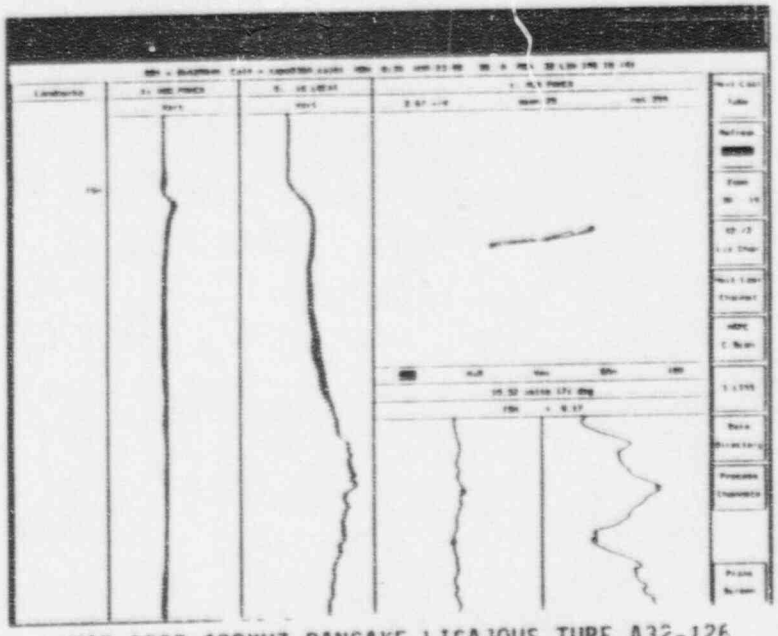

MAR 1992 400KHZ PANCAKE LISAJOUS TUBE A32-126

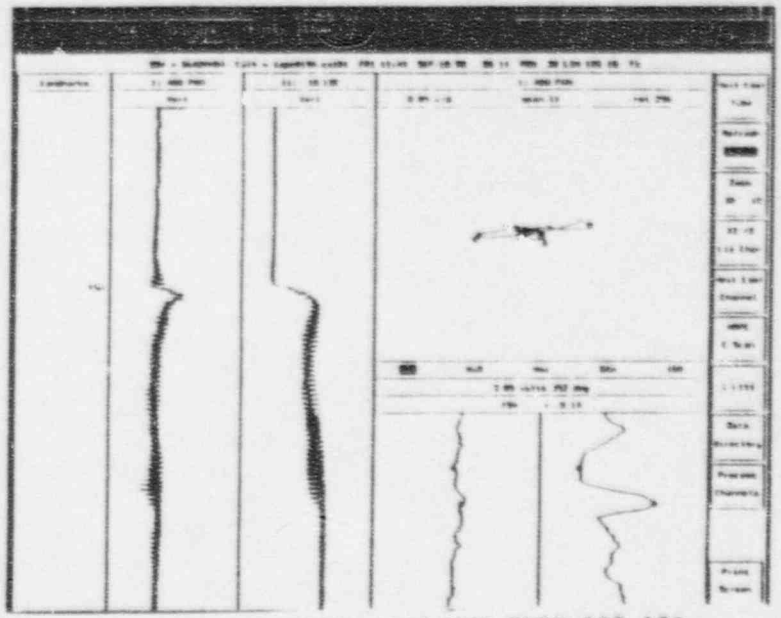

SEP 1992 400KHZ PANCAKE LISAJOUS TUBE A32-126

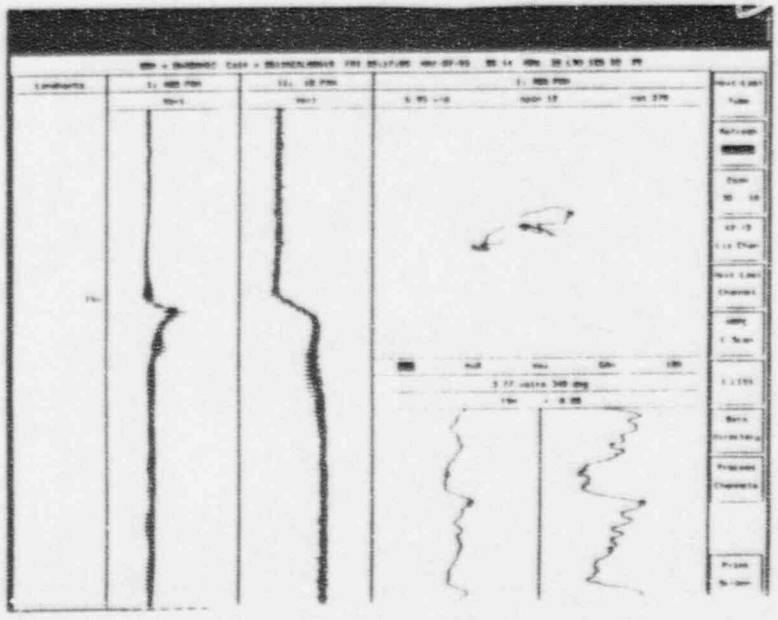

MAY 1993 400KHZ PANCAKE LISAJOUS TUBE A32-126

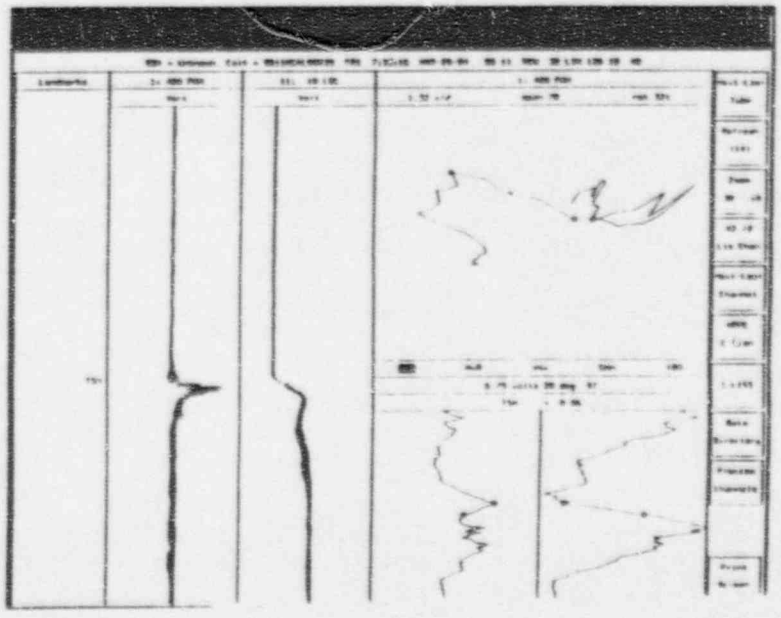

MAR 1994 400KHZ PANCAKE LISAJOUS TUBE A32-125

Figure 5.1-5
Lisajous Data for Tube 32-126

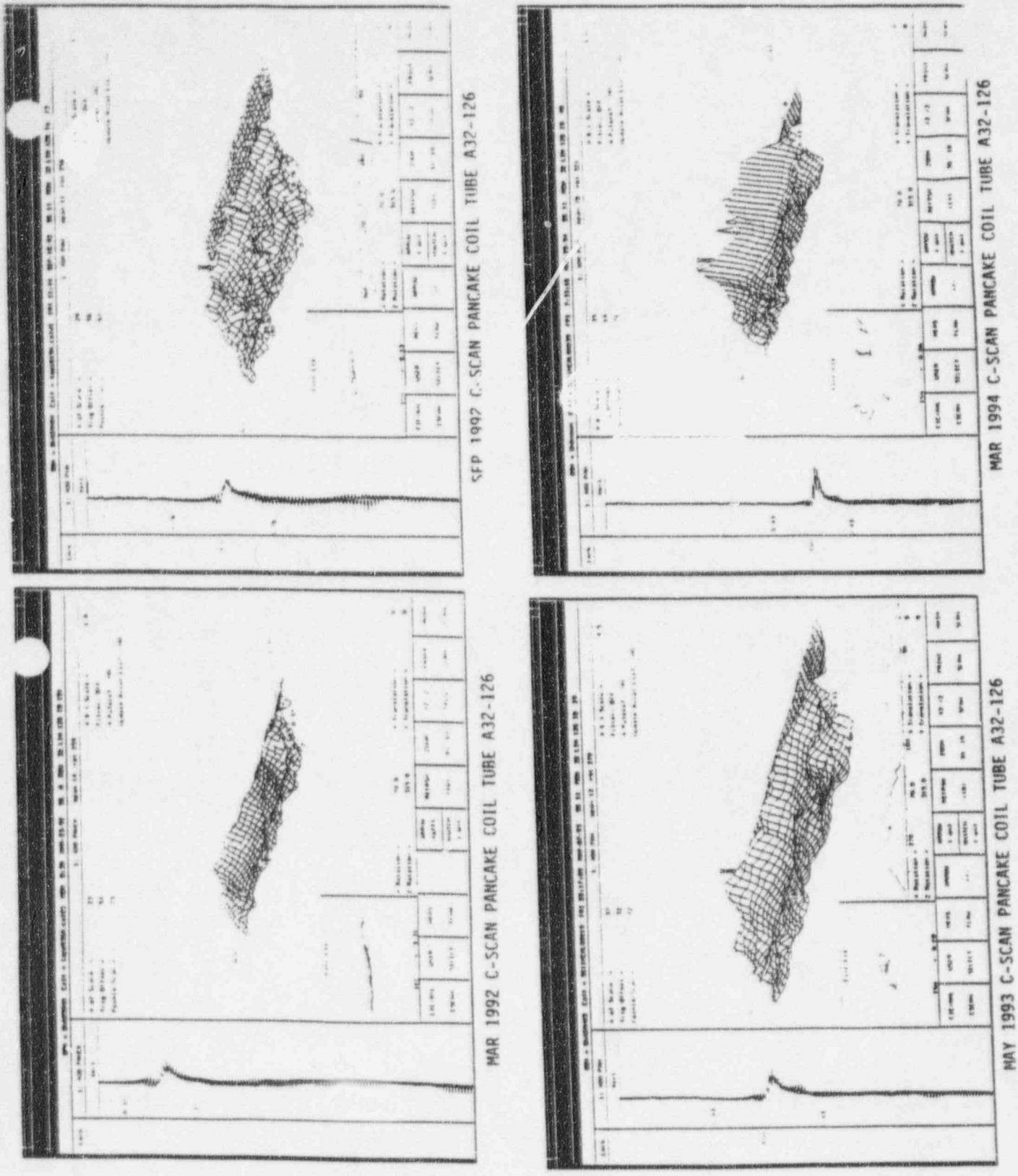

Figure 5.1-6
C-Scans of Tube 32-126

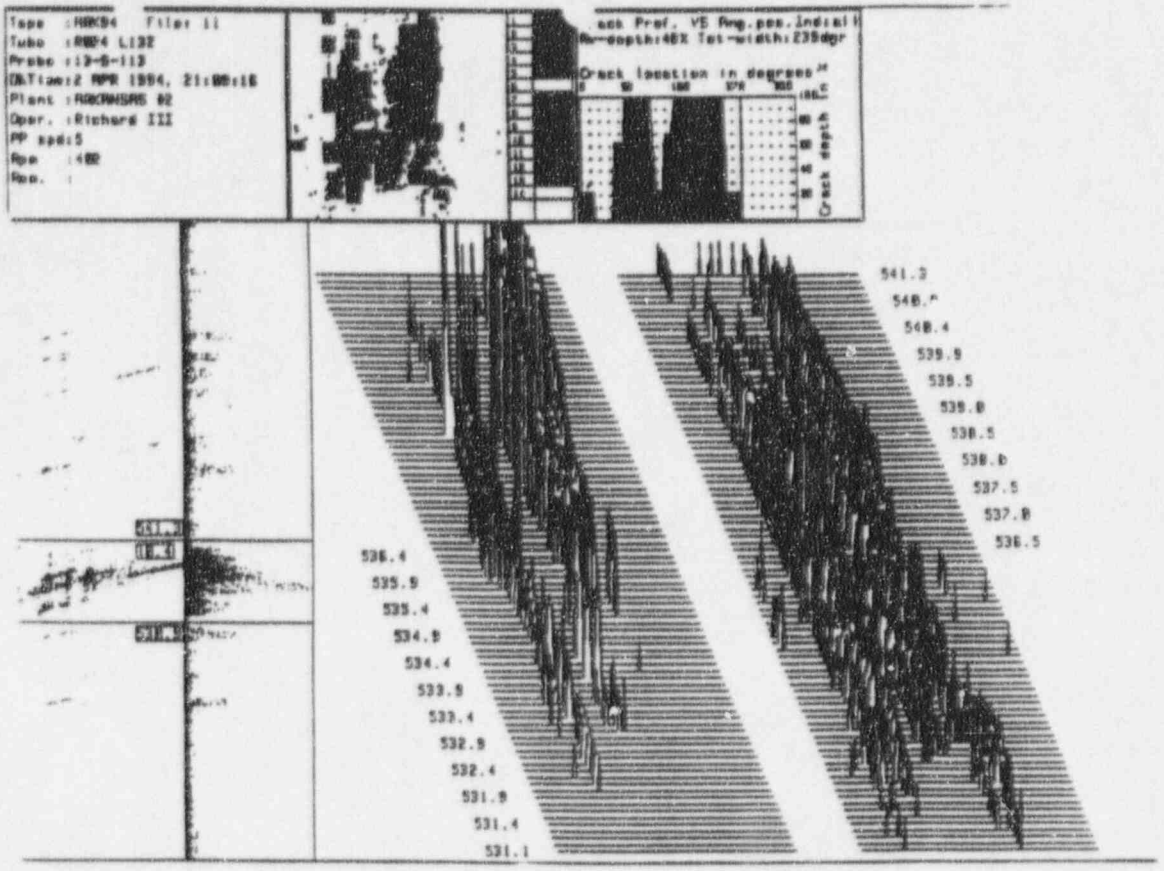

UT Plot

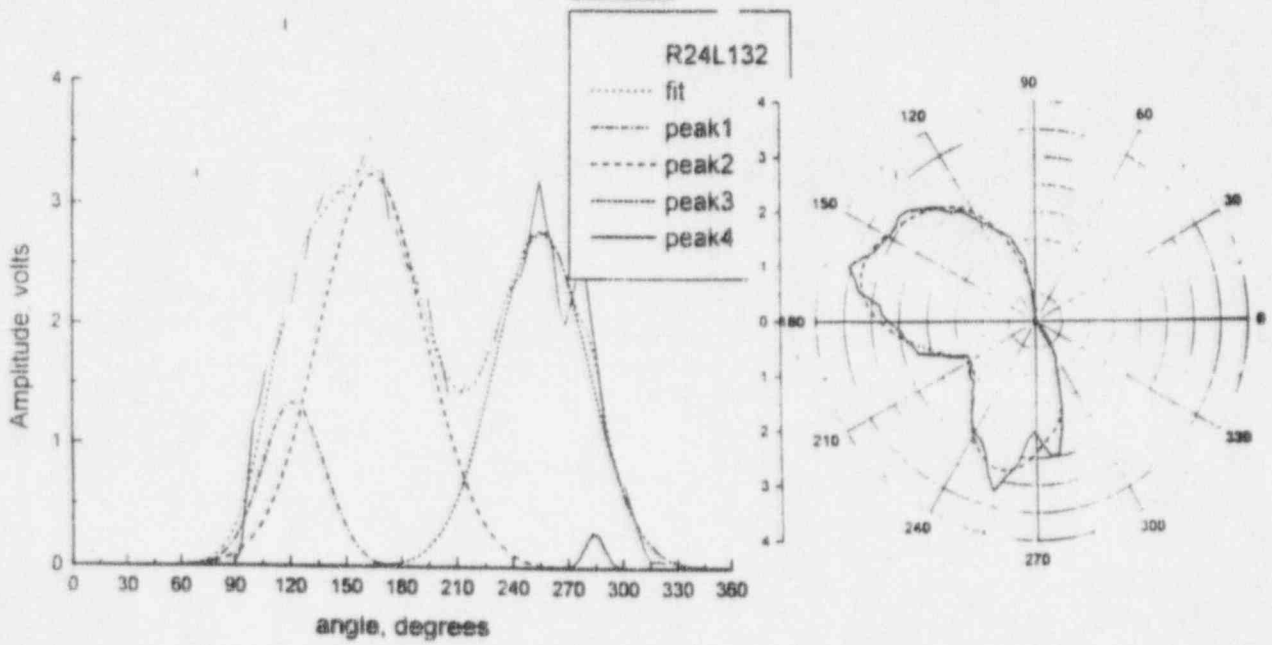

RPC Deconvolution Analysis

Figure 5.1-7
Comparison of UT to Deconvolution Analysis for Tube 24-132

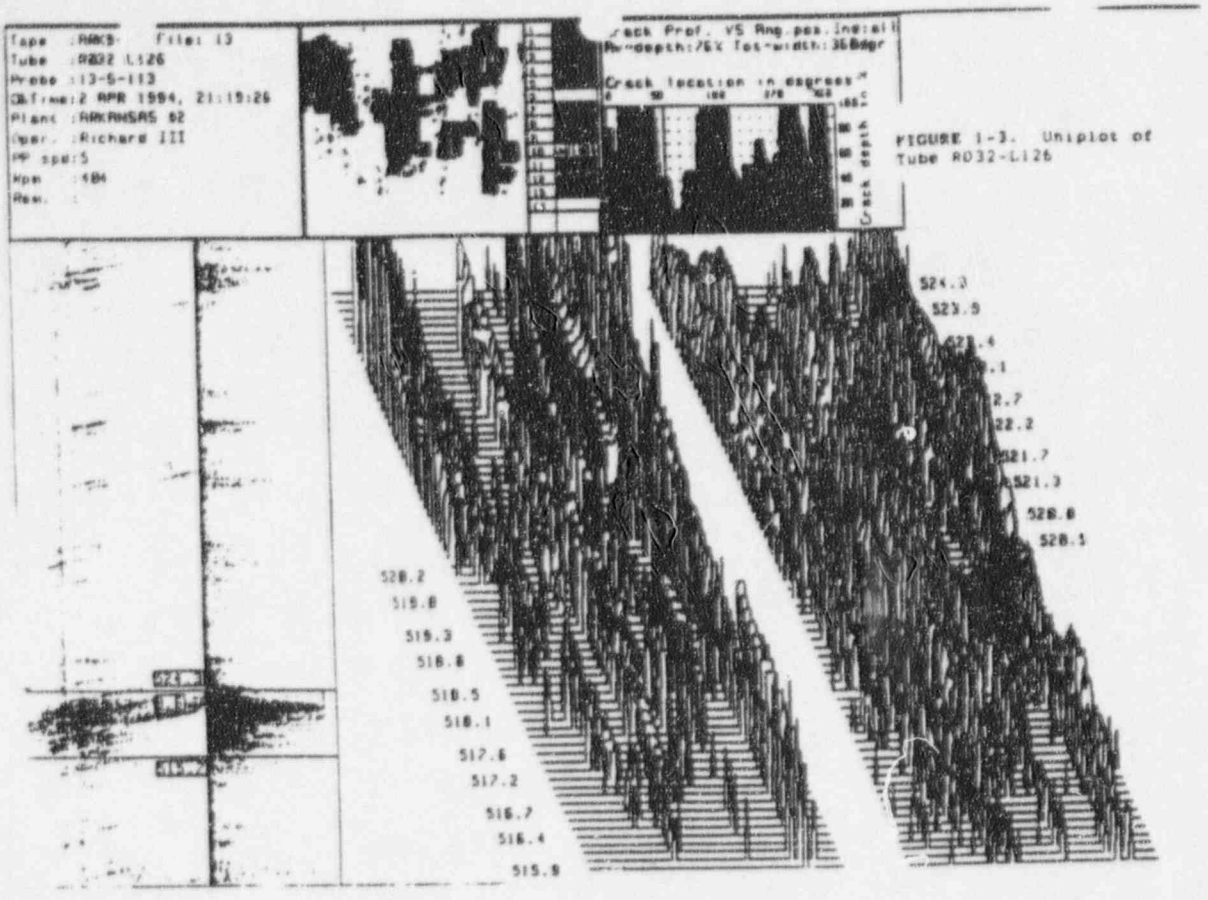

FIGURE 1-3. Uniplot of Tube R032-L126

UT Plot R32_126

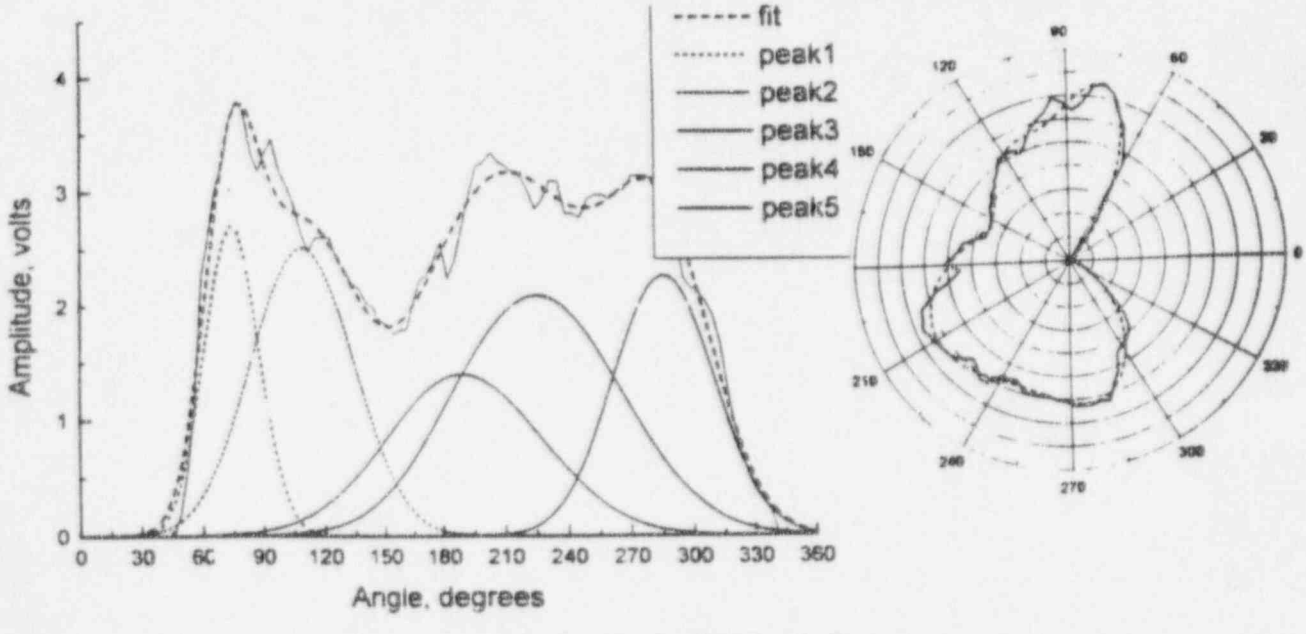

RPC Deconvolution Analysis

Figure 5.1-8
Comparison of UT to Deconvolution Analysis for Tube 32-126

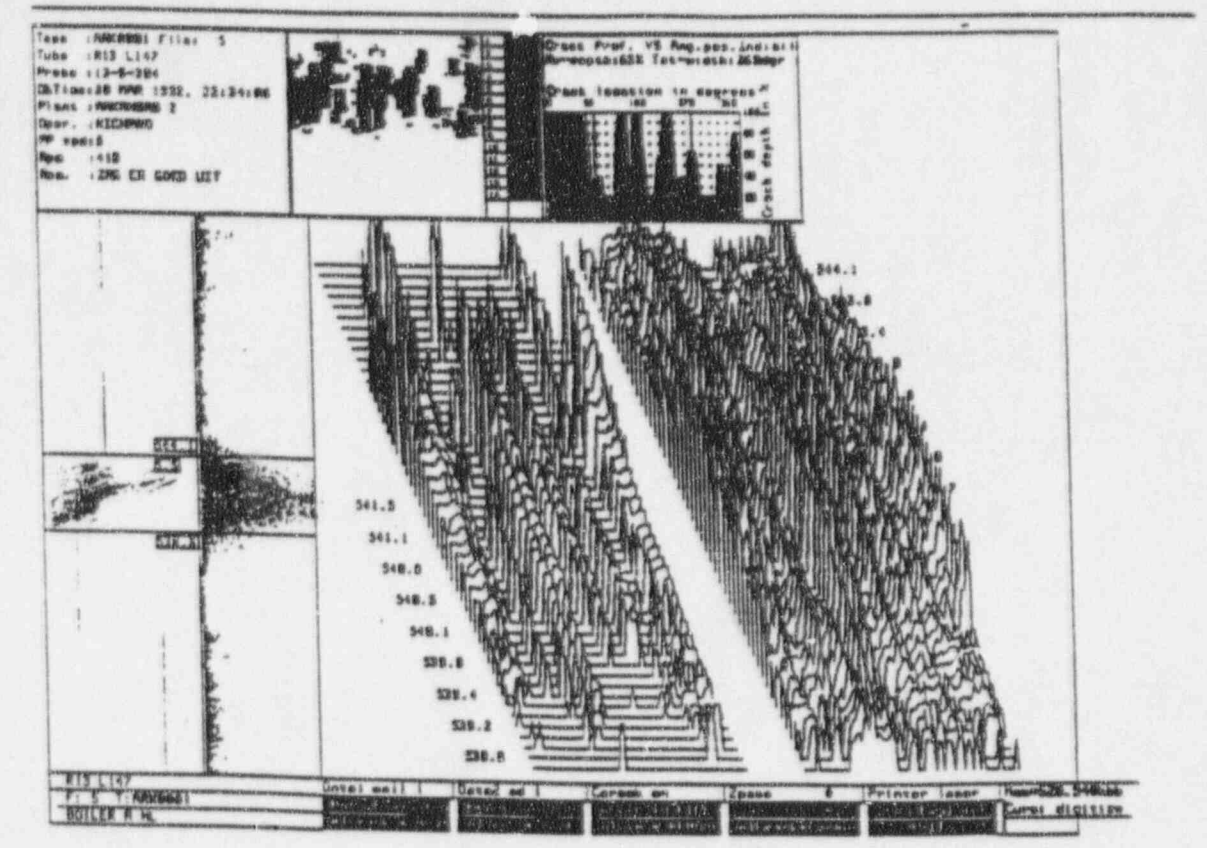

UT Plot

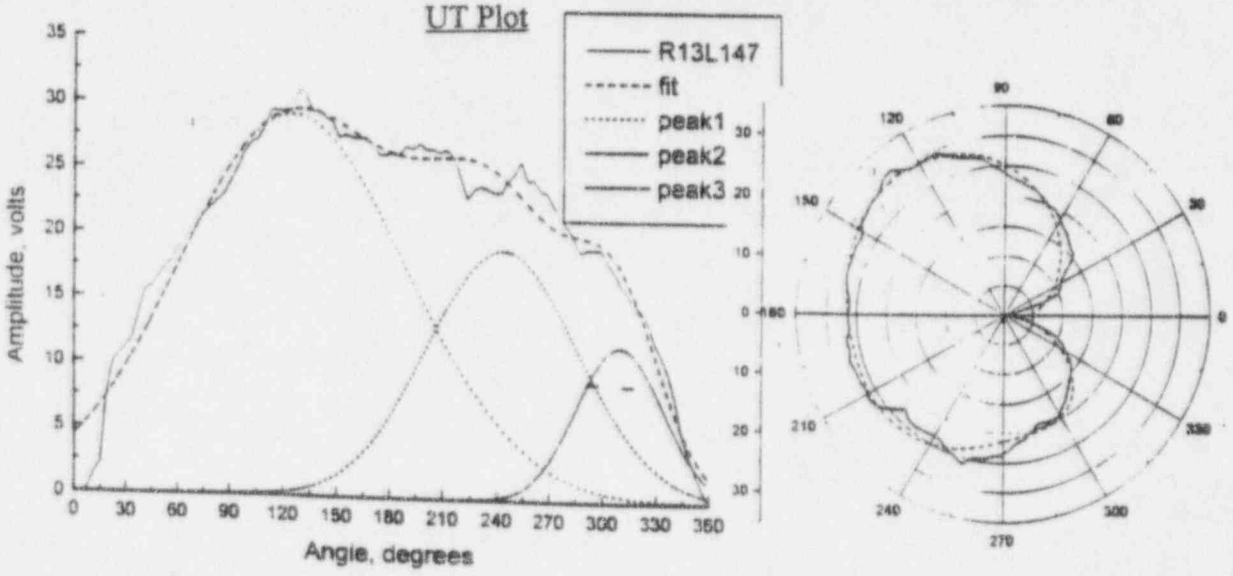

RPC Deconvolution Analysis

Figure 5.1-9
Comparison of UT to Deconvolution Analysis for Tube 13-147

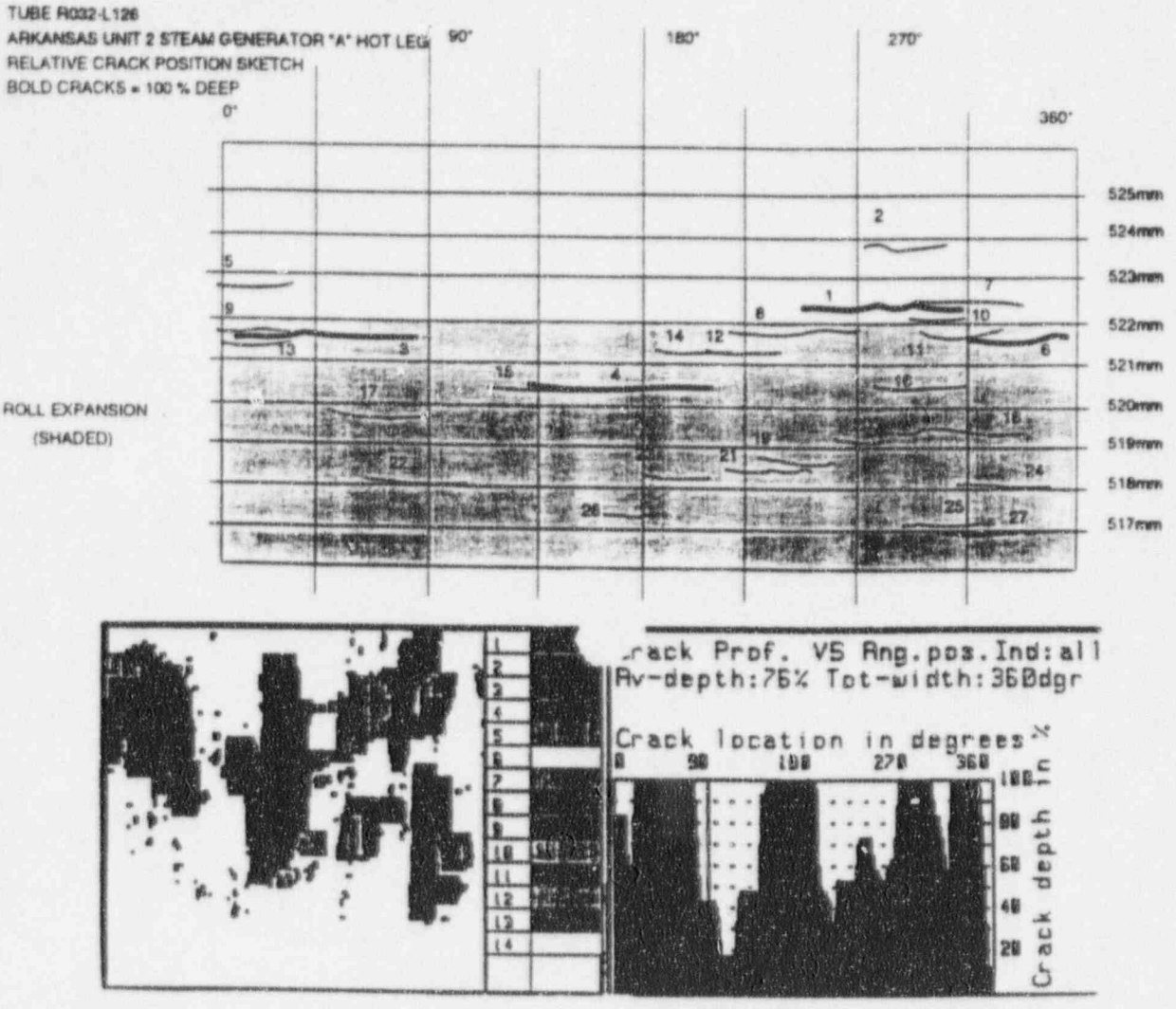

Figure 5.1-10
UT Plot (Largest Flaw in 2R10)

5.2 Statistical Analysis

In order to adequately assess the margin of safety provided by the steam generator tubes, it is necessary to be able to conservatively predict the probability of the existence of cracks that are of sufficient size to challenge the tube integrity during design basis events. This can be accomplished by statistically analyzing data from past inspection campaigns and industry data where applicable. Specifically, for ANO-2, this is accomplished by combining the most probable distribution of crack sizes and the expected number of cracks based upon plant operation time.

The use of statistical evaluations to support safe operation of ANO-2 was initially applied following the forced outage in the spring of 1992. Since this was the first inspection conducted at ANO-2 specifically to detect circumferential flaws at the ETR, the initial data base was limited. This data base was supplemented by using Millstone-2 (MP-2) plant data. MP-2 is a similar Combustion Engineering (CE) designed plant that had experienced circumferential cracking prior to ANO-2. MP-2 characterized the average %TW degradation as exhibiting the form of a gamma distribution (similar to Figure 5.2-1). The ANO-2 data demonstrated this same statistical distribution. Because of the limited plant specific data, ANO-2's data was combined with that of MP-2 to provide a reasonable assessment of the distribution of the flaws expected to be present at the end of the operating cycle (approximately four additional months of operation) to predict the probability of a flaw in the SGs which would exceed the RG 1.121 acceptance criteria. This analysis showed that ANO-2 was safe to operate the remainder of that cycle with a greater than 95% probability that no tube would have a flaw in excess of the acceptance criteria of RG 1.121.

This same basic statistical approach has been applied following each subsequent SG inspection. Entergy Operations has now performed five major inspections for circumferential cracks at ANO-2. Because of the expanded site specific data base, recent predictions have been based on ANO-2 specific data. As the data base increases, statistical confidence increases. Sections 5.2.1 and 5.2.2 describe this statistical approach. Section 6 combines this information with a plant specific failure mode analysis to assess core melt probabilities.

5.2.1 Crack Size Indication Distribution

This section provides a review of the circumferential crack data for ANO-2. Appendix A contains summary data tables of all cracks identified in the five inspections. Random variations in steam generator tube mechanical properties, local stresses, chemistry conditions, and individual crack growth rates result in variations in the circumferential length and depth of these cracks. The frequency of occurrence of specific crack lengths and depths can be characterized by statistical probability distributions. These distributions are not well characterized by the "standard" Gaussian probability distribution. This fact is consistent with the experience at other sites where SG circumferential cracking has occurred[12]. Standard non-Gaussian probability distributions can

be fit to the data which provide consistent and statistically valid models of the variability of circumferential crack length, maximum depth, and average depth.

A statistical procedure known as a goodness-of-fit test is commonly used to test whether a particular set of measurements can be concluded to be represented by a specified probability distribution. In these methods, a "null-hypothesis" specifies an assumed probability distribution function. Various methods can then be used to assess whether the empirical distribution is consistent with the hypothesized distribution. If the tests indicate that there is not good agreement, then the hypothesized distribution is abandoned in favor of an alternative[12].

Three candidate families of probability distributions were considered for representing the distribution: beta, gamma, and extreme value. The results indicate that the gamma probability distribution has the best goodness-of-fit for crack length and average depth. Figures 5.2-1 and 5.2-2 show the distribution of all flaws for average depth and arc length, respectively. Figures 5.2-3 and 5.2-4 show the distribution of flaws for the 2R10 outage for average depth and arc length, respectively. Figures 5.2-5 and 5.2-6 show the distribution of flaws for the 2P95-1 outage for average depth and arc length, respectively.

5.2.2 Projection of Number of Cracks

For most of the degradation mechanisms, it was assumed that the time dependence of the best estimate number of tubes requiring repair as the result of that degradation mechanism is described by a Weibull probability distribution. The Weibull distribution is perhaps the most widely used lifetime distribution model[13]. The basic Weibull distribution for failure times is:

$$F = 1 - \exp[-(t/\theta)^b]$$

where F is the fraction of the tube population that has failed at time t. Characteristic time (θ) and Weibull slope (b) are adjustable parameters of the Weibull distribution. These parameters are determined by fitting observed data for the plant being analyzed, or from analyzed industry experience for a given degradation mechanism[9].

Because the actual number of cracks found in 2R10 was significantly higher than predicted (170 found vs. 110 predicted), a more conservative approach using a 95% confidence level has been adopted. This work built upon the extensive work originally performed which used industry data and ANO-2 data up to 2R9[14]. Current efforts concentrate on the ANO-2 specific data and includes the results of all inspection campaigns to date. The observed data for all five ANO-2 inspections (for both the "A" and "B" SGs) is plotted in Figure 5.2-7. The best fit function to the last two inspection campaigns (2R10 and 2P95-1) conservatively results in θ and b values of 16.436 and 6.197 for the "A" SG and 14.228 and 15.539 for the "B" SG, respectively.

5.2.3 Statistical Projection of Degradation Expected at the End of Cycle 11

Utilizing the Weibull distribution derived above and applying it to the ~ nine months of operation remaining in Cycle 11, the number of anticipated circumferential cracks at the next refueling outage (2R11), which occurs at 11.6 EFPY, is anticipated to be 276 in the "A" SG and 200 in the "B" SG. Applying this projection to the gamma distribution derived from the data plotted in Figure 5.2-1 results in the conclusion, with a greater than 95% confidence level, that no flaw is anticipated to exist in either the "A" or "B" SGs at the end of Cycle 11 which would exceed the structural limits established by RG 1.121.

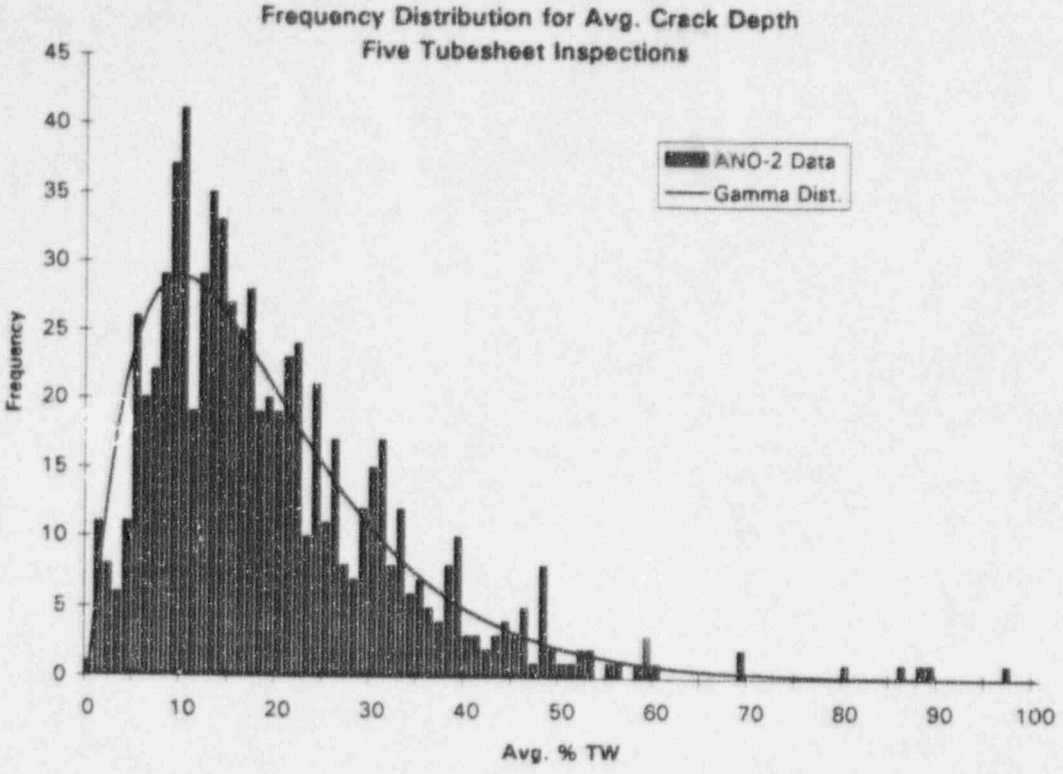

Figure 5.2-1

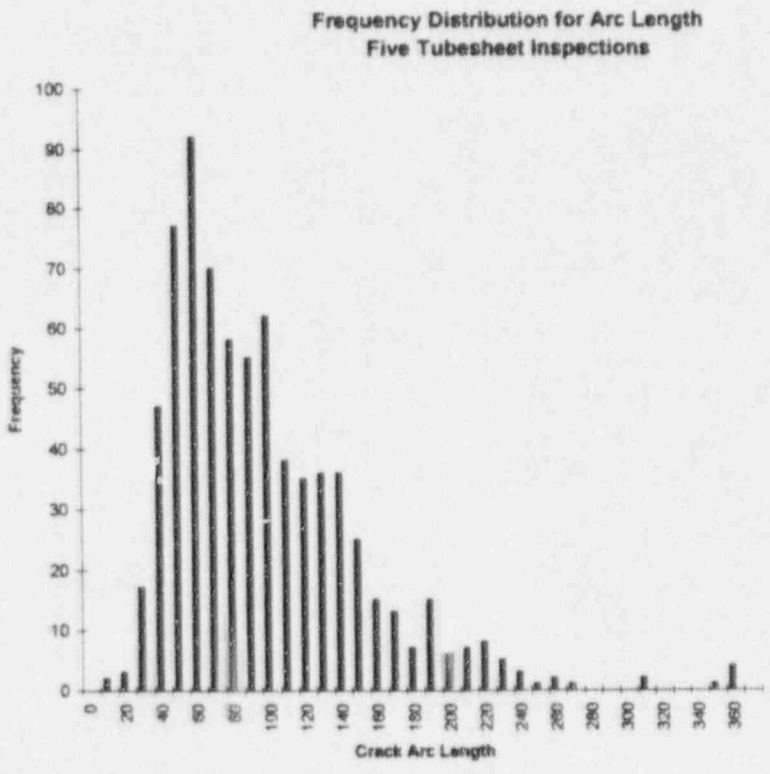

Figure 5.2-2

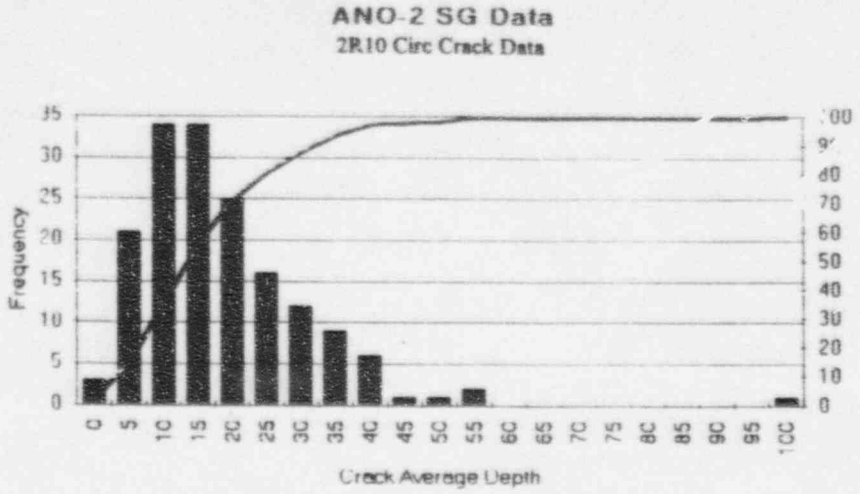

Figure 5.2-3

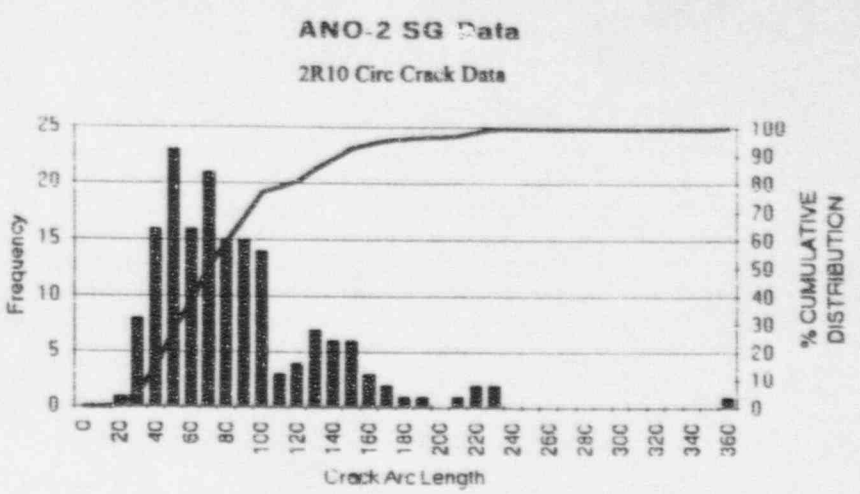

Figure 5.2-4

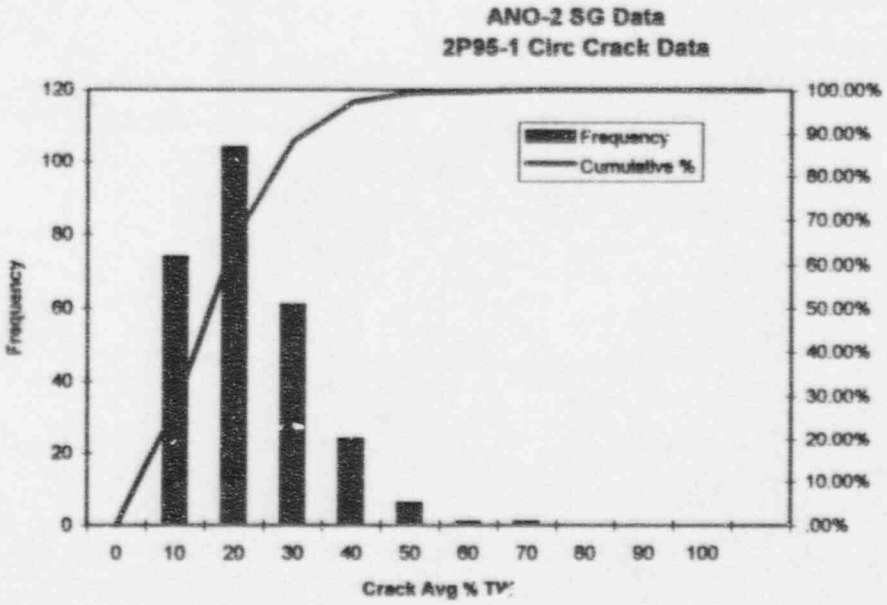

Figure 5.2-5

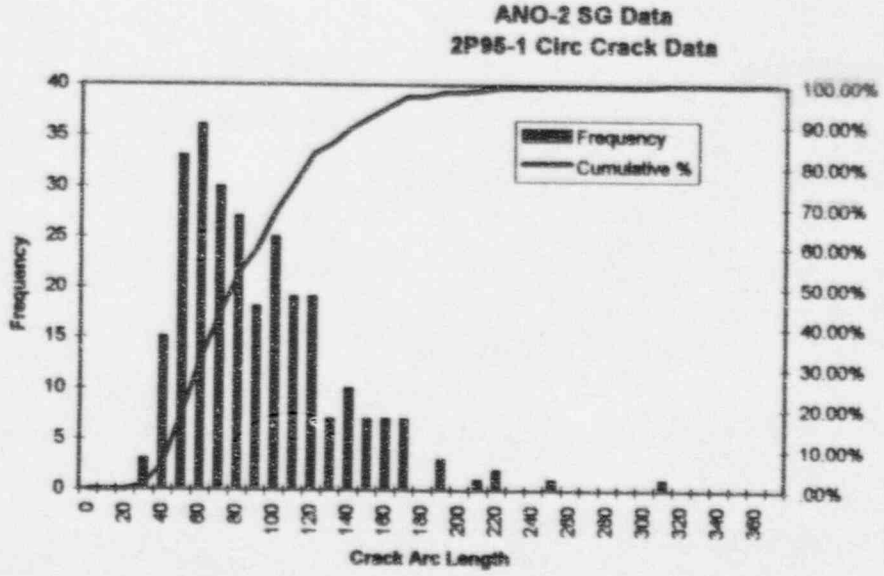

Figure 5.2-6

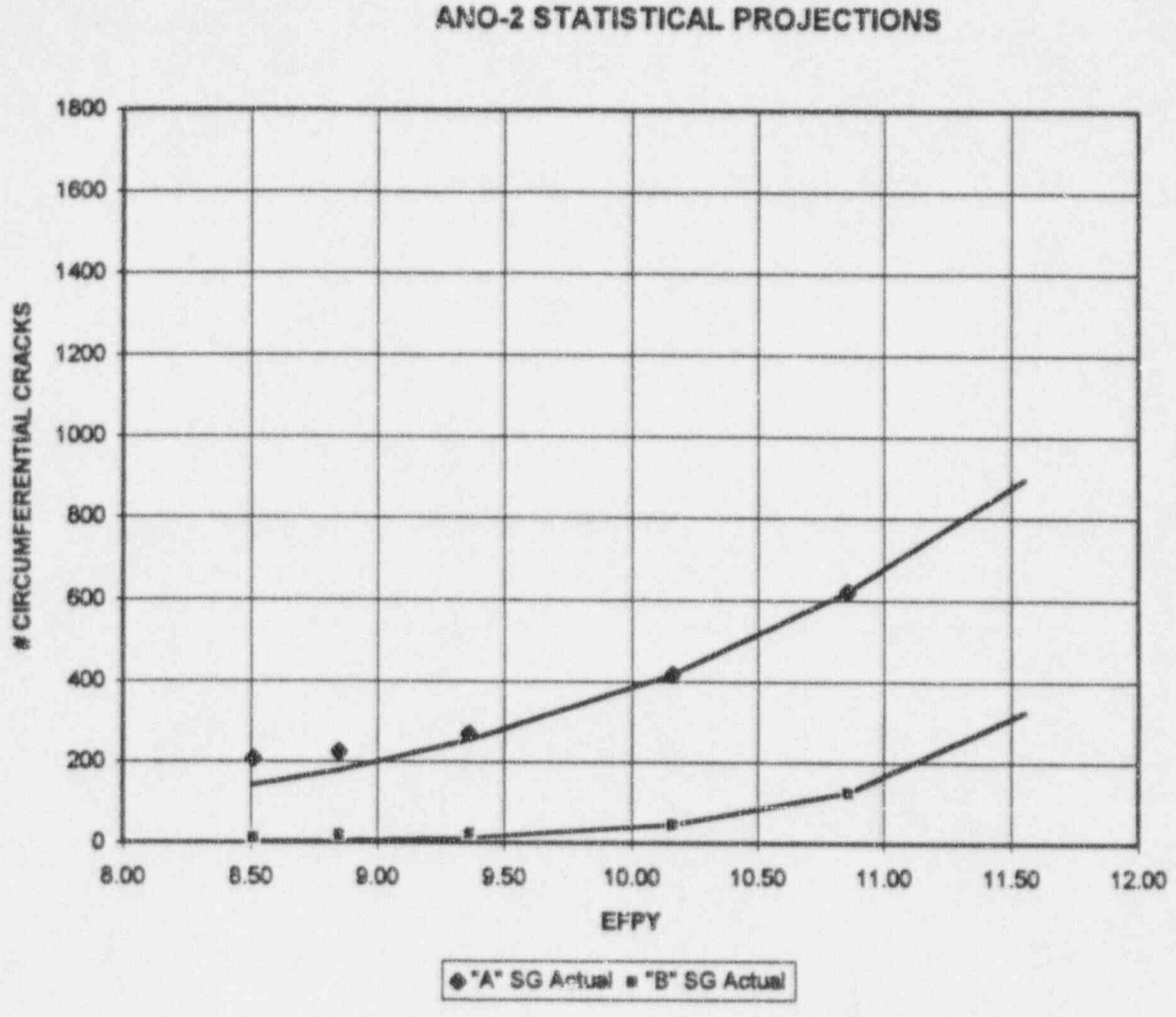
ANO-2 STATISTICAL PROJECTIONS
CIRCUMFERENTIAL CRACKS
1800
1600
1400
1200
1000
800
600
400
200
0
8.00
8.50
9.00
9.50
10.00
10.50
11.00
11.50
12.00
EFPY
"A" SG Actual
"B" SG Actual

Figure 5.2-7

5.3 Structural Analysis

5.3.1 Regulatory Guide 1.121 Evaluation

A. Summary

The following is a brief summary of the requirements contained in RG 1.121 relating to the analysis and testing to determine the necessary margins against steam generator tube rupture:

1) Normal Operation

Tubes with throughwall or part throughwall cracks should have a margin of at least three to burst, determined analytically either by tests or by refined finite element or fracture mechanics techniques. The material stress/strain characteristics at temperature, fracture toughness, stress intensity factors, and material flow properties should be considered in making this determination. The American Society of Mechanical Engineers (ASME) Section III code requirements must also be met. For ANO-2, $3\Delta P$ is 4050 psi.

2) Accident Conditions

The margin of safety against failure under accident conditions, concurrent with safe shutdown earthquake (SSE), should be consistent with NB-3225 of Section III, and be accommodated by the ultimate tube burst strength determined experimentally at the operating temperature.

NB-3225 suggests use of Appendix F, "Rules for Evaluation of Faulted Conditions":

Appendix F allows the use of any of the following methods:

a) Elastic analysis
b) Stress ratio
c) Collapse load determination
d) Plastic instability load or stress determination
e) Strain limit loss or stress determination
f) Inelastic analysis

B. Approach Options for RG Analysis

A number of different analytical and test methods may be used to determine allowable tube degradation per the above RG requirements. Accordingly, some variation can be expected in the final answer, depending on the methodology chosen. These variations are typically small, and are

accommodated, with margin, by the requirements of RG 1.121, e.g., by the safety factor of three required for normal operating pressure.

Among the factors which can influence the outcome of the results are the following:

1) Analysis methods:

a) The type of defect analyzed (e.g., the direction of controlling stress can be different for a circumferential defect than for an axial defect, depending on the size of the defect: testing has shown that circumferential defects up to about 58% throughwall, 360 degree extent, or 100% throughwall for 90 degrees will fail with axial splitting due to circumferential stresses, at pressures equivalent to a virgin tube)[15]. Also, an OD circumferential defect will have a higher allowable percent throughwall penetration than an ID defect, due to the difference in remaining cross sectional area, and the additional load imposed on an ID defect.

b) The type of analysis technique chosen (e.g., Appendix F alternatives).

c) The method chosen to accommodate variations of material properties (lot variations) which occur in the steam generator tubing.

d) The method of determining flow stress (burst strength).

e) The method of adjusting material properties from room temperature to operating temperatures.

2) Use of Burst Test Results

a) The method of accommodating variations in test specimen material properties.

b) The method of accommodating variations in tubing wall thickness and diameter (e.g., ANO-2 tubing is 0.048" wall, 3/4" OD tubing and Westinghouse tubing [largest data base] is 0.043").

c) Burst test configuration: for circumferential cracks at the face of the tubesheet, testing has shown that use of a simulated tube support structure above the defect will essentially eliminate bending loads[15]. Testing with

bending support, as would be provided within the steam generator, will significantly increase tube rupture pressure, compared to an unsupported test specimen.

C. Original ANO-2 Analysis

The original ANO-2 RG evaluation[16] is based upon analysis performed by CE and independently reviewed by MPR Associates. This evaluation utilizes the following methodologies for analyzing circumferential cracks:

1) Normal Operation

An evaluation of burst strength for circumferential cracks was done based on burst test data from PNL-2684, "Steam Generator Tube Integrity Program," Annual Progress Report, January 1 - December 31, 1977. CE evaluated the results of a 0.875" diameter tube with a 77% throughwall circumferential crack that burst at 5100 psi (> three times normal operating ΔP). The ratio of wall thickness to diameter was compared to ANO-2 tubing and it was determined that the test was bounding; and accordingly, the allowable defect penetration was greater than 77% for ANO-2. MPR performed a more specific analysis, in which the flow stress was calculated for the burst tube, then corrections were calculated to account for the variations in wall thickness and diameter, with minimum ANO-2 material properties assumed. It was also conservatively assumed that the cracks initiated from the ID. The equivalent flow stress for ANO-2 tubing was then limited to 1/3 (i.e., to attain the margin of three to burst), and the minimum wall thickness was calculated which corresponds to this stress. This stress corresponds to a remaining wall thickness of 21%, or an allowable defect depth of 79% throughwall.

2) Accident Conditions

The 77% penetration was analyzed in accordance with ASME Section III, Appendix F, by the elastic analysis method for components, to confirm that the resultant stresses for accident conditions were less than the allowable; i.e., stresses were less than 2.4 S_m and less than 0.7 S_u. (Note: the factor of 0.7 also has been used by others to indirectly define a requirement for a 1.4 margin for accidents (1/0.7 = 1.43) but this value is not specified within the RG, as is the factor of three for normal operation). The calculated stress levels were well below the allowable, such that the 79% value for normal operation also covered accident conditions. Note: the RG states that the margin should also be accommodated by the ultimate tube burst strength determined experimentally at the operating temperature). However, using the Code values for S_m and S_u conservatively bounds this consideration. Although these Code values do not vary with temperature for Alloy

600 material, they are lower than the actual burst stress values at operating temperatures[15].

D. Subsequent ANO-2 Analysis

Additional analysis has been utilized to confirm the validity of the original ANO-2 approach[15].

1) Analysis Techniques

a) A statistical analysis was performed of actual ANO-2 tube properties (certified material test reports) to establish the proper input for analysis, providing a 95/95 confidence level. Results showed that the properties used in the original analysis were conservative.

ANO-2 lower bound material properties (room temperature):

Category	Ultimate Strength	Yield Strength
SG "A"	91.92	39.83
SG "B"	91.68	39.95
avg.	91.8	39.9

b) An evaluation of Alloy 600 flow stress was performed to refine the necessary analysis input. This evaluation considered all burst testing whose configurations simulate the correct ANO-2 configuration. It was done prior to the secondary screening discussed in 2) below such that it includes a significant number of known low (Westinghouse) data. This evaluation determined that the best correlation of burst stress to material properties at room temperature (rt) is:

$$\text{Flow Stress}_{rt} = 0.507\ (\text{Ultimate}_{rt} + \text{Yield}_{rt})$$

c) An evaluation of material property corrections from room temperature to operating temperature (ot) was performed. This evaluation determined that:

$$\text{Ultimate}_{ot} = .97\text{Ultimate}_{rt}$$
$$\text{Yield}_{ot} = .87\text{Yield}_{rt}$$

Note that yield strength (Y) is more dependent on temperature than is ultimate (U). Others (e.g., Maine Yankee) have used the correction of yield strength to adjust

flow stress (FS); however, burst is controlled more by ultimate strength. The correction discussed below more closely approximates the actual effects of temperature on burst.

d) These corrections are applied together, such that burst strength is adjusted for effects on both yield and ultimate strengths, as follows:

$$FS_{ot} = 0.507(.97U_{rt} + .87Y_{rt})$$

Note: Based on actual burst test results (see 2 below), this approach is additionally conservative, as expected, due to the inclusion of a large number of known low data. Using this approach, the corrected failure stress for analysis, including the lower bound 95/95 ANO-2 material properties, and compensating for operating temperature is:

$$FS_{ot} = 0.507\ (.97(91.8) + .87(39.9)) = 62{,}745\ \text{psi}$$

Using this failure stress to calculate allowable wall penetration (avg. 360 degree OD crack) yields 77%

For comparison, flow stress from the original ANO-2 RG 1.121 analysis was assumed to be 0.85(best estimate Ultimate) = 0.85(90,000) = 76,500. Using this failure stress yields an allowable (360 degree ID crack) of 79%.

2) Tube Burst Test Data

a) Industry burst data was reviewed and screened to eliminate non-representative data. Applicable test results are shown on Figure 5.3-1. The largest set of non-representative data was determined to be the Westinghouse data for MP-2. This data was eliminated based on Reference 17 where it was determined that a conservative methodology for determining remaining wall thickness after electrical discharge machining (EDM) resulted in low apparent burst pressures. The remaining burst test results were then normalized to account for lower bound ANO-2 properties and corrected for operating temperature. Also included in Figure 5.3-1 is the ANO-2 pulled tube which was burst tested (after correction for bending stresses). A tube from the ANO-2 lab crack program that had sufficient cracking to fall within the area of interest is also included in the CE data shown on the figure.

5.3.2 Finite Element Model

To augment the analytical RG evaluation, an approach to evaluate the response of certain flaws utilizing finite element techniques was developed.

Two types of models were developed:

1) 2-D axisymmetric model for analysis of 360° circumferential crack

2) 3-D models for analysis of specific flaws (e.g., Tube 32-126 containing the largest 2R10 flaw)

The failure criteria used assumed failure when the average effective stress across a given section is equal to the flow stress at temperature. The effective stress from the non-linear analysis is similar to von Mises stresses of a linear analysis.

A. 2-D Axisymmetric Model

2-D axisymmetric finite element models (FEMs) are appropriate for modeling 360° circumferential cracks. The following crack sizes (average %TW) were considered in this analysis: 1) 74%, 2) 79%, and 3) 82%.

The results were as follows:

Ave. %TW	Burst Pressure for $\sigma_{eff\ avg}$
74	5330
79	4740
82	4090

B. 3-D Finite Element Analysis

3-D finite element analysis (FEA) is appropriate for modeling a tube with flaws that are not symmetric. Tube 32-126 is considered in this analysis. Two 3-D models were developed for this tube: 1) a model consisting of first order elements, and 2) a model consisting of second order elements.

1) First Order 3-D FEA for Tube 32-126

In this case, four cracks were modeled on three planes. The stress contours for a pressure of 3ΔP (4050 psi) demonstrate the tube would not be expected to burst at 3ΔP since $\sigma_{eff} < \sigma_o$. However, a more

accurate solution (and higher stresses) will be realized with the model consisting of second order elements.

2) Second Order FEA for Tube 32-126

The model consisting of second order elements is being run in steps at the time of this writing. A more accurate prediction of the burst pressure can be made when these results are available.

C Conclusion

The finite element model is an additional technique used to assess the structural significance of flaws. The results of the FEM work demonstrate that the original limit of 79% is realistically conservative for the ANO-2 circumferential cracks, and will be maintained as the appropriate RG limit. Based on the UT data and RPC deconvolution analysis evaluation results, all flaws from the ANO-2 steam generators have met the RG 1.121 margin requirements. This is based on the largest flaw being 76% average depth (UT Average %TW). UT has been successfully utilized by others to evaluate the presence of ligaments for the purpose of performing structural evaluations[18].

5.3.3 In-Situ Pressure Testing

A. Purpose

Per the requirements of RG 1.121, the effects of defects on steam generator tube burst strength must be determined and found to be within the margins defined in the RG. Both analysis technique and NDE inaccuracies must be accommodated in assessing actual defects against the allowable defect size. Traditionally, to demonstrate this, defective tubes have been pulled from steam generators and burst testing is then performed in the laboratory. However, the removal of tubes for testing has the following drawbacks: 1) the radiation dose during the tube pulls, and the subsequent handling of the pulled tube during shipping, handling, and testing, 2) the costs associated with the extraction and handling, 3) the inaccuracy of burst test results due to damage that occurs to the tube during the pulling process, 4) the potential problems which can occur associated with aborted tube pulls (e.g., if a tube breaks or becomes stuck during the pull, the potential for loose parts or vibration induced wear of adjacent tubes is significantly increased), and 5) tube lateral support is often missing or is roughly simulated in lab tests. In order to eliminate these problems, an in-situ pressure test device has been developed to allow testing of a defective tube within the steam generator without the need to pull the tube, thereby avoiding the above drawbacks. The process discussed below is being used for this purpose at ANO-2. This discussion is limited to the use of the CE supplied in-situ testing device which is used for testing of ANO-2 steam generator tubes with circumferential defects at the secondary face of the tube sheet. However, similar evaluations can be used to justify this method for other types of defects.

B. Tube Loading

For the deep penetration circumferential defects of interest, the main loading which is significant for burst testing is the axial load imposed by the tube internal/external pressure differential times the tube cross sectional (nondefective ID) area[16]. Accordingly, the in-situ pressure test device must transmit this axial load across the defected region for the test to be valid. This is accomplished by the CE tool, which has a slip joint design between the two sealing bladders as shown in Figure 5.3-2. This design allows each end of the device to move independently of the other when the chamber between the bladders is pressurized, such that the pressure load is transmitted to the tube in a manner equivalent to a full tube hydro. This is also equivalent to the ΔP loading for a laboratory burst test, where each end of the tube is capped. This equivalency was demonstrated by CE in a comparison test, where strain gauges were installed in a tube that was hydro tested in a manner equivalent to the lab type burst test, and then compared to strain gauge results using the in-situ device. The test showed essentially identical results for axial loads in each configuration[19]. This is shown in Figure 5.3-3. Accordingly, the in-situ device can impose the proper loading on the tube.

C. Evaluation of Potential Effects of Locked Support Plates

Experience with various tube support plate designs has shown that a non-protective magnetite formation in the crevice between the tube and plate can grow to the extent that the tube can be deformed (called denting). The conversion of iron to magnetite is accomplished by a two-fold volume increase. This increased volume squeezes the tube resulting in tube dents (relatively uniform contraction of the diameter) at support plates and ovalization of tubes at eggcrate supports. The presence of these corrosion products can potentially lock the tubes into the support. Because of the open nature of the eggcrate support, the locking forces are confined to the four line contact crevices. Thus, tubes will be less severely locked into eggcrate supports than drilled supports, but if significant denting has occurred, significant loads may be required to remove tubes from the eggcrate. In one model boiler test where corrosion was so extensive that the eggcrate had begun to breakup, a hydraulic jack was required to pull tubes from the eggcrate[20]. Locked supports can cause several negative effects. The potential effects on in-situ pressure testing will be discussed here.

If a tube is locked in the supports, then the full axial load imposed by the in-situ test device may not be carried by the defective tube. The non-protective magnetite that produces denting (and locked tubes) develops only at operating temperatures. Because of the greater coefficient of thermal expansion for Alloy 600, when cooled, the tubes will shrink more than the carbon steel parts of the generator (shroud, etc.) which would result in a tensile load during shutdown. However, the eggcrates and the partial drilled support plates are flexible in the axial direction. A recent CE analysis indicates that with wide scale tube lockup the axial stress for most tubes is near zero[20]. The exception to this is the normal hard spots adjacent to tie-rods and the lugs where the eggcrates are attached to the shroud; axial stresses at these locations may be 2000 psi during shutdown.

For those tubes with near zero shutdown load, the axial load imposed by the pressure test would be reduced by the resistance provided by a locked support; i.e., the adjacent tubes which would not be pressurized would carry some of the in-situ test load that would not be carried if all the tubes were pressurized. While this effect is thought to be small, its significance is additionally mitigated by the lack of any indication of locked tube supports at ANO-2, as discussed further below.

For ANO-2, the maximum loading would result from main steam line break (MSLB). During this accident, a concern exists that if a significant number of excessively defective and locked tubes were loaded the TSP could fail, resulting in multiple tube failures, perhaps with the failed support causing even more failures than those which had been excessively defective. A part of this concern is that an in-situ pressure test might pass an excessively defected and

locked individual tube, leading to an incorrect conclusion regarding the expected behavior of the steam generator during an accident loading, when all the tubes would see the maximum loading. This potential condition has been evaluated, and it has been determined that it is not a factor which affects the intended function of performing the in-situ pressure test at ANO-2. This is based on the following: 1) the determination that ANO-2 tubes are not likely locked in their supports, and 2) the limited number of excessively defected tubes which would affect the supports, as discussed below.

D. Assessment of Potential for ANO-2 Locked Supports

For the evaluation of chemical cleaning of the ANO-2 steam generators, CE performed an assessment of the effects of cleaning on tube supports, considering existing corrosion[21]. This evaluation concluded that corrosion of the ANO-2 eggcrates was not significant (based primarily on limited denting, as confirmed by NDE). Significant denting has not been detected at ANO-2 (very small dents have been observed in less than ten tubes out of 16,822) in the lower eggcrates. This indicates that it is unlikely that the tubes are locked within the lower supports, where denting could affect the in-situ results. Although the drilled upper partial supports at ANO-2 are dented, these supports encompass only the outer periphery of the steam generator and are outside the region of the majority of the detected circumferential cracks. Also, the drilled plates are well above the in-situ tested defects of interest at the tubesheet.

In addition, two tubes (19-55 and 96-166) from the "B" steam generator were pulled through the 1st and 2nd eggcrates. The absence of locking is further evidenced by the results of these tube pulls:

1) Examination of the tubes in the area of the eggcrate supports shows no evidence of locking: the tubes are not dented, and crevice corrosion indications are limited to a small region at the lines of contact with the eggcrates.

2) The pull forces required to remove these tubes were not significantly different from those pulled from below the eggcrates, suggesting that no locking had occurred[22]. However, the forces required to pull all the tubes was quite high, indicating the tubes were locked in the tubesheet, which may have masked any effects from the eggcrates.

E. Assessment of Effects of Locked Supports

In the unlikely event a few tubes could be locked, the possible effects were considered. As discussed elsewhere in this report, the number of large circumferential defects which could occur between inspections is very small. Also note that the in-situ pressure test loads the tube well above the actual

loads that would be imposed during an accident. Accordingly, if the small number of tubes which are excessively degraded also happen to be locked in place, the load transfer to the adjacent tubes during the in-situ testing is not likely to occur, since clustering of locked tubes is not expected. Therefore, the results of the in-situ pressure test will be conservatively indicative of the tube's actual behavior during an accident condition.

F. Test Pressure Correction

The in-situ pressure test should be run such that the RG requirements are demonstrated for normal operation, and for accident (faulted) conditions.

1) Normal Operation

For normal operation, the required pressure is three times normal operating pressure differential. Normal operating pressure is 2250 - 900 = 1350 psi, and the required pressure is 3(1350) = 4050 psi. This pressure must be corrected for 1) temperature effects, and 2) instrument error.

a) Temperature Effects

Material strength is somewhat reduced at operating temperature. Thus, the in-situ test run at room temperature must be increased to account for this effect. From Reference 15, this correction is 6.5%, or (4050)(1.065) = 4314 psi.

b) Instrument Error

This correction depends on the particular pressure gauge used for the test and should be reviewed at each application. For the 2R10 use, the correction was ½% of span (5000 psi), or an additional 25 psi[15].

Based on the above, the required test pressure for three times normal operating pressure is 4339 psi. During 2R9 and 2R10, 4700 psi was selected as a target pressure for the test. This value is high and was chosen to ensure the temperature and instrument corrections were adequate.

2) Accident Conditions

The maximum accident loading occurs during a MSLB, where the differential pressure is 2500 psi[16]. There is no dynamic amplification of the tube loads involved since the pressure change rate inside the steam generator is not sufficiently rapid. In essence, the saturated temperature water on the secondary side acts similar to that in a

pressurizer and retards the rate of pressure reduction during a MSLB accident. The RG requirements for accident conditions impose ASME Section III, NB-3225, which in turn refers to Appendix F, "Rules for Evaluation of Faulted Conditions." Appendix F offers several analysis options for the evaluation. For the method normally chosen for tubing (elastic component analysis), Appendix F imposes a design limit of the lesser of $2.4S_m$ or $0.7S_u$. Neither of these limits varies with temperature for Alloy 600 material. Accordingly, a temperature correction is not required for this limit. From Reference 15, the required pressure is 3500 psi.

a) Instrument Error

This pressure should be corrected for instrument error as discussed under the "Normal Operation" section above. Accordingly, the required test pressure for accident loads is 3525 psi.

G. Conclusion

The in-situ pressure test is an acceptable means of demonstrating structural integrity of defective tubes in accordance with the requirements of RG 1.121. When considering the advantages of the in-situ test over a tube pull as discussed above, the in-situ test becomes the preferred method. The test should be performed at the pressures indicated above.

H. Experience

In-situ pressure testing was first conducted in the industry by Westinghouse at the San Onofre Nuclear Generating Station in the early 1980s. The second known use was by ABB-CE at ANO-2 during the ninth refueling outage, where the entire tube was pressurized following plugging at both ends. That tube held a pressure of 4700 psi for ten minutes with no leakage. During 2R10, three tubes were selected for testing. The pressure test device had been redesigned prior to the outage to allow for more tubes to be tested in a shorter time frame. The new device utilizes two expandable bladders approximately 3.5" apart, and allows the chamber between the bladders to be pressurized up to 5000 psi.

Three tubes were selected for testing in 2R10 based on their defect size and physical location in the SG to allow testing from one fixture location due to ALARA considerations. The results of all ANO-2 in-situ pressure testing are summarized at the end of this section.

The in-situ pressure test system utilized a small capacity positive displacement pump which could maintain a leak rate of up to 0.6 GPM at 4700 psi (0.94 GPM at 0 psi.). Tube 32-126 leaked in excess of the makeup capacity of the

system when tested, but did not burst as evidenced by the tube holding 2000 psi for measurement of a leak rate.

The leakage values shown below have not been corrected for operating temperature, but operating temperature values are estimated to be approximately 25% of the room temperature rates. The leakage for Tubes 24-132 and 32-126 is considered high due to the tube swelling during the pressurization to the higher value causing the crack to open slightly. Laboratory experience indicates this does not represent a decrease in the burst strength of the tube. The applied pressure differential leads to plastic deformation of the crack face such that any subsequent leak tests exceeded the expected leakage at the lower pressure differentials[9].

Based on their peak pressure, Tubes 64-48, 24-132 and 48-50 met the requirement of 3ΔP. Tube 32-126 was unable to be pressurized to the 3ΔP pressure due to leakage, but did exceed the 1.4 times MSLB pressure of 3500 psi. Based on the UT results, coupled with finite element modeling and the in-situ pressure test results where applicable, all ANO-2 circumferential cracks tested met the RG 1.121 structural margin requirements.

During outage 2P95-1, three tubes were in-situ pressure tested using an improved tool. The new tool had the capability to perform pressure testing of tubes experiencing leakage in excess of makeup pump capacity by utilizing a bladder over the crack area (as is done in laboratory pressure test). All three of the tubes tested in 2P95-1 held the maximum pressure with no leakage, and thus the use of the bladder to seal the crack was not required.

Table 5.3-1

In-Situ Pressure Test Results

Outage	Tube	RPC Avg %TW	Max. Pressure	Leakage
2R9	64-48	58	~4700 psi	0
2R10	24-132	51	~4600 psi	0.05 GPM @ 2000 psi
2R10	32-126	97	~3600 psi	0.15 GPM @ 2000 psi
2R10	48-50	48	~4700 psi	0.04 GPM @ 4700 psi
2P95-1	23-135	69	~4550 psi	0
2P95-1	77-97	34	~4550 psi	0
2P95-1	24-134	39	~4550 psi	0

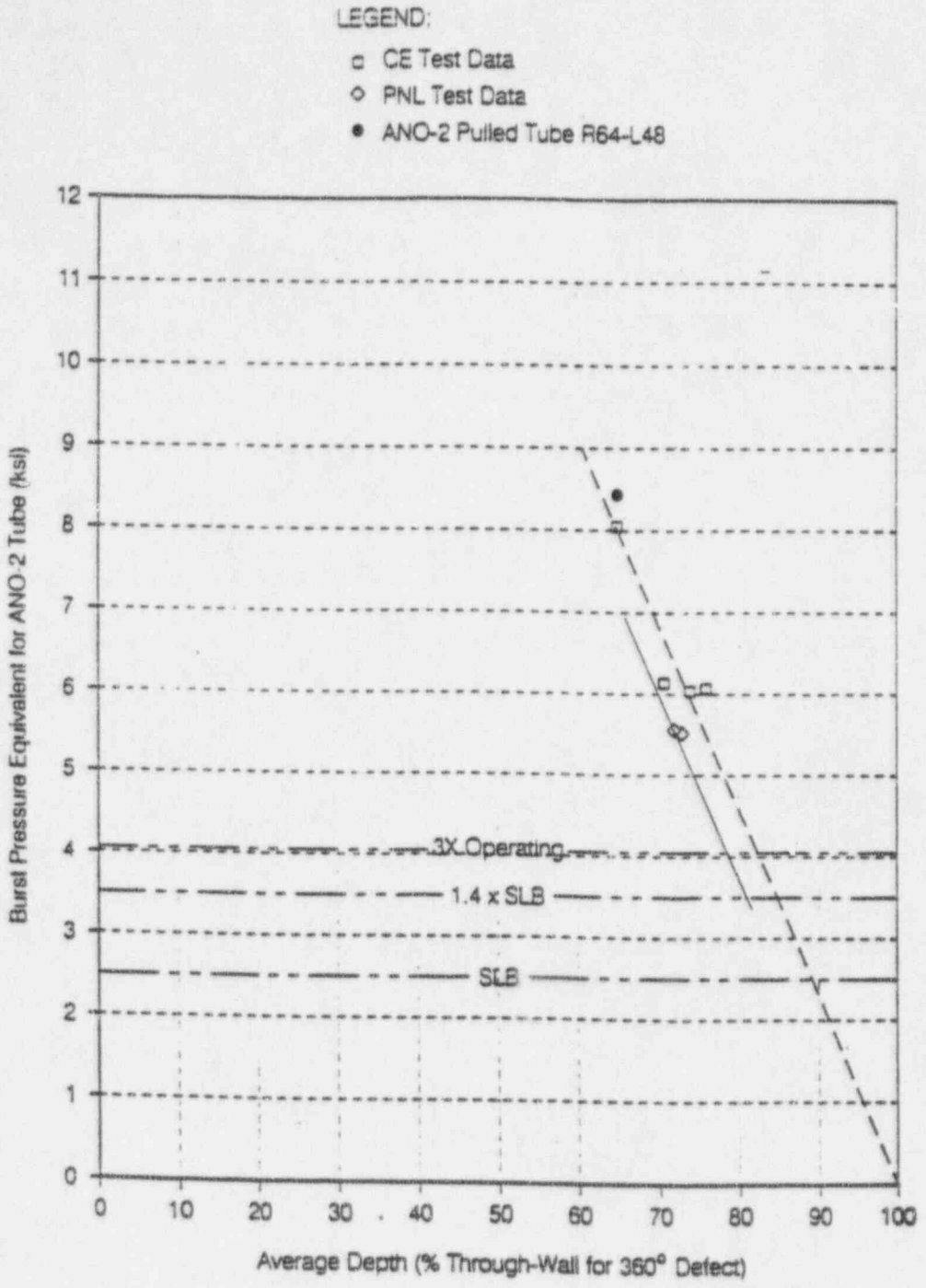

Figure 5.3-1
Comparison of Burst Tests to RG Limits

This figure indicates a RG limit of 82% for best fit, or a lower bound limit of 79%.

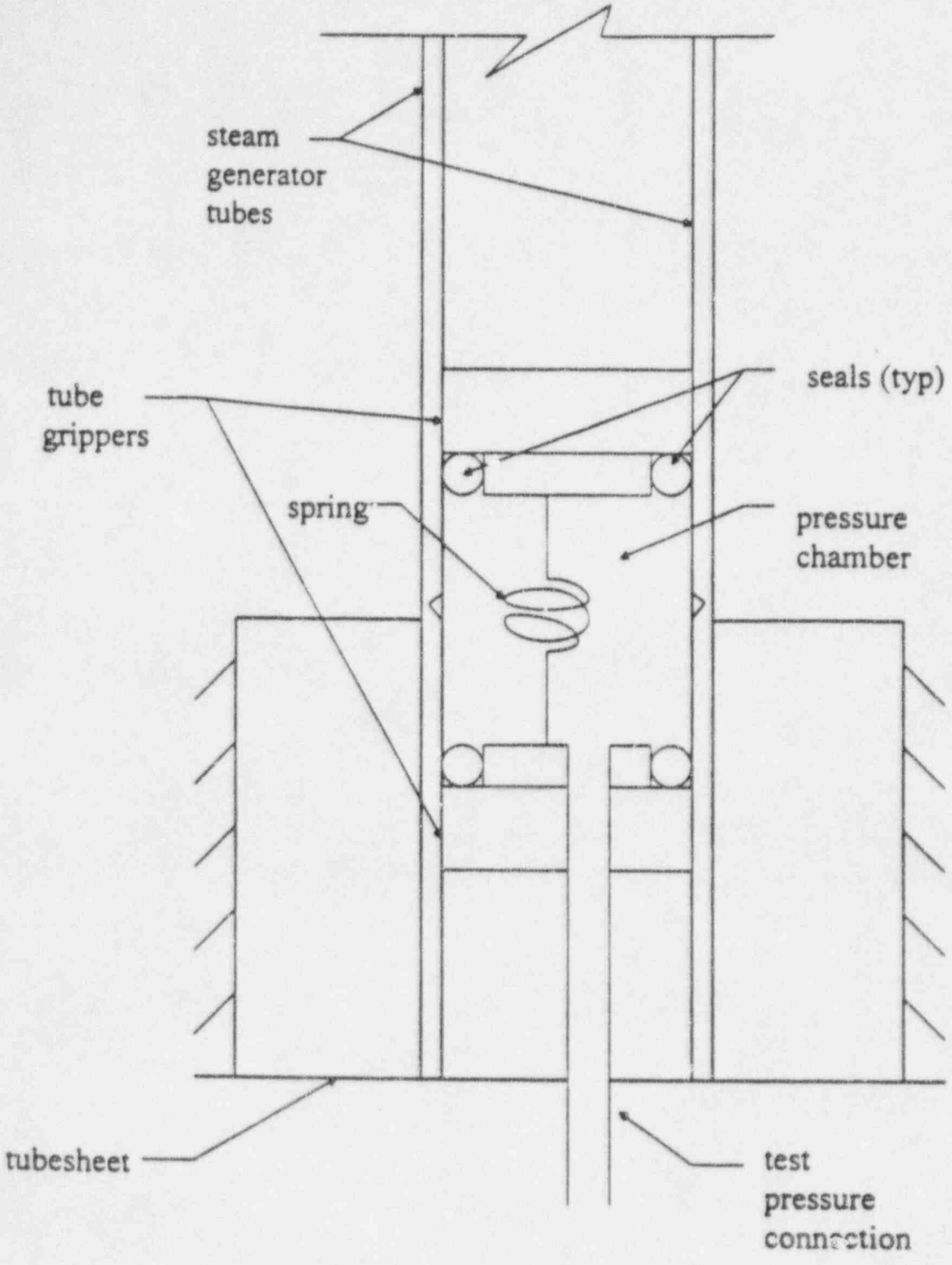

Figure 5.3-2
Schematic Drawing of CE In-Situ Pressure Test Device

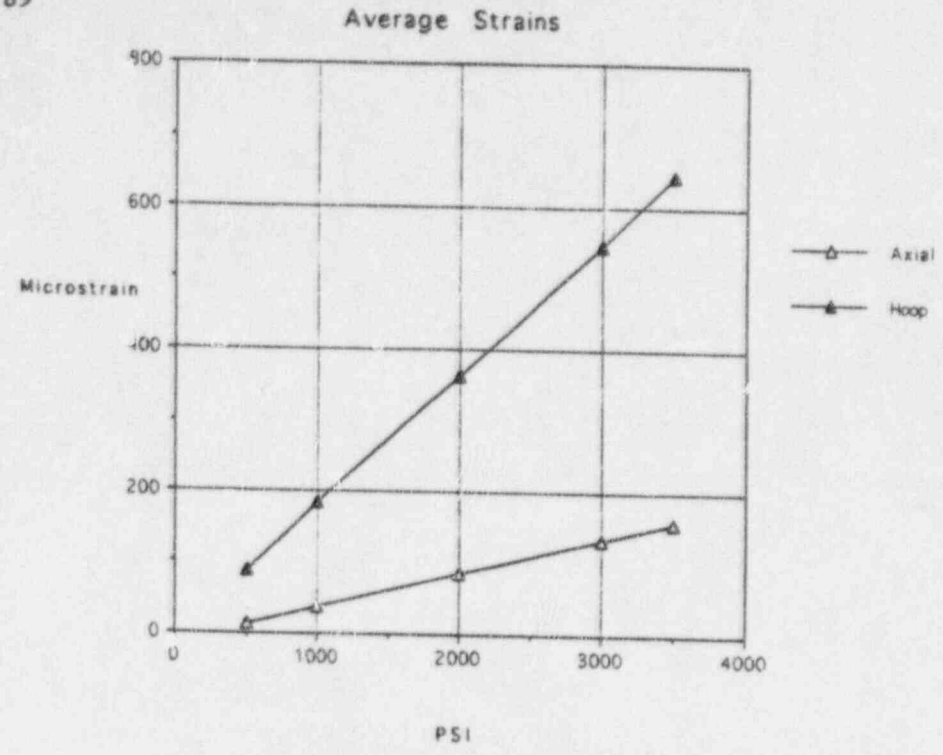

Capped Tube hydrostatic Test Strain Results

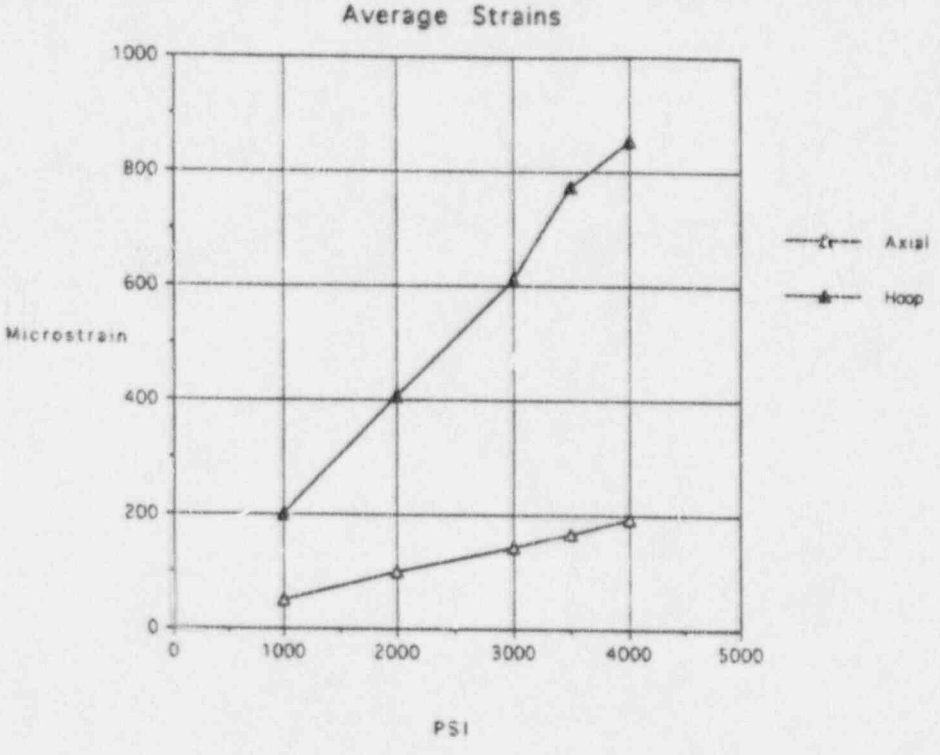

In-Situ Pressure Test Tool Strain Results

Figure 5.3-3

5.4 Leak Rate Analysis

Leak rates for individual cracks were calculated using a basic calculational technique which is presented in Reference 6 and deals with leak rates through axial cracks caused by primary water stress corrosion cracking (PWSCC) in expansion transitions. The leak rate, expressed in gallons per minute at the primary fluid temperature, is proportional to the crack opening area, a flow discharge coefficient and the square root of the "effective differential pressure."

Crack opening areas for circumferential cracks were calculated and then benchmarked versus test measurements on a tube with a 200° (total) throughwall crack. The presence of structures in the steam generator which limit the lateral displacement of tubes was considered.

The flow discharge coefficient is a function of the total crack opening. The semi-empirical equation of Reference 6 was used. The total opening is composed of the initial crack opening under no load and the opening under a differential pressure. A tight PWSCC crack was assumed. Cracks produced in the laboratory may have substantial initial openings and this has to be considered in the comparison of measured and calculational leak rates.

While the crack opening is a function of the primary to secondary pressure differential, the "effective differential pressure" driving the leak rate is a hydraulic parameter. If the primary fluid flashes to vapor, a back pressure opposing the flow will be created. If heat transfer/friction is minimal during the flow process, the "effective differential pressure" will be essentially the primary pressure minus the saturation pressure at the primary temperature.

This is the condition assumed in calculating leak rates under steam line break conditions. If flow is not isentropic, then the "effective differential pressure" will be somewhat higher than that assumed since the back pressure will be lower. For steam line break conditions and larger crack sizes, the assumption of isentropic flow is appropriate. For smaller cracks, the assumption of isentropic flow should lead to calculated leak rates which are low by about 20%. This difference is certainly overwhelmed by the uncertainties in leak rates resulting from variations in crack morphology, and the uncertainties in crack sizing[9].

This basic leakage model was utilized in conjunction with the statistical model to provide an assessment of potential end of cycle (EOC) leakage expected under MSLB loads. The distribution curve of arc lengths for 2R10 was used with the upper bound (95%) estimate for number of cracks at 2R11. For each crack it was assumed that ½ of the detected length was 100%TW. This is considered very conservative based on tube pull data where the average 100%TW extent has been ~ 20% of the total length, with the largest ~ 47%[23]. It is also conservative since the leakage calculations are based on the length of a single crack; whereas, the ANO-2 cracking is comprised of multiple smaller cracks. At EOC, the total summed leakage from all cracks under

MSLB loads (2500 psid at operating temperature), is ~ 9 GPM. This would lead to an offsite dose well below the applicable 10CFR100 limit.

5.5 Crack Growth Rate

Crack growth during the three operating periods between four inspections was used to develop growth rates expected for Cycle 11. Growth rate data for the interval between 2R10 and 2P95-1 are being calculated and were not available at the time of this report.

A review of the ECT data from the inspections was used to determine the maximum and average growth rate, which could then be used to assess the postulated end of cycle conditions.

Growth rate predictions are difficult due to the fact that all detected flaws are repaired when detected. One must rely on indications not being detected in previous outages to obtain growth information. Based on knowing the existence of cracks, a review of previous outage data shows evidence of a flaw for a number of indications. A review of the 1993 outage data showed that only 22 of 147 circumferential cracks found in the "A" SG were clearly new. The largest circumferential crack in 2R10 does appear to be present in the previous outage, although quantification is difficult due to the influence of OD deposits. This flaw was conservatively assumed to have grown from no crack in 2P93-1 to its value in 2R10. Overall, however, the average growth rate indicates no significant change in the ANO-2 damage progression. This is shown in Figures 5.5-1 and 5.5-2, where 95% of the indications grew ≤35% average depth and/or ≤110° in arc length over the ten month operating interval. Further work is ongoing to assess the growth between all of the previous operating intervals.

As a result of the inherent difficulties in growth rate analysis, Entergy Operations believes flaw growth should be evaluated statistically. Such analysis was performed and is described in Section 6.2.

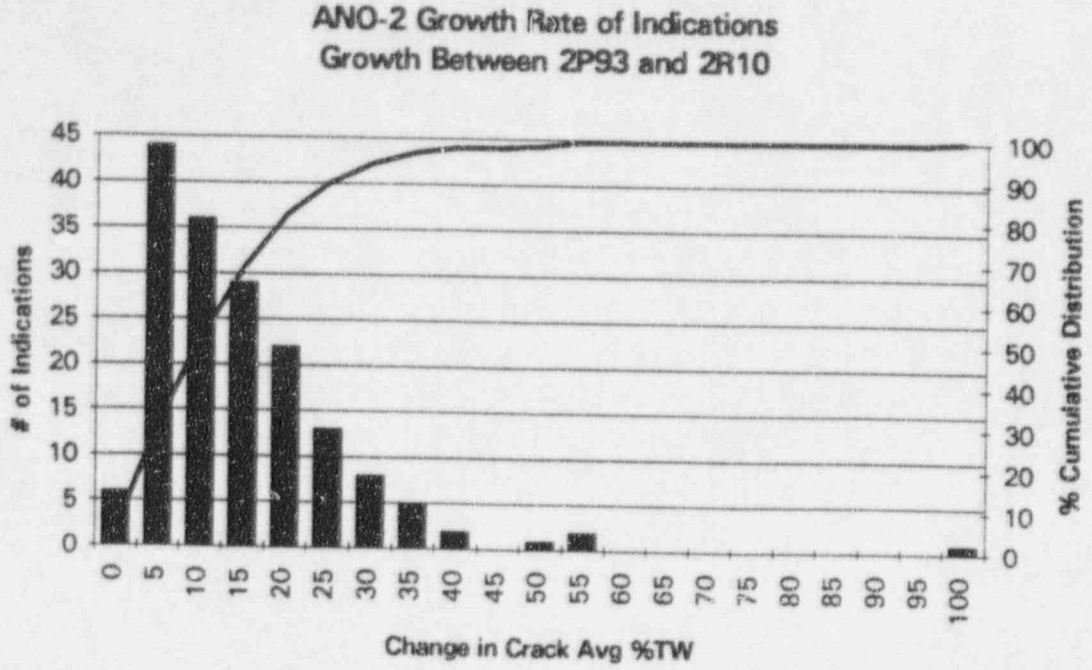

Figure 5.5-1

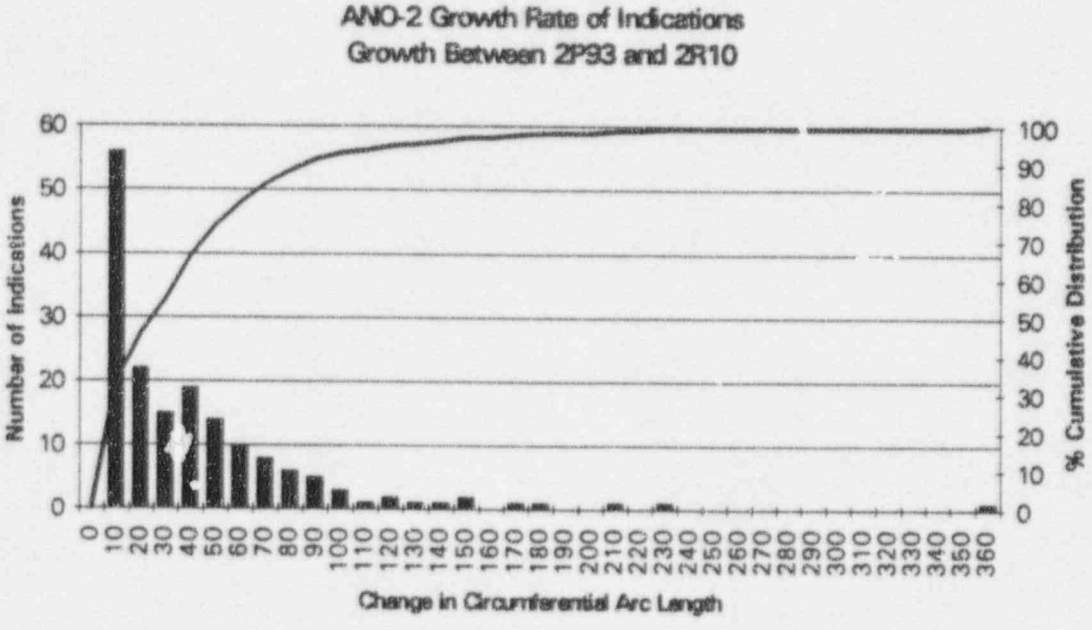

Figure 5.5-2

5.6 Laboratory Crack Project

Because of the limited amount of field data on circumferential cracks, a program was initiated to generate and analyze circumferential cracks typical of those found in the ANO-2 steam generators.

The defects were produced in 3/4 inch Alloy 600 tubing at the secondary face of a simulated tube sheet. The tubing was explosively expanded in the simulated tubesheet with the same process used for the initial fabrication of the steam generators. Seven tubesheet blocks containing six tubes each (for a total of 42) were assembled.

The objectives of the program were to:

- Provide additional data to support the RPC depth vs. actual depth correlation
- Provide insight into crack initiation and propagation
- Provide additional structural integrity/performance data to support further RG 1.121 correlations
- Provide insight into comparisons of various NDE techniques

The following summarizes the major areas of the project:

5.6.1 Nondestructive Examination

Eddy current and ultrasonic nondestructive testing was performed on the tube samples in an effort to assess NDE sizing error. Vendors with field ready nondestructive testing were invited to test the tube samples. Vendors performing eddy current testing included ABB Combustion Engineering Nuclear Operations, Babcock & Wilcox Nuclear Technologies, Westinghouse Electric Corporation, Electric Power Research Institute, Zetec, and Oak Ridge National Laboratories. Those performing UT were B&W Nuclear Technologies, Westinghouse Electric, and NUSON.

In addition to the NDE techniques normally utilized, a dye penetrant system was used to measure the 100% throughwall extent of the circumferential cracks in several of the defects. The tubes were inspected prior to leak and burst testing.

5.6.2 Residual Stress Measurements

Residual stress measurements were conducted to determine the stress level in the explosive expansions of the tubes. All residual stress measurements were performed by an X-ray diffraction technique. This technique has been recognized for some years as a reliable means for measuring surface residual stresses and, by electropolishing to remove layers of metal, the variation of

stress with depth. In X-ray diffraction residual stress measurement, the strain in the crystal lattice is measured, and the residual stress producing the strain is calculated, assuming a linear elastic distortion of the crystal lattice.

5.6.3 Metallurgical Analysis

In order to evaluate the real size of the flaws, destructive examinations were performed. The tubes were pulled apart using a tensile machine. The depth and length of the defect was determined by measuring the depth of the crack every 10° around the tube using a light optical stereo microscope (LOM) with graduated eye piece. The depths at 10° intervals were plotted on a schematic sketch of a tube cross-section to provide a graphic representation of the size and shape of each flaw.

5.6.4 Leak/Burst Testing

All of the samples were leak tested at normal operating pressure and at peak accident pressure. Some of the tubes were leak tested to a pressure of $3\Delta P$ to provide information on crack opening under the higher pressure for comparison to in-situ pressure tests previously performed. All samples were subsequently burst tested.

While laboratory cracks are questionably similar to actual cracks in the SG, certain data is valuable and presents conservative results. Information on NDE performance and leakrates may be dependent on crack dimensions such as crack width and may provide misleading results. The complete results of the program are currently under final review and should be available later in 1995.

6.0 SAFETY ASSESSMENT

6.1 Safety Analysis

An important aspect of any safety analysis is the demonstration that calculated offsite doses are within the NRC staff criteria given in the Standard Review Plan (SRP), NUREG-0800. Steam generator tube leakage is especially significant since it has the potential to lead to a containment bypass[24].

For ANO-2, the analysis utilized guidance from Reference 25, SRP assumptions, realistic assumptions for RCS activity, and a best estimate methodology (ANO-2 specific CEPAC Model), examining both pre-existing and event-generated iodine spike (PIS and GIS) consequences.

Using best estimate methodologies, the following were evaluated:

- Valid emergency operating procedure (EOP) guidance
- Acceptable offsite dose consequences
- Adequate refueling water tank (RWT) inventory

The evaluation was performed for the following events:

- Steam generator tube rupture (SGTR) - single tube
- SGTR - multiple tubes
- MSLB induced tube leak(s) or rupture(s)*

  * The MSLB induced single and multiple tube rupture event is limiting.

The general methodology was to use the ANO-2 simulator and operating crews to determine the best estimate operator response times for representative MSLB/SGTR scenarios. These results were then incorporated into the ANO-2 specific CEPAC evaluations of various MSLB/SGTR scenarios. The CEPAC results were then compared to "hand" calculations.

The safety analysis performed for ANO-2 yielded the following results:

- EOP guidance was valid for event induced tube ruptures; therefore, no significant changes or improvements to the existing EOPs were needed.

- The offsite dose limits of 10CFR100 and the control room dose limits of General Design Criterion (GDC) 19 can be satisfied using realistic assumptions.

- Based on generic system calculations and demonstration in the ANO-2 simulator, there is sufficient RWT inventory to shut down and depressurize the plant before depleting the RWT and sustaining core damage.

Details of this analysis were presented to the NRC staff on August 30, 1993[4].

6.2 Probabilistic Safety Analysis

The avoidance of a severe accident leading to core damage is an important part of assuring adequate protection of the public health. Such severe accidents are important because, although extremely unlikely, they have the potential of releasing large quantities of fission products to the environment. A probabilistic safety analysis (PSA) was performed in order to assess the impact of the SG tube degradation mechanism on the probability of such a severe accident at ANO-2[26]. The objective of this PSA was to identify the optimum ANO-2 SG inspection interval: one which assures adequate protection to the public, yet minimizes ANO-2 operational costs and radiation worker exposure.

The severe accident safety impact was evaluated by estimating the change in the ANO-2 core damage frequency (CDF) as a function of the time between SG inspections since the beginning of Cycle 11 (BOC11) steam generator inspection. Several proposed inspection interval lengths were considered: (1) a half-cycle interval at the middle of Cycle 11 (MOC11), (2) a full cycle interval at the end of Cycle 11 (EOC11), and (3) strictly for comparison purposes, a two cycle interval at the end of Cycle 12 (EOC12). The formal analysis was based upon steam generator inspection results through 2R10 (BOC11). The results of these analyses were qualitatively extended to include the 2P95-1 SG tube inspection findings in order to assess the risk of operating for the remainder of Cycle 11.

The CDF estimates were developed via the use of a modified version of the ANO-2 PSA plant model. The ANO-2 SG inspection interval risk analysis was performed via the development and quantification of event tree and fault tree models in a manner similar to that done in the ANO-2 individual plant examination (IPE)/PSA analysis[27]. The subject ANO-2 SG inspection interval safety analysis differed from the ANO-2 IPE/PSA analysis in that the subject analysis was limited to accidents involving SGTRs, since its intent was to estimate the change in ANO-2 CDF for several inspection interval options. In addition, the subject analysis accounted for the risk contributions due to both spontaneous SGTR initiators (R) and SGTRs induced by other initiators. The ANO-2 IPE/PSA did not account for SGTRs induced by other initiators.

The ANO-2 SGTR CDF analysis included the following steps:

1. Review and identification of events which could lead to spontaneous or induced SGTRs (either initiators or subsequent events),

2. Assessment of the SGTR conditional probability (CP) given an initiator or subsequent event which could cause a SGTR,

3. Identification of the safety functions important to assuring adequate core cooling,

4. Development of event tree logic which accounts for combinations of safety function failures which lead to core damage (i.e., core damage accident sequence),

5. Development of system fault tree logic to account for component failures which contribute to safety function failures, and

6. Quantification of the above event and fault trees to estimate the frequency of core damage involving SGTRs.

The frequency of spontaneous SGTRs (i.e., those occurring during power operation which are not due to significant changes in the primary-to-secondary pressure differential) was estimated to be 5.77E-3/rx-yr per the ANO-2 IPE/PSA[27]. The frequency of induced SGTRs (i.e., those occurring during power operation which are a result of a significant change in the primary-to-secondary pressure differential) required the review of the transient and loss of coolant accidents (LOCAs) described in the ANO-2 Safety Analysis Report (SAR)[28], NUREG-0844[24], and other sources of information. The potential for a SGTR event in each of these accidents was assessed by estimating the maximum primary-to-secondary differential pressure (PSdP) occurring in each and estimating the probability that one or more SG tubes will fail as a result of this differential pressure. An accident was considered a candidate for inducing a SGTR only if its maximum PSdP exceeded the nominal operating PSdP of 1350 psid (2250 psia - 900 psia).

Based on a review of the ANO-2 SAR and other sources, three accident initiators were identified to produce PSdPs significantly greater than the nominal 1350 psid PSdP: the steam line break (SLB), the feed line break (FLB), and the anticipated transient without scram (ATWS). Other initiators, including LOCAs, were not considered significant SGTR initiators. Due to differences in the plant response, the FLB/SLB accidents are assessed together followed by the ATWS-induced SGTR accidents.

6.2.1 FLB/SLB Analysis

In order to account for the ANO-2 plant response dependencies on the SLB location and to distinguish the FLB from the SLB, the ANO-2 IPE/PSA

combined SLB/FLB initiator (T5) was split into four parts and given a unique initiating event designator:

1. Steam line piping outside of the main steam isolation valves (MSIVs) (T5-1),

2. Steam line piping inside of MSIVs and outside of the containment (CNMT) on both SGs (T5-2),

3. Steam line inside of the CNMT on both SGs (T5-3), and

4. Feedwater line inside of the feedwater check valves on both SGs (T5-4).

The frequency of each initiation was taken as the fraction of the total lengths of the steam line (SL) and feedwater line (FL) that each section represents times the total ANO-2 IPE/PSA SLB/FLB frequency. A summary of these calculated SGTR frequencies is provided in Table 6.2-1 below.

Table 6.2-1
Summary of SGTR Initiating Event Frequencies

Initiating Event	ANO-2 IPE/PSA Frequency (/rx-yr)	Fraction of Total SL/FL Length	SGTR Analysis Frequency (/rx-yr)
R	9.77E-3	not appl.	9.77E-3
T5-1	1.1E-3	0.699	7.690E-4
T5-2	1.1E-3	0.107	1.182E-4
T5-3	1.1E-3	0.114	1.258E-4
T5-4	1.1E-3	0.079	8.710E-5

The probability of a tube rupturing in a given accident was assessed by developing an estimate of the probability of a tube wall failure as a function of average tube wall defect depth (i.e., %TW) at selected ANO-2 burnups and comparing each of these "fragility curves" with the expected population of ANO-2 SG tube defects at each of these burnups.

The expected population of ANO-2 SG tube defects, i.e., the number of tube defects as a function of defect size (%TW), was estimated using SG tube inspection data collected in past ANO-2 SG inspection campaigns through 2R10. It has been shown in Reference 14 that the Weibull function can be used to predict the total number of defective tubes as a function of operating time (see Section 5.2). Furthermore, the data collected at ANO-2 through 2R10 and including the recent 2P95-1 inspection indicates that the sizes of the defects (avg %TW) can be described by a Gamma probability distribution function (see Section 5.2). Using these two relationships, estimates of the

defect population after a half-cycle, a full-cycle, and two-cycles of operation were developed. The results of these analyses were qualitatively extended to include the 2P95-1 SG tube inspection findings in order to assess the risk of operating for the remainder of Cycle 11.

The SG tube "fragility curves" were based on experimental SG tube burst pressure test data. These burst tests were performed for a wide range of tube wall defect sizes based upon metallurgical examination of the tubes after failure. For use in this study, these test results were corrected for temperature and to an average RPC %TW indication (see Section 5.3). The resulting data was used to estimate the probability a tube will, as a function of its defect average depth, fail for a given PSdP. The likely number of SG tube failures resulting from an accident is the combination (i.e., convolution) of the SG tube defect population and the SG tube fragility distribution for a given burnup and PSdP and is depicted graphically in Figure 6.2-1.

The conditional probability of tube failure for a PSdP of 2500 psid based on the expected number of tube defects at 2R11 obtained by this convolution technique was approximately 2.2E-03 which is less than the 1.0E-02 threshold value provided in the draft Generic Letter for Voltage-Based Repair Criteria[25]. This value is the sum of the EOC11 SG "A" and SG "B" conditional probabilities at the 95% confidence level (0.87846 for SG "A" plus 0.14689 for SG "B" per Table 6.2-2, below) divided by the sum of the expected number of tube defects at 2R11 (276 for SG "A" plus 200 for SG "B" per Section 5.2). In order to assure conservative results, the EOC11 SG "A" and SG "B" tube rupture probabilities (the numerator) assume that a single defective tube randomly distributed between 60%TW and 100%TW was not detected during the BOC11 tube inspection campaign. **This single defective tube assumption dominates the SGTR conditional failure probability estimate.** For SLB- and FLB-induced SGTRs, the PSdP was assumed to be 2500 psid. This is the maximum credible differential pressure between the primary and secondary systems and represents the primary pressure at approximately the primary code safety relief valve setpoint with the secondary pressure at atmospheric conditions. For these conditions, if the number of tubes susceptible to rupture for a given accident was estimated to be less than one tube, this value was conservatively interpreted as the conditional probability of a single tube rupture in the PSA analysis of CDF. A summary of these SGTR conditional probabilities are provided in Table 6.2-2 below.

Table 6.2-2

SGTR Conditional Probabilities for Accidents Involving a SLB or FLB Event

SG Inspection	SGTR Conditional Probability Used (+1 tube @ 95% CL)	
	SG "A"	SG "B"
BOC11	0.3688	0
MOC11	0.61434	0.06532
EOC11	0.87846	0.14689
EOC12	1.0	0.41861

These SGTR conditional probabilities were applied directly to the SLB and FLB initiating event frequencies provided in Table 6.2-1 to obtain the frequency of SGTR in a given SG following a SLB or FLB at the specified time after the BOC11 SG inspection.

Consistent with that performed in the ANO-2 IPE/PSA, the spontaneous SGTR, the SLB-induced SGTR, and the FLB-induced SGTR CDF analyses were performed via use of event trees and fault trees. Event trees specific to the SGTR accident were developed in order to provide a more detailed account of the accident progression than that in the ANO-2 IPE/PSA. The safety functions listed in Table 6.2-3 below were identified to be important for the SGTR accidents involving spontaneous, SLB-induced, and FLB-induced SGTRs.

Table 6.2-3

Spontaneous and SLB/FLB-Induced SGTR Safety Functions

Safety Function	Descriptor	Description
Reactivity control	K	Insert sufficient negative reactivity to stop nuclear reaction and maintain reactor subcritical
SGTR isolable with RCS intact	I_{RCS}	Ruptured SG can be isolated from environment and Containment
SGTR isolable within containment	I_{CNMT}	Ruptured SG can be isolated from environment
Feedwater (FW) available to intact SG	B_{1I}	Main feedwater (MFW), emergency feedwater (EFW), or auxiliary feedwater (AFW) provides feed to intact SG
FW available to intact or ruptured SG	B_{1N}	MFW, EFW, or AFW provides feed to either intact or ruptured SG
Secondary system pressure control via intact SG	B_{2I}	Operation of atmospheric dump valves (ADVs) and/or turbine bypass valves (TBVs) on intact SG
Secondary system pressure control via intact or ruptured SG	B_{2N}	Operation of ADVs and/or TBVs on either intact or ruptured SG
RCS inventory control	U	High pressure safety injection (HPSI) or, if sufficient, charging
Once through cooling	F	RCS depressurization via emergency core cooling system vent valve or low temperature overpressure protection vent valves
Long-term cooling	X	Shutdown cooling (SDC) or HPSI recirculation

These safety functions were used to develop a spontaneous and SLB/FLB-induced SGTR event tree. This event tree identifies the combinations of initiating events and functional failures expected to lead to core damage resulting in fifty-two (52) accident sequences of importance. Using these event trees and Boolean algebra, the ANO-2 CDF due to spontaneous and SLB/FLB-induced SGTR was quantified at BOC11, MOC11, EOC11, and EOC12. These CDF values are "point estimates," i.e., they correspond to their respective burnup conditions. These CDF values were averaged over the intervals between BOC11, MOC11, EOC11, and EOC12 in order to determine the average ANO-2 CDF due to spontaneous and SLB/FLB-induced SGTRs in each interval. These CDF values are reported in Section 6.2.3.

6.2.2 ATWS Analysis

Due to its severe thermohydraulic challenge to the plant, the ATWS-induced SGTR safety analysis was performed separately from that of other initiators. As in the ANO-2 IPE/PSA, the dominant ATWS-induced core damage risk was assumed to be associated with only three transient groups: turbine trips (T1), loss of MFW (T2), and loss of off-site power (T3) initiators. The safety functions listed in Table 6.2-4 below were identified to be important in the ATWS-induced SGTR core damage accidents. Note that these functions were selected to be relatively independent of each other in order to ensure that the ATWS-induced SGTR CDF is conservatively quantified.

Table 6.2-4

ATWS-Induced SGTR Safety Functions

Safety Function	Descriptor	Description
Reactivity control	K	Control rods insert sufficient negative reactivity to stop nuclear reaction and maintain reactor subcritical
Emergency AC power	AC	Emergency AC power
Turbine trip (TT) successful	TT	Turbine Trip successful
MFW available	MFW	MFW available
EFW available	E	EFW available
Moderator temperature coefficient	MTC	Moderator temperature coefficient for TT/MFW/E and burnup condition produces RCS-SG pressure differential less than 3700 psid
SG integrity	SGI	SG tube integrity remains intact following ATWS pressure excursion
Primary relief secured	W	Primary relief following ATWS pressure excursion secured
Borated water	BW	Borated water injection inserts sufficient negative reactivity to stop nuclear reaction and maintain reactor subcritical
Long-term cooling	LTC	SDC successful

These safety functions were used to develop three ATWS-induced SGTR event trees which identify forty-two (42) accident sequences of importance. Using these event trees, the ANO-2 CDF due to ATWS-induced SGTR was arithmetically quantified for the intervals between BOC11, MOC11, EOC11, and EOC12. The arithmetic quantification of the ATWS-induced SGTR CDF is consistent with that performed in the ANO-2 IPE/PSA and with the screening nature of the ATWS analysis. The ATWS-induced SGTR CDF values are averaged over the intervals between BOC11, MOC11, EOC11, and

EOC12 (the averaging is accounted in the ATWS event trees). These CDF values are included in the combined CDF values reported in Section 6.2.3.

6.2.3 PSA Analysis Results

The results of the ANO-2 SG inspection interval safety analyses are listed in Table 6.2-5 below and are graphically depicted in Figure 6.2-2. These results include the combined core damage contributions of the spontaneous SGTR, the SLB- and FLB-induced SGTR, and the ATWS-induced SGTR accidents.

Table 6.2-5
ANO-2 Spontaneous, SLB/FLB-Induced, and ATWS-Induced SGTR
CDF Results Averaged @ MOC11, and EOC11 and EOC12
w/95% +1 Confidence Level

Case	BOC11 to MOC11	BOC11 to EOC11	BOC11 to EOC12
Spontaneous and Induced SGTR CDF w/ SG Insp @ BOC11 only	3.79E-07	3.98E-07	5.25E-07
Spontaneous and Induced SGTR CDF w/ SG Insp @ Mid-Cycles	3.79E-07	3.39E-07	3.39E-07
CDF Increase	0	5.92E-8	1.86E-7

These results, slightly revised from those presented to the NRC staff on July 14, 1994[5], show that the extension of the ANO-2 SG inspection interval from one half cycle (MOC11) to a full cycle (EOC11) interval has a negligible increase on the average ANO-2 CDF due to a SGTR. Specifically, using the 95% confidence level CDF, the increase in ANO-2 CDF due to spontaneous and induced SGTRs is only 0.59E-07/rx-yr or about 0.2% of the ANO-2 CDF due to internal events reported in the ANO-2 IPE/PSA[27]. This increase in CDF is small and is well within the NO ACTION recommendation category per SECY 91-270[29]. In addition, it is below the NO ACTION recommendation per NUREG/CR 91-04[30] and within the NON-RISK SIGNIFICANT classification per the draft PSA Applications Guide. Since the increase in the ANO-2 SGTR CDF over a half cycle is small, the greater than expected SG defect population found during 2P95-1 at MOC11 indicates that the continued operation of ANO-2 for the remainder of Cycle 11 is not risk significant.

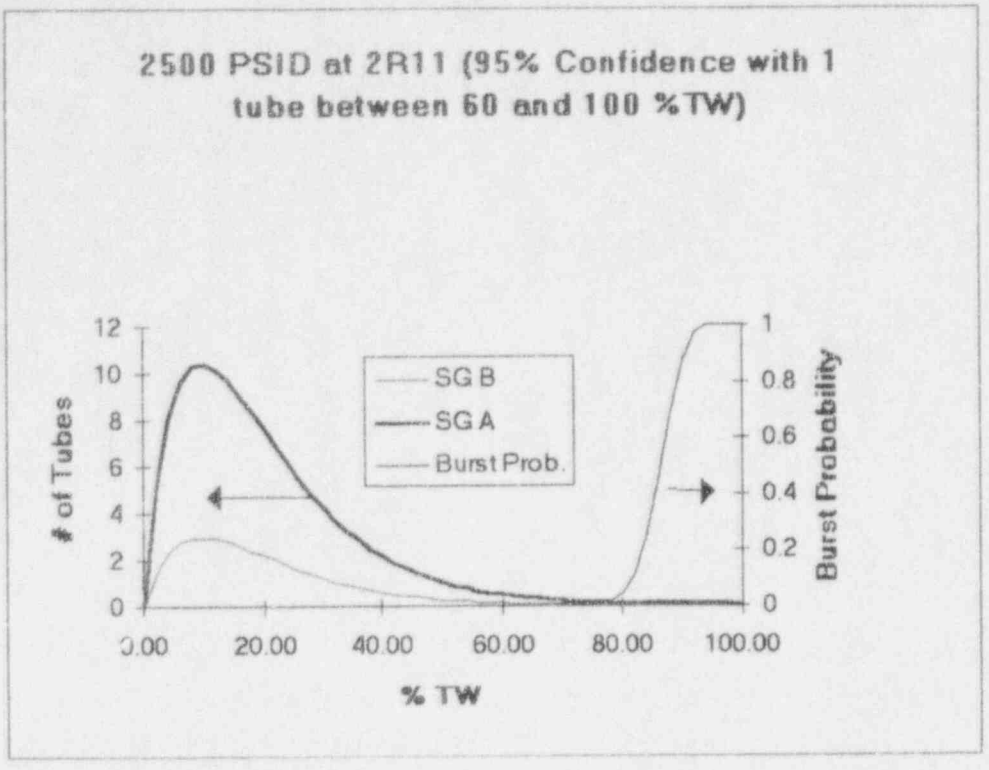

Figure 6.2-1

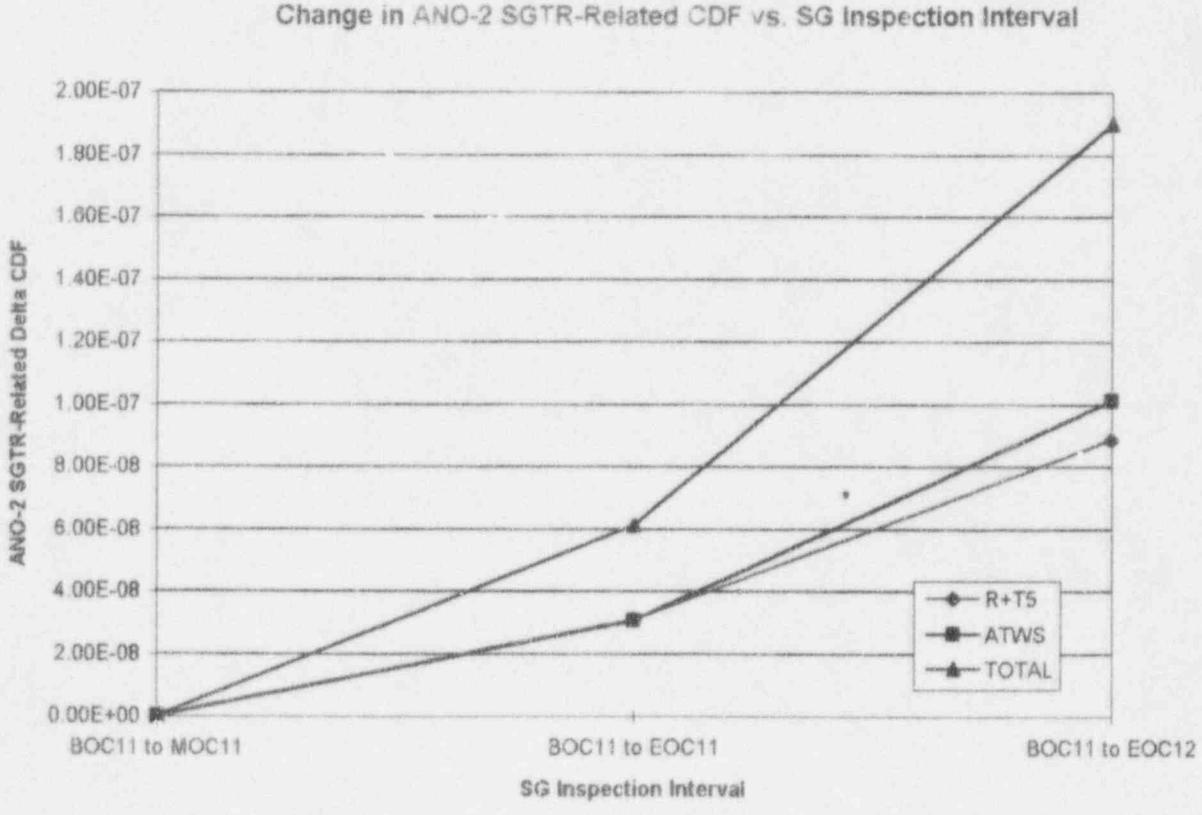

Figure 6.2-2

7.0 OPERATIONAL RESPONSE

An operational leak rate limit is established to provide reasonable assurance that flaws either missed during inspection or growing more rapidly than expected will not render the tube vulnerable to tube rupture in the event of a MSLB. The ANO-2 Technical Specification limit is 0.5 GPM per SG, but an administrative procedural limit of 0.1 GPM (144 GPD) exists to provide for added margin against burst. In addition, rate of change limits exist to ensure rapidly propagating cracks or damage will be addressed at the earliest possible stages.

Upon any control room alarm indicating primary to secondary leakage, the Operations and Chemistry Departments enter abnormal operating procedures. If the leak rate is ≥0.1 GPM, a plant shutdown is procedurally required. In addition, a plant shutdown is procedurally required if the leak rate is projected to be ≥0.1 GPM in one hour. Stable leak rates of >0.01 GPM procedurally require management awareness for continued plant operations.

7.1 Inservice Leakage Detection/Response

There are several methods and techniques utilized by the Operations and Chemistry Departments to identify the presence of a primary to secondary leak. The need to provide leakage monitoring is given in the Bases for Section 3.4.6.2 of the ANO-2 Technical Specifications and denotes that a maximum total leakage of 1.0 GPM (0.5 GPM per steam generator) provides assurance that off-site release limits will not be exceeded (small fraction of 10CFR100 limits) in the event of a steam line break or a steam generator tube rupture, and guards against tube severance or rupture under the extreme differential pressure conditions imposed during a steam line break or LOCA. ANO-2 Technical Specification 3.4.6.2.c requires that when primary to secondary leakage is greater than 0.5 GPM through one SG or 1.0 GPM through both SGs the reactor is to be in hot standby within 6 hours and in cold shutdown within the following 30 hours. The plant is administratively shutdown at ≥0.1 GPM.

The Operations Department trends the steam, condenser off-gas, and steam generator sample systems in determining indication of steam generator tube leak. Steam lines are monitored via radiation monitors and nitrogen sixteen (N-16) gamma detectors, which provide the chemists and operators with the capability of quantifying leakage. The amount of N-16 present in the secondary system is influenced by the size of the leak, the location of the leak in the steam generator, and the power level. The ANO-2 N-16 monitors have the capability of correcting the leak rate for changes in power level, and are set to detect or discriminate for the high energy gamma rays emitted from N-16 only; therefore, other isotopes that leak into the secondary system will not have an effect on the N-16 values. Because of the short half-life of N-16, the amount of N-16 seen by the detector will vary depending on the location of the leak. ANO-2 N-16 monitors can be adjusted to display a leak rate for the hot leg bottom of the tube, the U-bend, the cold leg bottom of the tube, or an average and thus make it possible to gather more accurate leak rate information. Condenser off-gas monitoring provides a means to measure the gaseous activity levels released to the system vent (located on spent fuel pool floor) using a Geiger Mueller tube (determines gross levels of beta and gamma radiation) and an off-line gaseous sampler. The steam generator monitoring

system continually takes steam generator blowdown samples downstream of their respective sample coolers to detect for fission product activity (primarily Cs-137) and allows for determining which generator is leaking. Procedures (e.g., EOP 2204.004 and abnormal operating procedure (AOP) 2203.038) are utilized when the monitors or trend recorders for the aforementioned systems exhibit increasing trends. The Operations Department enters these procedures to place the plant in a stable condition and to mitigate the consequences of a steam generator tube leak. AOP 2203.038 (Primary to Secondary Leakage) is used when any of the following entry conditions exist:

(Increasing trends on any of the following)

- Main steam radiation monitors or secondary system trend recorders
- Steam generator sample line monitors (samples taken off blowdown)
- Condenser off-gas monitors
- Steam generator tube leak N-16 monitors
- Unexplained "Secondary System Radiation HI" annunciator alarm
- Increasing fission product activity through chemistry sampling
- Unexplained "Trouble/Leak rate HI" annunciator alarm
- Unexplained "Rate of Change HI" annunciator alarm

EOP 2204.004 (Steam Generator Tube Rupture) is used when any of the following conditions exist:

(Increasing trends on any of the following)

- Main steam radiation monitors or secondary system trend recorders
- Steam generator sample line monitors
- Condenser off-gas monitors
- Steam generator tube leak N-16 monitors

The Chemistry Department routinely samples both the primary water and secondary water systems to identify primary to secondary leakage and trends the sample results to identify possible primary to secondary occurrences. Off-gas samples (extracted from the condenser vacuum pump discharge) are taken for Ar-41 and samples for tritium (taken from condensate as liquid sample) are taken to quantify activity levels in the secondary system. Argon-41 levels yield more of an indicative measure of instantaneous levels of primary to secondary leakage. Tritium levels (in the secondary system) will increase linearly over time during a primary to secondary leak. By knowing the tritium level in the primary system and the time delay from the initial indication of a leak to the tritium analysis in the secondary system, a primary to secondary leakrate can be determined. Secondary liquid samples are taken to measure fission product activity on such radioisotopes as I-131, I-132, I-133, I-134, Xe-133, and Cs-134 via gamma spectroscopy, which can identify the presence of radioisotopes in the sample based on the energies of the incident radiation particles. Resin from the startup & blowdown demineralizers is also sampled for increased activity (gamma spectroscopy is used to identify and quantify activity levels).

The following is a list of primary to secondary monitoring devices and their current setpoints:

• SG sample (2RITS-5854, 5864)	~ 130 cpm
• Steam line radiation (2RR-1007, 1057)	1 mr/hr
• N-16 monitors (2RE-0200, 0201)	0.01 GPM, 2X current leakrate
• Condenser off-gas monitors	~ 600 cpm

8.0 CONCLUSIONS

Entergy Operations has performed an extensive investigation into the circumferential cracking occurring at ANO-2. The investigation includes comprehensive inspections, application of appropriate safety factors, use of statistically valid (95/95) material properties, degradation projections, and tube burst test data. Probabilistic evaluations were performed to assess the validity for continued operation for the unit, and concluded that the ANO-2 steam generators can safely operate for the remainder of the fuel cycle with an acceptable level of risk. The acceptable level is based on not compromising the structural integrity margin requirements for the tubing and a minimal change in the SGTR-related core damage frequency.

The evaluations also considered the previous large flaws found at ANO-2 during inspections. Based on a combination of analytical evaluations, in-situ pressure tests, laboratory testing, finite element modeling, and use of advanced NDE techniques (UT and RPC deconvolution analysis), all of the circumferential cracks previously found would have met the RG 1.121 structural margin requirements.

9.0 REFERENCES

1) Information Update ANO-2 Steam Generator Tube Leak Outage, April 16, 1992.

2) Information Update Concerning the ANO-2 Steam Generators, August 26, 1992.

3) Information Update Concerning the ANO-2 Steam Generators, December 3, 1992.

4) Information Update Concerning the ANO-2 Steam Generators, August 30, 1993.

5) Information Update Concerning the ANO-2 Steam Generators, July 14, 1994.

6) "PWR Steam Generator Tube Repair Limits: Technical Support Document for Expansion Zone PWSCC in Roll Transitions," EPRI NP-6864L - Rev. 2.

7) Summary of Meeting on July 15, 1993 Concerning Eddy Current Methodologies Used at Arkansas Nuclear One, Unit 2 (ANO-2), dated August 6, 1993.

8) "Circumferential IGSCC: UT The Only Choice?," by D. Dobbeni and D. Degreve, presented at the 12th EPRI Steam Generator NDE Workshop, Park City, Utah, August 1993.

9) "Some NDE, Leak Rate and Burst Pressure Considerations in Support of the Analysis of Circumferential Cracking Incidents at ANO Unit 2," by S.D. Brown and J.A. Begley, Packer Engineering Report No. B51677-R1, Revision 0, September 1994.

10) "Coil Design and Technique Parameter Development for Early Detection of O.D. Cracking," by Jeff Siegel and Marty Klatt, ZETEC, Inc., presented at the EPRI 13th SG NDE Workshop, July 25-27, 1994.

11) NRC Inspection Report 50-313/94-17; 50-368/94-17, Section 6.2.3, July 13, 1994.

12) "Statistical Evaluation of ANO-2 Circumferential Crack Data," Tetra Engineering Group, Inc., Report TR-94-7201, January 1994.

13) "Statistical Analysis of Steam Generator Tube Degradation," EPRI NP-7493.

14) "ANO-2 Steam Generator Tube Life Prediction Analysis," Dominion Engineering, Inc., February 1993, Revision 1.

15) "ANO-2 Steam Generator Tube Burst Pressures for Circumferential Defects at Top of Tubesheet," MPR Associates, November 11, 1994.

16) "ANO-2 Steam Generator Degraded Tube Analysis Per Reg. Guide 1.121," ANO Engineering Report 92-R-2025-01.

17) Packer Engineering memo dated June 3, 1993, to A. Buford.

18) Westinghouse Owners Group/NRC SG Circumferential Cracking Issue Meeting, September 26, 1994.

19) "Final Report for the Steam Generator Tube In-Situ Hydrostatic Test Tool," CE Report TR-ESE-1030.

20) "In-Situ Pressure Test Information," CE Memo A-PENG-94-025, November 20, 1994.

21) "Tasks 3 and 6 Report: Effects of Chemical Cleaning on Steam Generator Defects; Chemical Cleaning Qualification Testing for ANO-2," CE Report TR-MCC-274, Revision 0, December 1, 1993.

22) "Arkansas Nuclear One Unit 2 Leaker Outage Steam Generator Tube Repair Summary (Final Report)," B&W Report.

23) "ANO-2 Eddy Current Data Evaluation and Leak Rate Estimation," Westinghouse Report, NSD-JLH-3347, SG-93-09-011, CARK-501, September 20, 1993.

24) "NRC Integrated Program for the Resolution of Unresolved Safety Issues A-3, A-4, and A-5 Regarding Steam Generator Tube Integrity, NUREG-0844, September 1988.

25) "Voltage-Based Interim Plugging Criteria for Steam Generator Tubes - Task Group Report," Draft NUREG-1477, June 1, 1993.

26) "ANO-2 SG Inspection Interval Risk Analysis Based on Inspection Data through 2R10," Calc. 93-E-0079-05, Rev. 0.

27) "ANO-2 Probabilistic Risk Assessment (PRA), Individual Plant Examination (IPE) Submittal," Report 94-R-2005-01, Revision 0.

28) ANO-2 Safety Analysis Report, Amendment 12.

29) "Interim Guidance on Staff Implementation of the Commission's Safety Goal Policy," Letter form J.M. Taylor (NRC) to the Commissioners, SECY 91-270, August 27, 1991.

30) "Severe Accident Issue Closure Guidelines," NUMARC 91-04, January 1992.

Appendix A

Data Tables

Steam Generator "A"

	TOTAL	2F92	2R9	2P93-1	2R10	2P95-1
# of Cracks	620	208	17	45	147	203
Crack Length						
Average =	97.04	115.79	102.76	90.56	85.57	86.98
Std. Dev. =	54.31	61.43	63.85	54.45	50.60	42.17
Minimum =	4	4	30	21	18	25
Maximum =	360	360	239	252	360	304
Max %TW						
Average =	71.33	72.73	71.29	71.76	71.56	69.66
Std. Dev. =	21.50	20.34	15.08	17.09	21.96	23.60
Minimum =	0	2	41	27	0	1
Maximum =	100	100	88	97	97	100
Average %TW						
Average =	19.77	24.30	21.48	17.89	17.52	17.02
Std. Dev. =	13.57	15.95	15.93	11.60	12.45	10.41
Minimum =	0.00	0.33	5.24	4.48	0.00	0.15
Maximum =	96.88	89.00	57.76	51.31	96.88	68.40

Steam Generator "B"

	TOTAL	2F92	2R9	2P93-1	2R10	2P95-1
# of Cracks	125	11	8	3	23	80
Crack Length						
Average =	75.51	82.91	63.13	67.27	56.98	81.36
Std. Dev. =	44.62	93.51	40.18	41.58	20.96	39.36
Minimum =	25	35	30	30	25	30
Maximum =	360	360	139	112	93	220
Max %TW						
Average =	69.80	64.55	58.50	52.33	63.61	74.09
Std. Dev. =	23.50	22.63	20.44	36.96	22.21	23.13
Minimum =	2	9	24	30	17	2
Maximum =	100	91	84	95	93	100
Average %TW						
Average =	15.01	15.96	11.83	7.51	10.17	16.87
Std. Dev. =	11.21	21.68	10.90	2.02	5.09	10.31
Minimum =	1.00	1.28	2.00	5.33	1.49	1.00
Maximum =	80.00	80.00	32.43	9.33	20.44	47.27

Both Steam Generators

	TOTAL	2F92	2R9	2P93-1	2R10	2P95-1
# of Cracks	745	219	25	48	170	283
Crack Length						
Average =	93.42	114.14	90.08	89.10	81.66	85.39
Std. Dev. =	53.39	63.53	59.54	53.68	48.61	41.40
Minimum =	4	4	30	21	18	25
Maximum =	360	360	239	252	360	304
Max %TW						
Average =	71.07	72.32	67.20	70.54	70.45	70.91
Std. Dev. =	21.84	20.48	17.62	18.82	22.10	23.51
Minimum =	0	2	24	27	0	1
Maximum =	100	100	88	97	97	100
Average %TW						
Average =	18.97	23.88	18.39	17.24	16.53	16.98
Std. Dev. =	13.31	16.32	15.00	11.52	11.99	10.36
Minimum =	0.00	0.33	2.00	4.48	0.00	0.15
Maximum =	96.88	89.00	57.76	51.31	96.88	68.40

Circumferential Crack Data

OUTAGE	SG	ROW	LINE	VOLTS	MAX %TW	LENGTH	AVG %TW
2F92	A	63	59	1.77	2	60	0.33
2F92	A	114	72	1.53	4	44	0.49
2F92	A	55	65	1.76	87	4	0.97
2F92	A	102	72	3.69	83	5	1.15
2F92	B	100	106	4.43	9	51	1.28
2F92	A	18	34	1.75	11	54	1.65
2F92	A	110	62	1.87	12	75	2.50
2F92	A	60	66	3.84	91	11	2.78
2F92	A	67	77	1.90	19	58	3.06
2F92	A	66	58	2.27	20	56	3.11
2F92	A	32	50	2.98	20	68	3.78
2F92	A	113	71	1.06	34	40	3.78
2F92	A	37	37	5.86	82	19	4.33
2F92	A	36	50	1.43	21	81	4.73
2F92	A	8	16	1.15	20	88	4.89
2F92	A	46	54	1.70	24	74	4.93
2F92	A	50	38	1.05	33	54	4.95
2F92	A	34	42	2.12	37	56	5.76
2F92	A	105	63	1.12	41	54	6.15
2F92	A	101	79	4.12	87	28	6.77
2F92	B	103	65	2.56	60	42	7.00
2F92	A	81	127	2.51	83	33	7.61
2F92	A	45	49	1.60	86	32	7.64
2F92	A	14	152	1.27	45	62	7.75
2F92	A	63	77	2.34	20	140	7.78
2F92	A	41	39	0.98	61	47	7.96
2F92	A	76	80	1.71	82	35	7.97
2F92	A	107	71	1.94	66	44	8.07
2F92	A	11	45	1.35	55	54	8.25
2F92	B	106	82	2.66	86	35	8.36
2F92	B	84	42	2.82	69	44	8.43
2F92	A	86	124	8.38	73	42	8.52
2F92	A	95	119	5.07	96	32	8.53
2F92	A	15	31	1.04	35	90	8.75
2F92	A	5	53	1.94	44	72	8.80
2F92	.	113	67	3.18	43	74	8.84
2F92	B	104	60	4.08	49	65	8.85
2F92	A	71	73	0.89	61	53	8.98
2F92	B	104	68	2.19	54	60	9.00
2F92	B	105	89	3.34	80	42	9.33
2F92	A	24	34	2.87	43	79	9.44
2F92	A	64	76	1.97	51	67	9.49

OUTAGE	SG	ROW	LINE	VOLTS	MAX %TW	LENGTH	AVG %TW
2F92	A	13	151	1.02	61	57	9.66
2F92	B	84	42	3.01	66	53	9.72
2F92	A	23	53	3.21	40	88	9.78
2F92	A	32	46	1.10	55	65	9.93
2F92	A	90	122	1.60	45	80	10.00
2F92	A	34	98	2.24	78	47	10.18
2F92	A	27	39	1.79	51	72	10.20
2F92	A	56	54	3.22	36	102	10.20
2F92	A	67	81	2.18	81	46	10.35
2F92	A	36	38	2.20	72	53	10.60
2F92	A	106	82	1.45	48	83	11.07
2F92	A	36	44	1.29	79	54	11.85
2F92	A	21	149	6.30	74	58	11.92
2F92	A	81	63	1.35	85	51	12.04
2F92	A	88	46	0.93	55	79	12.07
2F92	A	14	28	1.21	41	107	12.19
2F92	A	13	27	2.74	72	61	12.20
2F92	A	87	43	2.22	85	53	12.51
2F92	A	87	43	5.20	89	51	12.61
2F92	A	94	46	1.63	65	70	12.64
2F92	A	105	77	1.22	73	63	12.78
2F92	A	46	74	0.95	55	86	13.14
2F92	A	9	151	6.95	77	62	13.26
2F92	A	32	130	3.21	58	83	13.37
2F92	A	8	54	2.33	55	88	13.44
2F92	A	19	35	5.50	73	67	13.59
2F92	A	60	68	4.39	93	53	13.69
2F92	A	107	81	1.09	62	83	14.29
2F92	A	111	95	4.12	87	60	14.50
2F92	A	70	74	2.48	39	135	14.63
2F92	A	4	38	1.65	53	100	14.72
2F92	A	59	57	6.64	82	65	14.81
2F92	A	30	114	2.07	89	60	14.83
2F92	B	113	99	3.81	91	61	15.42
2F92	A	15	149	3.17	67	83	15.45
2F92	A	27	33	2.47	85	67	15.82
2F92	A	32	20	2.75	85	67	15.82
2F92	A	34	24	1.66	60	97	16.17
2F92	A	62	64	5.10	97	60	16.17
2F92	A	104	96	3.92	72	82	16.40
2F92	A	51	45	6.49	63	95	16.63
2F92	A	59	63	1.92	56	107	16.64
2F92	A	21	53	5.79	77	79	16.90

OUTAGE	SG	ROW	LINE	VOLTS	MAX %TW	LENGTH	AVG %TW
2F92	A	65	77	1.54	63	98	17.15
2F92	B	111	73	2.06	66	99	18.15
2F92	A	11	149	1.20	58	113	18.21
2F92	A	79	81	4.32	94	70	18.28
2F92	A	31	41	3.80	65	102	18.42
2F92	A	63	111	2.00	42	158	18.43
2F92	A	71	107	2.54	85	79	18.65
2F92	A	37	39	7.07	80	84	18.67
2F92	A	41	35	1.18	54	125	18.75
2F92	A	41	35	6.65	97	70	18.86
2F92	A	13	153	0.99	50	137	19.03
2F92	A	32	124	7.78	92	75	19.17
2F92	A	113	73	4.07	76	91	19.21
2F92	A	100	122	6.67	73	95	19.26
2F92	A	106	98	5.88	95	73	19.26
2F92	A	17	151	1.71	67	104	19.36
2F92	A	101	73	2.34	87	81	19.58
2F92	A	78	130	8.19	94	75	19.58
2F92	A	96	46	2.50	85	84	19.83
2F92	A	84	126	4.17	56	128	19.91
2F92	A	13	17	5.03	87	84	20.30
2F92	A	28	112	1.72	53	140	20.61
2F92	A	27	35	4.05	73	102	20.68
2F92	A	79	79	1.74	90	83	20.75
2F92	A	68	32	6.58	87	86	20.78
2F92	A	31	123	4.70	90	84	21.00
2F92	A	5	55	2.69	73	104	21.09
2F92	A	68	108	1.29	61	125	21.18
2F92	A	28	126	3.46	77	100	21.39
2F92	A	43	119	2.13	83	93	21.44
2F92	A	108	74	2.59	79	98	21.51
2F92	A	31	51	2.41	81	97	21.83
2F92	A	21	151	0.91	69	114	21.85
2F92	A	46	58	3.84	83	43	9.91
2F92	A	55	77	9.57	82	96	21.87
2F92	A	55	77	5.08	54	146	21.90
2F92	A	105	67	2.14	79	102	22.38
2F92	A	46	88	7.44	87	93	22.48
2F92	A	51	111	6.87	73	111	22.51
2F92	A	82	80	2.46	73	112	22.71
2F92	A	25	131	3.41	86	97	23.17
2F92	A	47	121	6.32	87	96	23.20
2F92	A	70	78	3.30	67	125	23.26

OUTAGE	SG	ROW	LINE	VOLTS	MAX %TW	LENGTH	AVG %TW
2F92	A	16	148	1.41	63	134	23.45
2F92	A	35	127	2.42	80	106	23.56
2F92	A	44	46	2.39	68	125	23.61
2F92	A	101	69	4.27	92	93	23.77
2F92	A	92	46	10.02	87	100	24.17
2F92	A	51	119	14.30	75	118	24.58
2F92	A	59	65	1.59	86	104	24.84
2F92	A	32	48	4.90	94	97	25.33
2F92	A	12	146	3.39	61	150	25.42
2F92	A	20	52	1.64	79	116	25.46
2F92	A	57	65	5.00	73	126	25.55
2F92	A	15	145	5.65	91	102	25.78
2F92	A	68	76	10.13	78	123	26.65
2F92	A	97	121	8.49	75	128	26.67
2F92	A	55	53	20.30	81	121	27.23
2F92	A	107	69	2.27	79	128	28.09
2F92	A	52	106	5.35	71	143	28.20
2F92	A	18	138	1.66	83	125	28.82
2F92	A	11	151	11.39	82	128	29.16
2F92	A	45	119	1.34	75	140	29.17
2F92	A	96	118	16.64	92	115	29.39
2F92	A	109	77	7.14	92	116	29.64
2F92	A	47	49	3.27	83	130	29.97
2F92	A	19	137	7.78	90	120	30.00
2F92	A	58	56	10.50	88	123	30.07
2F92	A	108	94	9.19	76	143	30.19
2F92	A	26	52	5.71	90	121	30.25
2F92	A	71	105	17.46	75	146	30.42
2F92	A	83	127	9.97	83	133	30.66
2F92	A	22	146	1.37	75	148	30.83
2F92	A	11	19	2.98	77	146	31.23
2F92	A	28	128	7.99	81	139	31.28
2F92	A	42	118	3.26	81	139	31.28
2F92	A	49	49	3.51	85	135	31.88
2F92	A	103	109	5.76	87	132	31.90
2F92	A	64	68	4.20	95	121	31.93
2F92	A	108	76	6.79	83	139	32.05
2F92	A	102	106	10.55	89	130	32.14
2F92	A	93	45	6.52	86	135	32.25
2F92	A	105	69	4.90	87	135	32.63
2F92	A	106	64	9.62	91	130	32.86
2F92	A	106	64	6.16	87	137	33.11
2F92	A	23	133	9.05	89	134	33.13

OUTAGE	SG	ROW	LINE	VOLTS	MAX %TW	LENGTH	AVG %TW
2F92	A	108	72	2.39	72	170	34.00
2F92	A	106	76	13.95	84	149	34.77
2F92	A	105	61	6.24	95	132	34.83
2F92	A	62	66	5.93	100	126	35.00
2F92	A	103	107	6.78	85	156	36.83
2F92	A	60	112	9.92	94	142	37.08
2F92	A	56	62	7.21	84	160	37.33
2F92	A	13	149	3.01	72	188	37.60
2F92	A	52	54	3.09	73	188	38.12
2F92	A	106	96	9.84	68	202	38.16
2F92	A	88	126	9.94	80	172	38.22
2F92	A	21	135	6.78	88	157	38.38
2F92	A	15	147	17.59	78	178	38.57
2F92	A	14	144	5.35	84	167	38.97
2F92	A	63	69	4.29	84	167	38.97
2F92	A	15	143	3.05	80	176	39.11
2F92	A	104	108	19.90	77	186	39.78
2F92	A	12	28	9.93	67	221	41.13
2F92	A	20	136	4.04	85	183	43.21
2F92	A	45	121	14.89	86	181	43.24
2F92	A	97	115	1.90	82	194	44.19
2F92	A	106	68	16.37	87	184	44.47
2F92	A	107	73	6.58	88	183	44.73
2F92	A	63	61	4.39	89	183	45.24
2F92	A	17	147	1.51	81	202	45.45
2F92	A	30	120	1.70	94	175	45.69
2F92	A	28	130	7.77	90	183	45.75
2F92	A	31	127	14.42	84	197	45.97
2F92	A	29	129	5.21	81	209	47.03
2F92	A	110	74	21.86	80	212	47.11
2F92	A	52	52	18.11	88	193	47.18
2F92	A	101	109	8.48	7°	218	47.23
2F92	A	101	109	6.80	87	196	47.37
2F92	A	31	125	6.92	95	183	48.29
2F92	A	104	78	6.14	57	309	48.93
2F92	A	30	124	12.69	100	180	50.00
2F92	A	66	106	2.27	86	218	52.08
2F92	A	51	51	4.87	91	207	52.33
2F92	A	14	142	6.80	88	225	55.00
2F92	A	34	40	36.46	83	240	55.33
2F92	A	52	116	3.37	91	230	58.14
2F92	A	110	68	12.81	88	238	58.18
2F92	A	28	132	19.44	82	257	58.54

OUTAGE	SG	ROW	LINE	VOLTS	MAX %TW	LENGTH	AVG %TW
2F92	A	44	48	3.30	91	270	68.25
2F92	B	36	130	7.09	80	360	80.00
2F92	A	68	78	13.10	89	347	85.79
2F92	A	55	63	39.80	88	360	88.00
2F92	A	13	147	80.29	89	360	89.00
2R9	B	92	122	0.95	24	30	2.00
2R9	B	18	18	1.16	40	41	4.56
2R9	B	108	64	0.51	48	36	4.80
2R9	A	93	117	1.39	41	46	5.24
2R9	A	47	57	1.18	43	55	6.57
2R9	A	96	120	2.39	49	51	6.94
2R9	A	50	50	2.31	88	30	7.33
2R9	B	66	136	0.63	66	43	7.88
2R9	A	57	51	1.46	76	39	8.23
2R9	B	25	147	1.48	69	46	8.82
2R9	B	84	80	1.13	57	57	9.03
2R9	A	60	64	0.55	69	51	9.78
2R9	A	104	110	1.36	76	58	12.24
2R9	A	11	17	1.66	74	78	16.03
2R9	A	98	122	1.80	74	92	18.91
2R9	A	58	62	0.56	83	88	20.29
2R9	A	69	131	2.76	69	107	20.51
2R9	A	95	117	2.63	62	123	21.18
2R9	B	101	65	2.61	80	113	25.11
2R9	A	96	116	0.83	67	148	27.54
2R9	B	108	86	3.38	84	139	32.43
2R9	A	102	110	3.32	88	143	34.96
2R9	A	79	83	0.99	87	181	43.74
2R9	A	67	79	2.78	79	218	47.84
2R9	A	64	48	6.34	87	239	57.76
2P93-1	A	111	91	0.89	46	35	4.48
2P93-1	A	24	38	1.55	35	53	5.15
2P93-1	B	90	48	0.83	32	60	5.33
2P93-1	A	98	86	3.87	97	21	5.66
2P93-1	A	45	45	0.91	66	33	6.05
2P93-1	A	53	79	1.25	36	65	6.50
2P93-1	A	114	90	1.2	74	35	7.20
2P93-1	A	52	118	0.95	27	96	7.23
2P93-1	A	101	77	2.79	70	39	7.50
2P93-1	A	54	50	1.79	85	33	7.79
2P93-1	B	66	128	3.04	95	30	7.86
2P93-1	A	33	129	1.46	56	54	8.40
2P93-1	A	53	51	1.69	75	43	8.96

OUTAGE	SG	ROW	LINE	VOLTS	MAX %TW	LENGTH	AVG %TW
2P93-1	A	114	96	1.19	66	51	9.32
2P93-1	B	82	44	0.97	30	112	9.33
2P93-1	A	62	50	1.93	92	37	9.46
2P93-1	A	49	115	2.26	58	63	10.15
2P93-1	A	54	52	1.83	67	58	10.79
2P93-1	A	27	127	3.14	90	44	11.00
2P93-1	A	15	33	2.42	87	49	11.84
2P93-1	A	30	126	2.09	70	63	12.25
2P93-1	A	10	130	2.56	85	53	12.41
2P93-1	A	105	91	0.91	78	58	12.53
2P93-1	A	103	75	2.59	82	60	13.57
2P93-1	A	64	108	2.11	48	102	13.60
2P93-1	A	101	81	4.54	86	58	13.81
2P93-1	A	104	88	2.4	90	56	14.02
2P93-1	A	106	90	0.87	45	117	14.68
2P93-1	A	27	131	2.80	60	95	15.83
2P93-1	A	31	129	1.96	60	102	16.94
2P93-1	A	34	130	2.55	80	81	18.00
2P93-1	A	72	130	4.27	87	75	18.13
2P93-1	A	30	52	2.96	84	79	18.43
2P93-1	A	77	77	2.22	72	96	19.27
2P93-1	A	20	34	1.21	74	100	20.56
2P93-1	A	104	90	5.76	88	84	20.56
2P93-1	A	4	56	1.74	57	144	22.80
2P93-1	A	111	79	3.09	89	105	25.99
2P93-1	A	105	89	1.67	83	121	27.87
2P93-1	A	101	85	2.94	77	137	29.30
2P93-1	A	109	73	1.19	67	159	29.59
2P93-1	A	106	102	2.11	80	137	30.44
2P93-1	A	77	79	2.64	50	252	35.04
2P93-1	A	16	30	3.72	75	179	37.29
2P93-1	A	100	56	1.47	75	194	40.52
2P93-1	A	42	46	1.72	76	193	40.74
2P93-1	A	35	45	4.8	93	163	42.11
2P93-1	A	82	126	5.92	91	203	51.31
2R10	A	6	110	2.7	93	96	24.90
2R10	A	8	34	1.0	N/A	33	20.00
2R10	A	8	40	2.0	88	95	23.13
2R10	A	12	30	7.1	86	130	30.97
2R10	A	13	29	3.6	91	49	12.40
2R10	A	15	29	8.0	94	163	42.55
2R10	A	13	145	0.7	41	72	8.18
2R10	A	17	29	1.8	87	75	18.21

OUTAGE	SG	ROW	LINE	VOLTS	MAX %TW	LENGTH	AVG %TW
2R10	A	17	31	1.2	71	110	21.77
2R10	A	17	139	1.5	48	165	21.96
2R10	A	19	53	4.7	91	95	23.92
2R10	A	20	138	3.7	89	56	13.86
2R10	A	20	150	2.4	82	68	15.57
2R10	A	21	19	2.9	89	70	17.33
2R10	A	21	29	2.8	72	142	28.39
2R10	A	21	137	2.7	76	184	38.84
2R10	A	22	54	4.0	89	72	17.76
2R10	A	22	114	2.1	39	54	5.88
2R10	A	22	150	2.4	72	135	26.98
2R10	A	23	39	2.1	88	72	17.56
2R10	A	24	130	2.0	84	138	32.30
2R10	A	24	132	9.3	90	205	51.25
2R10	A	25	133	4.0	87	124	30.06
2R10	A	27	37	1.6	78	79	17.08
2R10	A	29	39	4.0	88	124	30.41
2R10	A	31	39	7.8	88	142	34.69
2R10	A	31	43	3.6	88	98	23.99
2R10	A	32	40	5.1	97	67	17.94
2R10	A	32	42	1.6	72	84	16.82
2R10	A	32	122	7.4	90	151	37.67
2R10	A	32	126	6.8	97	360	96.88
2R10	A	33	43	1.5	86	35	8.37
2R10	A	33	53	2.7	71	81	15.90
2R10	A	33	123	0.9	71	154	30.41
2R10	A	33	125	2.6	55	105	16.06
2R10	A	34	48	1.4	71	42	8.29
2R10	A	34	58	1.7	75	67	13.87
2R10	A	35	41	4.2	84	N/A	20.00
2R10	A	35	53	2.9	67	89	16.63
2R10	A	36	42	1.1	74	37	7.56
2R10	A	36	128	1.9	93	112	28.97
2R10	A	37	35	2.3	76	63	13.32
2R10	A	37	43	1.7	N/A	65	20.00
2R10	A	38	36	1.8	83	47	10.91
2R10	A	38	38	1.0	83	88	20.20
2R10	A	38	40	7.3	94	109	28.37
2R10	A	38	42	1.7	86	56	13.39
2R10	A	38	44	4.5	92	63	16.12
2R10	A	44	118	1.4	80	42	9.34
2R10	A	46	42	3.3	87	75	18.21
2R10	A	48	48	1.5	70	56	10.90

OUTAGE	SG	ROW	LINE	VOLTS	MAX %TW	LENGTH	AVG %TW
2R10	A	48	50	4.2	79	217	47.68
2R10	A	48	120	1.5	58	63	10.16
2R10	A	49	41	0.4	51	70	9.93
2R10	A	49	107	1.8	N/A	142	20.00
2R10	A	50	144	0.7	50	30	4.14
2R10	A	51	43	N/A	N/A	N/A	20.00
2R10	A	51	113	1.2	67	65	12.07
2R10	A	51	115	0.8	61	42	7.13
2R10	A	52	104	1.0	48	42	5.61
2R10	A	52	120	1.6	61	96	16.33
2R10	A	54	64	3.0	82	68	15.57
2R10	A	54	106	2.2	N/A	65	20.00
2R10	A	55	105	1.2	40	39	4.28
2R10	A	57	63	2.1	73	98	19.90
2R10	A	58	54	1.2	33	39	3.53
2R10	A	58	66	9.8	96	96	25.70
2R10	A	59	55	1.8	41	88	9.98
2R10	A	59	113	1.0	25	54	3.77
2R10	A	59	115	2.5	97	46	12.27
2R10	A	61	133	0.5	70	18	3.41
2R10	A	62	60	1.9	50	67	9.25
2R10	A	62	82	1.5	50	98	13.63
2R10	A	63	63	1.3	24	74	4.91
2R10	A	63	137	1.5	85	21	4.96
2R10	A	64	60	3.2	79	116	25.38
2R10	A	65	61	1.5	49	37	5.01
2R10	A	65	107	1.6	60	79	13.14
2R10	A	65	109	1.2	32	51	4.52
2R10	A	66	60	1.1	59	228	37.33
2R10	A	66	110	5.7	86	47	11.30
2R10	A	67	61	1.6	58	149	23.99
2R10	A	67	65	0.9	35	149	14.48
2R10	A	67	107	1.4	62	179	30.78
2R10	A	68	66	4.0	95	84	22.19
2R10	A	68	104	2.0	75	126	26.28
2R10	A	70	106	2.5	85	121	28.55
2R10	A	71	35	9.2	81	223	50.07
2R10	A	71	103	1.7	0	98	0.00
2R10	A	71	111	2.7	92	47	12.09
2R10	A	73	41	1.5	81	33	7.49
2R10	A	74	36	1.8	3	51	0.42
2R10	A	75	37	4.0	94	61	16.01
2R10	A	75	79	3.6	76	68	14.43

OUTAGE	SG	ROW	LINE	VOLTS	MAX %TW	LENGTH	AVG %TW
2R10	A	75	81	1.6	3	63	0.53
2R10	A	75	133	1.0	66	26	4.82
2R10	A	76	36	1.0	84	39	8.99
2R10	A	76	130	3.2	84	117	27.39
2R10	A	77	129	4.2	91	91	23.03
2R10	A	77	131	3.3	94	49	12.81
2R10	A	78	80	1.2	54	84	12.62
2R10	A	79	127	1.1	48	46	6.07
2R10	A	82	82	7.0	90	131	32.85
2R10	A	84	84	3.6	90	46	11.39
2R10	A	87	125	6.7	82	154	35.12
2R10	A	88	44	3.4	89	51	12.56
2R10	A	89	125	0.8	73	39	7.82
2R10	A	90	124	2.1	79	40	8.84
2R10	A	93	85	3.1	76	79	16.65
2R10	A	94	84	11.2	88	123	29.98
2R10	A	95	115	4.7	92	63	16.12
2R10	A	96	52	7.1	87	96	23.29
2R10	A	97	45	0.7	63	46	7.97
2R10	A	97	51	1.3	68	44	8.27
2R10	A	97	79	2.3	88	39	9.42
2R10	A	97	83	2.9	90	86	21.46
2R10	A	98	118	4.8	86	67	15.91
2R10	A	99	55	1.5	44	91	11.14
2R10	A	100	84	2.1	73	72	14.57
2R10	A	102	78	6.7	97	131	35.41
2R10	A	102	86	2.5	80	39	8.57
2R10	A	102	92	1.5	4	103	1.15
2R10	A	102	108	5.5	78	131	28.47
2R10	A	103	61	1.2	63	28	4.91
2R10	A	103	77	2.4	97	28	7.55
2R10	A	103	81	1.4	46	51	6.49
2R10	A	103	83	1.4	69	51	9.74
2R10	A	103	85	1.6	61	128	21.67
2R10	A	103	87	0.7	33	21	1.93
2R10	A	104	74	2.1	95	42	11.10
2R10	A	104	76	1.3	65	53	9.49
2R10	A	104	84	2.8	60	217	36.21
2R10	A	105	65	1.4	74	46	9.36
2R10	A	105	75	1.4	91	137	34.55
2R10	A	105	87	1.2	58	88	14.11
2R10	A	105	109	1.1	71	79	15.55
2R10	A	106	60	1.3	1	81	0.22

OUTAGE	SG	ROW	LINE	VOLTS	MAX %TW	LENGTH	AVG %TW
2R10	A	107	61	2.4	87	51	12.28
2R10	A	107	83	2.9	91	82	20.82
2R10	A	107	85	1.1	57	60	9.43
2R10	A	108	70	1.2	70	42	8.18
2R10	A	108	96	5.4	97	58	15.58
2R10	A	108	102	2.1	82	63	14.37
2R10	A	111	73	2.1	63	147	25.76
2R10	A	111	75	1.3	48	32	4.21
2R10	A	111	107	3.6	83	93	21.41
2R10	A	112	92	1.8	73	70	14.21
2R10	B	18	150	3.3	91	53	13.29
2R10	B	18	152	1.7	91	67	16.83
2R10	B	20	18	1.4	17	32	1.49
2R10	B	20	114	1.1	50	35	4.87
2R10	B	24	146	1.1	83	63	14.54
2R10	B	40	126	2.5	93	25	6.34
2R10	B	42	66	1.0	57	93	14.70
2R10	B	43	135	3.0	80	46	10.12
2R10	B	71	55	1.8	21	47	2.76
2R10	B	83	95	2.0	44	58	7.07
2R10	B	93	121	0.9	62	37	6.34
2R10	B	94	116	2.0	90	39	9.64
2R10	B	97	115	2.1	41	44	4.99
2R10	B	98	50	0.8	52	65	9.36
2R10	B	101	53	0.6	53	28	4.13
2R10	B	102	62	0.8	67	49	9.13
2R10	B	104	70	1.6	69	89	17.13
2R10	B	106	84	0.7	35	89	8.69
2R10	B	106	98	1.0	57	65	10.26
2R10	B	107	83	2.3	84	88	20.44
2R10	B	107	85	3.1	71	72	14.17
2R10	B	110	96	1.5	74	81	16.57
2R10	B	114	72	7.4	81	49	11.04
2P95-1	A	46	52	1.1	83	41	9
2P95-1	A	50	52	0.72	66	90	17
2P95-1	A	32	66	1.8	92	39	10
2P95-1	A	57	55	1.38	72	74	15
2P95-1	A	57	57	2.32	98	48	13
2P95-1	A	53	63	5.9	88	88	22
2P95-1	A	61	67	1.39	45	55	7
2P95-1	A	60	60	1.92	59	83	14
2P95-1	A	64	62	1.13	37	65	7
2P95-1	A	54	62	0.77	58	53	9

OUTAGE	SG	ROW	LINE	VOLTS	MAX %TW	LENGTH	AVG %TW
2P95-1	A	66	64	3.27	93	129	33
2P95-1	A	56	66	0.75	79	42	9
2P95-1	A	64	66	1.3	90	48	12
2P95-1	A	23	51	2.22	11	122	4
2P95-1	A	10	152	0.69	3	62	1
2P95-1	A	22	152	0.62	39	51	6
2P95-1	A	24	52	2.99	42	143	17
2P95-1	A	12	152	1.63	67	50	9
2P95-1	A	22	32	2.03	89	170	42
2P95-1	A	16	54	2.03	74	106	22
2P95-1	A	20	54	1.08	19	111	6
2P95-1	A	17	153	1.89	88	25	6
2P95-1	A	27	53	2.27	80	94	21
2P95-1	A	16	140	1.78	91	67	17
2P95-1	A	28	146	2.97	88	102	25
2P95-1	A	16	144	1.75	96	78	21
2P95-1	A	12	148	2.71	88	95	23
2P95-1	A	23	135	2.48	81	304	68
2P95-1	A	19	139	1.06	60	138	23
2P95-1	A	11	147	0.97	50	163	23
2P95-1	A	66	138	1.62	95	55	15
2P95-1	A	61	137	2.01	94	71	19
2P95-1	A	57	141	3.64	99	74	20
2P95-1	A	90	118	0.64	89	50	12
2P95-1	A	90	126	1.66	97	57	15
2P95-1	A	82	132	1.11	1	40	1
2P95-1	A	68	136	1.01	25	75	5
2P95-1	A	72	132	0.85	67	117	22
2P95-1	A	96	122	1.61	88	113	28
2P95-1	A	21	111	0.86	69	92	18
2P95-1	A	21	113	3.49	71	95	19
2P95-1	A	29	113	1.17	61	46	8
2P95-1	A	31	113	1.06	55	53	8
2P95-1	A	15	153	1.08	44	64	8
2P95-1	A	99	121	2.37	95	95	25
2P95-1	A	71	135	1.54	75	118	25
2P95-1	A	34	122	0.86	59	79	13
2P95-1	A	49	119	1.5	68	151	29
2P95-1	A	4	118	1.93	70	58	11
2P95-1	A	5	127	1.62	76	58	12
2P95-1	A	33	127	2.73	88	132	32
2P95-1	A	35	129	1.47	91	117	30
2P95-1	A	29	131	2.15	23	71	5

OUTAGE	SG	ROW	LINE	VOLTS	MAX %TW	LENGTH	AVG %TW
2P95-1	A	33	131	3.91	97	104	28
2P95-1	A	32	128	0.57	15	60	3
2P95-1	A	30	130	1.57	1	55	0
2P95-1	A	32	132	3.35	92	67	17
2P95-1	A	26	134	2.5	96	87	23
2P95-1	A	20	134	7.11	91	134	34
2P95-1	A	24	134	4.4	97	143	39
2P95-1	A	11	127	0.69	87	53	13
2P95-1	A	43	131	4.2	99	48	13
2P95-1	A	21	133	2.31	72	62	12
2P95-1	A	41	133	3.51	98	48	13
2P95-1	A	24	126	2.74	79	58	13
2P95-1	A	14	128	3.84	72	85	17
2P95-1	A	8	130	0.8	65	64	12
2P95-1	A	71	69	2.67	92	58	15
2P95-1	A	83	81	2.7	89	74	18
2P95-1	A	81	83	1.75	62	134	23
2P95-1	A	85	83	2.14	46	112	14
2P95-1	A	72	68	1.18	36	90	9
2P95-1	A	88	68	1.77	45	101	13
2P95-1	A	72	80	2.05	35	115	11
2P95-1	A	78	82	2.15	84	138	32
2P95-1	A	76	84	0.85	30	103	9
2P95-1	A	80	74	4.26	1	56	1
2P95-1	A	74	76	3.84	92	83	21
2P95-1	A	78	76	2.74	77	165	35
2P95-1	A	76	78	7.15	69	83	16
2P95-1	A	70	80	1.73	59	69	11
2P95-1	A	81	91	1.35	27	69	5
2P95-1	A	71	101	3.39	80	71	16
2P95-1	A	75	65	1.95	76	64	14
2P95-1	A	70	82	2.66	38	83	9
2P95-1	A	69	83	1.4	64	66	12
2P95-1	A	72	102	2.1	89	94	23
2P95-1	A	76	98	1.77	14	92	4
2P95-1	A	80	88	1.36	47	102	13
2P95-1	A	76	100	1.01	39	43	5
2P95-1	A	95	45	2.86	84	120	28
2P95-1	A	95	53	0.68	76	64	14
2P95-1	A	107	59	0.85	41	69	8
2P95-1	A	79	91	2.71	93	143	37
2P95-1	A	83	91	1.32	52	109	16
2P95-1	A	77	97	1.42	51	241	34

OUTAGE	SG	ROW	LINE	VOLTS	MAX %TW	LENGTH	AVG %TW
2P95-1	A	97	53	1.14	53	51	8
2P95-1	A	98	48	1.2	71	46	9
2P95-1	A	98	52	1.28	68	43	8
2P95-1	A	92	44	1.84	81	120	27
2P95-1	A	103	79	1.88	79	64	14
2P95-1	A	107	79	1.97	81	97	22
2P95-1	A	95	81	0.75	77	83	18
2P95-1	A	107	103	5.05	92	62	16
2P95-1	A	111	83	0.91	56	81	13
2P95-1	A	104	68	1.97	83	76	18
2P95-1	A	104	70	0.84	43	34	4
2P95-1	A	112	70	1.02	64	92	16
2P95-1	A	100	76	4.49	97	108	29
2P95-1	A	108	78	0.94	59	60	10
2P95-1	A	104	80	0.97	81	62	14
2P95-1	A	100	86	1.58	71	76	15
2P95-1	A	112	90	4.17	93	167	43
2P95-1	A	112	98	3.66	96	69	18
2P95-1	A	97	77	2.05	82	115	26
2P95-1	A	93	83	1.7	99	123	34
2P95-1	A	101	83	4.67	96	113	30
2P95-1	A	105	83	1.74	74	112	23
2P95-1	A	109	83	2.98	90	92	23
2P95-1	A	97	85	1.66	81	182	41
2P95-1	A	101	87	0.77	66	98	18
2P95-1	A	97	95	1.26	60	88	15
2P95-1	A	110	70	1.38	87	51	12
2P95-1	A	106	72	2.8	97	76	20
2P95-1	A	110	96	1.04	70	155	30
2P95-1	A	114	100	2.62	93	44	11
2P95-1	A	106	94	1.9	86	95	23
2P95-1	A	98	80	3.29	92	150	38
2P95-1	A	102	80	6.88	98	136	37
2P95-1	A	106	84	0.75	68	74	14
2P95-1	A	110	84	3.75	97	78	21
2P95-1	A	98	92	2.77	85	104	25
2P95-1	A	67	95	1.12	75	46	10
2P95-1	A	52	88	1.3	83	43	10
2P95-1	A	68	94	0.99	40	39	4
2P95-1	A	42	74	2	37	150	15
2P95-1	A	50	74	1.15	69	46	9
2P95-1	A	66	78	1.5	37	115	12
2P95-1	A	46	72	0.75	89	53	13

OUTAGE	SG	ROW	LINE	VOLTS	MAX %TW	LENGTH	AVG %TW
2P95-1	A	39	69	1.84	77	76	16
2P95-1	A	82	110	3.18	86	46	11
2P95-1	A	26	124	0.58	58	41	7
2P95-1	A	29	125	0.58	50	58	8
2P95-1	A	72	78	1.21	82	69	16
2P95-1	A	77	85	1.58	59	133	22
2P95-1	A	68	82	1.81	73	133	27
2P95-1	A	43	101	1.75	86	65	16
2P95-1	A	34	116	0.71	42	48	6
2P95-1	A	62	110	0.97	74	58	12
2P95-1	A	56	116	0.62	71	35	7
2P95-1	A	48	110	0.91	62	39	7
2P95-1	A	53	103	1.42	25	76	5
2P95-1	A	61	113	0.88	67	158	29
2P95-1	A	64	98	1.32	62	46	8
2P95-1	A	51	103	1.28	36	55	6
2P95-1	A	25	35	2.17	94	124	32
2P95-1	A	21	37	2.26	95	43	11
2P95-1	A	25	37	2.59	96	134	36
2P95-1	A	33	41	4.24	98	145	39
2P95-1	A	23	35	3.53	98	218	59
2P95-1	A	11	37	2	79	36	8
2P95-1	A	23	37	2.61	85	134	32
2P95-1	A	35	39	1.36	66	113	21
2P95-1	A	27	41	1.63	90	57	14
2P95-1	A	11	43	11.17	54	67	10
2P95-1	A	32	34	1.53	97	64	17
2P95-1	A	24	36	1.03	74	48	10
2P95-1	A	28	36	1.32	43	99	12
2P95-1	A	28	38	5.43	100	87	24
2P95-1	A	40	36	0.88	46	37	5
2P95-1	A	22	34	0.92	85	110	26
2P95-1	A	26	38	1	88	39	10
2P95-1	A	49	45	0.8	52	83	12
2P95-1	A	37	47	2.87	52	170	25
2P95-1	A	37	49	0.77	31	39	3
2P95-1	A	35	43	1.81	68	36	7
2P95-1	A	35	47	1.53	50	83	12
2P95-1	A	43	47	0.97	45	164	21
2P95-1	A	47	47	2.49	30	210	18
2P95-1	A	36	46	1.12	39	111	12
2P95-1	A	52	46	3.24	99	51	14
2P95-1	A	34	46	2.31	68	152	29

OUTAGE	SG	ROW	LINE	VOLTS	MAX %TW	LENGTH	AVG %TW
2P95-1	A	42	48	0.87	41	67	8
2P95-1	A	14	26	1.62	91	92	24
2P95-1	A	22	26	4.05	84	93	22
2P95-1	A	16	28	1.99	50	115	16
2P95-1	A	14	30	1.62	78	108	24
2P95-1	A	18	30	2.08	81	72	17
2P95-1	A	12	32	1.65	89	48	12
2P95-1	A	37	21	1.05	40	109	13
2P95-1	A	23	33	3.1	93	92	24
2P95-1	A	22	32	1.32	80	76	17
2P95-1	A	65	79	2.27	69	160	31
2P95-1	A	70	34	1.64	93	55	15
2P95-1	A	73	35	0.74	56	52	8
2P95-1	A	80	40	1.2	40	62	7
2P95-1	A	55	39	2.06	94	52	14
2P95-1	A	81	41	4.65	96	76	21
2P95-1	A	83	41	0.99	57	41	7
2P95-1	A	58	40	0.4	57	37	6
2P95-1	A	82	40	2.41	86	71	17
2P95-1	A	86	40	0.88	70	28	6
2P95-1	A	12	18	3.32	92	96	25
2P95-1	B	83	57	2.4	84	51	12
2P95-1	B	71	59	1.5	87	155	37
2P95-1	B	69	59	3.76	92	122	31
2P95-1	B	73	59	2.75	96	74	20
2P95-1	B	28	58	3.51	87	50	12
2P95-1	B	95	113	0.83	61	83	14
2P95-1	B	94	124	1.89	81	93	21
2P95-1	B	20	106	1	80	120	27
2P95-1	B	36	126	1.33	18	59	3
2P95-1	B	11	133	0.86	20	30	2
2P95-1	B	87	65	0.39	51	35	5
2P95-1	B	87	53	1.66	88	71	17
2P95-1	B	96	52	0.73	21	67	4
2P95-1	B	100	52	2.52	88	103	25
2P95-1	B	92	54	0.77	21	112	7
2P95-1	B	96	54	2.21	14	74	3
2P95-1	B	100	54	3.28	87	73	18
2P95-1	B	81	47	2.82	94	34	9
2P95-1	B	93	55	1.16	73	78	16
2P95-1	B	101	63	0.8	73	93	19
2P95-1	B	91	49	2.37	93	99	26
2P95-1	B	100	48	2.64	91	97	25

OUTAGE	SG	ROW	LINE	VOLTS	MAX %TW	LENGTH	AVG %TW
2P95-1	B	104	62	1.46	95	106	28
2P95-1	B	100	62	1.33	91	164	41
2P95-1	B	100	60	1.68	76	100	21
2P95-1	B	111	75	2.19	93	60	16
2P95-1	B	107	65	0.35	52	60	9
2P95-1	B	103	77	3.11	91	120	30
2P95-1	B	91	83	1.25	68	43	8
2P95-1	B	111	87	0.64	64	57	10
2P95-1	B	107	97	1.31	87	55	13
2P95-1	B	103	103	1.5	77	74	16
2P95-1	B	107	105	0.8	89	48	12
2P95-1	B	107	93	3.66	83	158	36
2P95-1	B	101	67	0.8	2	81	1
2P95-1	B	109	69	0.75	56	58	9
2P95-1	B	113	73	0.85	98	67	18
2P95-1	B	97	81	2.01	88	65	16
2P95-1	B	109	85	1.93	82	143	33
2P95-1	B	105	91	1.21	76	62	13
2P95-1	B	113	97	2.4	91	187	47
2P95-1	B	104	64	1.4	87	106	26
2P95-1	B	100	66	0.89	59	104	17
2P95-1	B	108	70	1.35	71	67	13
2P95-1	B	108	80	1.13	70	44	9
2P95-1	B	108	84	3.22	99	109	30
2P95-1	B	108	88	1.51	84	50	12
2P95-1	B	108	96	0.79	79	95	21
2P95-1	B	100	100	1.42	57	183	29
2P95-1	B	104	104	2.19	88	57	14
2P95-1	B	106	80	0.66	47	92	12
2P95-1	B	106	88	2.33	85	85	20
2P95-1	B	110	98	1.39	85	109	26
2P95-1	B	110	100	2.45	91	48	12
2P95-1	B	106	104	0.59	47	39	5
2P95-1	B	98	100	3.38	100	64	18
2P95-1	B	100	98	1.73	84	41	10
2P95-1	B	112	96	0.93	85	41	10
2P95-1	B	66	112	0.94	75	53	11
2P95-1	B	40	34	1.43	75	78	16
2P95-1	B	17	37	0.7	17	99	5
2P95-1	B	16	36	1.41	83	58	13
2P95-1	B	22	42	3.27	85	108	26
2P95-1	B	23	45	2.49	85	126	30
2P95-1	B	24	48	2.48	76	220	46

OUTAGE	SG	ROW	LINE	VOLTS	MAX %TW	LENGTH	AVG %TW
2P95-1	B	79	43	0.82	59	64	10
2P95-1	B	83	43	2.14	88	123	30
2P95-1	B	87	43	1.11	77	46	10
2P95-1	B	21	21	0.83	45	85	11
2P95-1	B	32	26	1.37	69	39	7
2P95-1	B	21	31	2.49	95	41	11
2P95-1	B	32	32	1.85	44	48	6
2P95-1	B	52	34	2.03	95	30	8
2P95-1	B	64	34	2.89	79	57	13
2P95-1	B	78	38	2.42	93	60	16
2P95-1	B	74	38	3.81	90	126	30
2P95-1	B	75	39	1.46	46	42	6
2P95-1	B	59	41	3.17	84	48	12
2P95-1	B	19	17	1.23	41	106	12
2P95-1	B	71	41	1.17	91	37	10

In addition, the following tubes with volumetric/axial indications were plugged in 2P95-1

OUTAGE	SG	ROW	LINE
2P95-1	A	31	101
2P95-1	A	59	51
2P95-1	A	88	84
2P95-1	A	74	86
2P95-1	A	69	97
2P95-1	A	79	61
2P95-1	A	99	83
2P95-1	A	48	72
2P95-1	A	33	103
2P95-1	A	34	104
2P95-1	A	51	49
2P95-1	A	117	65
2P95-1	B	74	84
2P95-1	B	79	85
2P95-1	B	64	96
2P95-1	B	67	75
2P95-1	B	66	98